DISSERTATION

ENGINEERED mRNA THERAPEUTIC ENCODING BETA-CATENIN INCREASED BONE FORMATION IN A MURINE TIBIAL FRACTURE MODEL

Submitted by

Anna Laura Nelson

School of Biomedical Engineering

In partial fulfillment of the requirements

For the Degree of Doctor of Philosophy

Colorado State University

Fort Collins, Colorado

Fall 2023

Doctoral Committee:

Advisor: Nicole Ehrhart
Co-Advisor: Chelsea Bahney

Johnny Huard
Ketul Popat
David Prawel

ABSTRACT

ENGINEERED mRNA THERAPEUTIC ENCODING BETA-CATENIN INCREASED BONE FORMATION IN A MURINE TIBIAL FRACTURE MODEL

Fractures continue to be a global economic burden and impaired fracture healing cases, like delayed and non-union, occurring in about 14% of all tibial shaft fractures. Current treatments to aid in fracture healing involve surgical interventions and osteoanabolic, bone-morphogenetic protein-2 (BMP-2), yet is challenged supraphysiological doses and adverse side effects. Given the limited treatment options available, there remains a clinical need to develop injectable therapeutics to accelerate fracture healing in impaired fracture healing cases. Mechanistic data reveals β-catenin as a molecular driver in endochondral ossification. The central hypothesis for this dissertation is a stabilized, non-destructive β-catenin mRNA delivered locally in the fracture callus can accelerate fracture healing in a murine tibia fracture healing model. Using mRNA therapeutically continues to be challenged with stability and immunogenicity of the mRNA. To circumvent these limitations, delivery carriers have been employed to maximize gene stability, minimize off-target effects, and reduce immunogenicity. Recent advancements in liposomal technologies have led to the development of lipid nanoparticles (LNPs), leading to successful clinical translation of several novel and highly effective therapies, like SARS-CoV-2 vaccine. Alternative delivery carriers have emerged involving use of mineral coated microparticles (MCMs) as a biomimetic and biocompatible system to deliver liposomes at the site of a fracture in a controlled manner. Here, we explore mRNA delivery carriers for fracture healing applications, including manufactured cationic liposomes, MCMs, LNPs and a combination of these carriers. Manufactured liposome, Lipofectamine™, was found to be prolong transfection when tested in a murine fracture model *in vivo* as compared to TransIT Transfection Reagent. Using Lipofectamine™ to deliver mRNA, chemically-doped MCMs enhanced transfection and stimulated bone *in vitro* when delivered in chondrocytes. When testing these platforms in a murine tibia fracture model,

chemically-doped MCM did not promote bone expression through testing RNA in the fracture callus for bone-related genes and through histomorphometry of the fracture callus 2 weeks post-fracture. The chemically doped MCM was found to prolong transfection of reporter gene, firefly luciferase mRNA, *in vivo* when compared to other treatment groups including the liposome and mRNA complex (lipoplex) alone. Ionizable-based LNPs are positively charged at a low pH and net neutral at physiological pH. Two FDA-approved ionizable phospholipids, MC3 and SM-102, were used to generate ionizable LNPs. First, MC3 LNP was tested for transfection capacity when combined with MCMs. While chemically-doped MCMs when combined with firefly luciferase mRNA encapsulated MC3 LNPs showed improved transfection *in vitro*, no improvements in transfection efficacy were found *in vivo*. Next, MC3 and SM-102 LNPs were then complexed with reporter gene, firefly luciferase mRNA to test transfection potential, immunogenicity, fracture interference and biodistribution *in vitro* and in a murine fracture healing model. SM-102 LNPs showed enhanced transfection efficacy *in vitro*, prolonged transfection *in vivo*, minimal fracture interference *in vivo* and showed no localized inflammatory response in the murine fracture callus. *Ex-vivo* IVIS images of main organs revealed no biodistributive effects when delivering SM-102 complexed with mRNA locally to the site of the fracture callus. Capitalizing on prior mechanistic data showing β-catenin's critical role in chondrocyte to osteoblast transdifferentiation, a non-destructive β-catenin, β-catenin^{GOF}, mRNA transcript was generated using nucleoside modification, N1-methyl-pseudouridine, and cap analog, CleanCap. When testing the generated β-catenin^{GOF} mRNA encapsulated in SM-102 LNPs *in vitro* for bioactivity, downstream canonical Wnt genes were significantly upregulated. When testing SM-102-β-catenin^{GOF} mRNA therapeutic in murine tibia fracture model, more bone and less cartilage composition compared to PBS control was determined when analyzing histomorphometry at 25 and 45 μg concentrations at 2 weeks post-fracture. To further confirm SM-102-β-catenin^{GOF} mRNA therapy's capabilities to promote bone *in vivo*, μCT was performed revealing significantly more bone volume over total volume with 45 μg dose as compared to PBS control. Taken together, we generated a novel mRNA based therapeutic encoding a non-destructive β-catenin mRNA and optimized ionizable LNP, SM-102, to maximize transfection

efficacy with a localized delivery. This SM-102-β-catenin^{GOF} mRNA therapeutic may accelerate fracture healing in a murine tibia fracture healing model.

ACKNOWLEDGEMENTS

The data generated in this dissertation was conceptualized based on collaborative meetings with Chelsea Bahney, Nicole Ehrhart and myself. I would specifically like to thank my advisors, Chelsea and Nicole, for their continued support and assistance throughout these past few years. Additionally, I would like to thank Dr. William Murphy and Dr. Francesca Taraballi for their support and collaborations in these projects and throughout my PhD journey. These sets of data were collected in part from Josh Choe, from Dr. Murphy's laboratory, and Chiara Mancino, from Dr. Taraballi's laboratory. Josh, Chiara and I have worked closely together on these projects, and I would like to thank them for their help, guidance and friendship.

Additionally, I would like to thank my labs at both Steadman Philippon Research Institute (SPRI) and Colorado State University (CSU) and specifically Laura Chubb, Kate Williams and Molly Czachor for their help in data collection. SPRI funded my PhD stipend and resources, while Dr. Ehrhart's lab at CSU also aided in funding resources. This work was funded in part through Orthoregeneration Network Kick-starter Grant (20-166), Mike and Sue Shannon Foundation and National Institutes of Health through NIAMS (NIAMS (R01-AR077761).

I'd like to recognize Dr. Tobet and Sara Mattern for their guidance and support throughout this journey and openness to putting together this collaborative program. Additionally, I'd like to thank the support from SPRI, specifically Dr. Huard and Suzanne Page. The remaining of my committee members – Dr. Prawel and Dr. Popat - have always been generous, kind and I am thankful for their support.

Lastly, my parents have been a tremendous help in all ways possible throughout my career and in life. I cannot thank you enough and I love you both so much. My lovely partner, Patrick, who has also been an enormous help in life – thank you for being you and for choosing me. I love you too.

DEDICATION

To my parents, Cindy and Steve Nelson, my partner, Patrick Schlehuber, and Jada.

TABLE OF CONTENTS

ABSTRACT……..ii
ACKNOWLEDGEMENTS……...v
DEDICATION……..vi
LIST OF TABLES……....ix
LIST OF FIGURES……...x
INTRODUCTION…….....1
Chapter I: STRATEGIES TO ACTIVATE CANONICAL WNT ..…….....12
I.1 Introduction……...12
I.2 Wnt Activating Therapeutics……15
I.2.1 Sclerostin Antibodies……16
I.2.2 Other Antibody-based Approaches to Modulate Wnt……17
I.2.3 Synthetic Wnts.……..……19
I.2.4 Lithium Chloride……19
I.2.5 Fluoride……..20
I.2.6 Strontium…….....21
I.2.7 Other Wnt Modifiers……..21
I.3 Tissue Engineering Strategies to Achieve Delivery……22
I.3.1 Liposomes…….....24
I.3.2 Scaffold Dopants……..…….....25
I.3.3 Hydrogels……....26
I.4 Future Directions……....26
I.4.1 mRNA Delivery…….....27
I.4.2 CRISPR Gene Editing……27
I.5 Conclusions……...….28
I.6 References……..30
Chapter II: MINERAL COATED MICROPARTICLES AS MRNA DELIVERY PLATFORMS FOR FRACTURE HEALING…….41
II.1 Introduction……...…41
II.2 Methods & Materials……43
II.2.1 Synthesis of MCM and FMCM……....43
II.2.2 MCM and FMCM formulations with lipoplexes for *in vitro* experiments.....…..44
II.2.3 Testing MCM and FMCM cytotoxicity *in vitro*……...……44
II.2.4 Testing immunogenicity and osteogenesis *in vitro*……..……45
II.2.5 Murine tibia fracture and stabilization model……..46
II.2.6 Localized MCM and FMCM injections…….…..47
II.2.7 Transfection efficacy and kinetics *in vivo*……48
II.2.8 *In vivo* immunogenicity and osteogenic testing…….…..48
II.2.9 Histology, histopathologic scoring and histomorphometric methodology……..49
II.2.10 Statistics……..……51
II.3 FMCM enhances transfection, promotes bone and minimizes immunogenicity *in vitro*…....51
II.4 FMCM prolongs transfection without altering fracture healing in a murine model……....54
II.5 Conclusions……..57
II.6 Limitations and Future Directions……...…59
II.7 References……....61
Chapter III: OPTIMIZING LIPID NANOPARTICLES FOR MRNA DELIVERY IN FRACTURES.....65
III.1 Introduction……65
III.2 Methods & Materials……...……68

III.2.1 LNP Formulations……..…...68
III.2.2 Testing transfection efficacy and cytotoxicity *in vitro*……..……..….69
III.2.3 Murine tibia fracture and stabilization model……..……70
III.2.4 Localized injections of cationic lipoplexes……..……71
III.2.5 Localized injections of MCM-LNPs…….....72
III.2.6 Localized injections of ionizable LNPs……..……...72
III.2.7 Transfection efficacy and kinetics *in vivo*……73
III.2.8 *In vivo* immunogenicity and fracture healing interference measurements……...73
III.2.9 Biodistribution Study……..…..74
III.2.10 Statistics……75
III.3 Lipofectamine™ prolongs expression of FLuc at the fracture site as compared to TransIT..75
III.4 MC3-MCM/FMCM complex did not prolong transfection i*n vivo*……76
III.5 SM-102 LNPs improved mRNA delivery characteristics as compared with MC3 LNPs *in vitro* and *in vivo*.....78
III.6 Biodistribution remained largely localized to the fracture site following LNP injection…...81
III.7 Conclusions…….....82
III.8 Limitations and Future Directions…….…86
III.9 References……...88
Chapter IV: NON-DESTRUCTIVE β-CATENIN MRNA PROMOTES BONE IN FRACTURE MODEL……...92
IV.1 Introduction……92
IV.2 Methods & Materials……..…95
IV.2.1 LNP Formulations……..…95
IV.2.2 Testing bioactivity of β-catenin mRNA *in vitro*……95
IV.2.3 Murine tibia fracture and stabilization model……96
IV.2.4 Localized injections of β-catenin mRNA – SM-102 LNPs……97
IV.2.5 Histology and histomorphometry……..98
IV.2.6 μCT analysis……..….98
IV.2.7 Statistics…….99
IV.3 β-catenin mRNA activates canonical Wnt *in vitro* and stimulates bone formation *in vivo*…99
IV.4 Conclusions……...101
IV.5 Limitations and Future Directions…….....103
IV.6 References…….....105
Chapter V: SUMMARY, IMPLICATIONS, CONCLUSIONS AND FUTURE DIRECTIONS……..…109
V.1 References……..117
APPENDIX A: SUPPLEMENTAL FIGURES AND TABLES...……....120
APPENDIX B: COPYRIGHT PERMISSION LETTER……..…124

LIST OF TABLES

TABLE 1. PRIMER SEQUENCES FOR MCM *IN VITRO* STUDIES……...46
TABLE 2. N-VALUES ASSOCIATED WITH TREATMENT GROUPS FOR MCM STUDIES……48
TABLE 3. PRIMER SEQUENCES FOR USE IN ALL MCM *IN VIVO* STUDIES……49
TABLE 4. PRIMER SEQUENCES FOR USE IN ALL LNP *IN VITRO* AND *IN VIVO* STUDIES……...74
SUPPLEMENTAL TABLE 1. HISTOLOGICAL SEMI-QUANTITATIVE SCORING METHOD..…123

LIST OF FIGURES

FIGURE 1. CANONICAL WNT SCHEMATIC ……...…14
FIGURE 2. SYSTEMIC AND LOCALIZED APPROACHES FOR WNT ……..23
FIGURE 3. TISSUE ENGINEERING STRATEGIES FOR WNT ……24
FIGURE 4. SCHEMATIC OF MCM DELIVERY OF LIPOPLEXES IN FRACTURE……...43
FIGURE 5. CHARACTERIZATION OF MCM AND FMCM……..52
FIGURE 6. *IN VITRO* TRANSFECTION ANALYSIS OF MCM AND FMCM……..53
FIGURE 7. MCM GENE EXPRESSION ANALYSIS WITHIN THE FRACTURE CALLUS..……..54
FIGURE 8. HISTOLOGICAL AND INFLAMMATORY ANALYSIS OF MCM-LPX……...55
FIGURE 9. MCM TRANSFECTION EFFICACY, KINETICS AND CHARACTERIZATION……..56
FIGURE 10. SCHEMATIC OF CATIONIC AND IONIZABLE LNPS……67
FIGURE 11. FLUC MRNA-LIPOFECTAMINE™ AND FLUC MRNA-TRANS-IT® IN FRACTURE……75
FIGURE 12. *IN VITRO* TRANSFECTION POTENTIAL OF IONIZABLE MC3 LNP……...…….76
FIGURE 13. TESTING MCM AND FMCM TO ENHANCE MC3 LNP TRANSFECTION……..…..77
FIGURE 14. MC3 AND SM-102 LNP CHARACTERIZATION……..……79
FIGURE 15. TRANSFECTION EFFICACY AND KINETICS OF IONIZABLE LNPS *IN VIVO*……...80
FIGURE 16. *IN VIVO* IMMUNOGENIC AND OSTEOGENIC EFFECTS OF IONIZABLE LNPS…...81
FIGURE 17. BIODISTRIBUTION OF LOCALIZED DELIVERY OF IONIZABLE LNPS…….…...82
FIGURE 18. CANONICAL WNT BIOACIVITY OF β-CATENIN-GOF MRNA *IN VITRO*……..…100
FIGURE 19. SM-102 LNPS-β-CATENIN-GOF MRNA PROMOTE BONE IN-VIVO…….……101
SUPPLEMENTAL FIGURE 1. OPTIMIZED β-CATENIN-GOF MRNA SEQUENCE……....120
SUPPLEMENTAL FIGURE 2. CACLULATING POWER ANALYSIS FOR IVIS OUTPUT……....121
SUPPLEMENTAL FIGURE 3. TRANSFECTION EFFICACY OF MC3 LNPS OVER TIME.……....122

INTRODUCTION

Fractures continue to be one of the most frequent type of hospitalized traumas with reports of about 32.7 million new cases of lower leg fractures globally in 2019.[1, 2] Additionally, tibial shaft fractures account for about 36.7% of all long-bone fractures in adults and are frequently associated with high-energy trauma events, like falls and transport accidents.[1, 3, 4] Open tibial fractures are often associated with higher rates of complications, like non-union or delayed union.[3, 5] In fact, reports of non-union have been found to occur up to 14% within tibial shaft fractures in a large study over the course of two years.[6] Non-union is typically treated through repeated surgeries resulting in long recovery times leading to increased frailty, depression, loss of independence, and, in some cases, a downward spiral that ends in death.[7, 8]

The process of fracture healing is a highly complex and regulated other involving many cell types, growth factors and other biological factors to form bone.[9] One particular cell type integral in fracture healing includes mesenchymal stem cells (MSCs), which undergo differentiation to either chondrocytes or osteoblasts depending on several factors, such as micromotion at the fracture gap.[9, 10] Bone forms through two distinct mechanisms: direct and indirect bone formation.[9] Direct bone formation, or intramembranous ossification, involves the direct transition of MSCs to osteoblasts, cells which deposit bone without a cartilaginous intermediary.[9] Indirect bone formation, or endochondral ossification, involves MSCs differentiating to chondrocytes prior to transitioning to osteoblasts.

The majority of fractures heal primarily through endochondral ossification, which involves can be characterized into 4 biological phases: 1) hematoma and inflammatory phase, 2) fibrocartilaginous phase, 3) hard callus phase and finally, 4) bone remodeling phase.[10] Within minutes of the fracture, a hematoma forms which released pro-inflammatory cytokines and recruits inflammatory cells. A robust pro-inflammatory response ensues involving macrophages and neutrophils, amongst other inflammatory cells.[9] While an inflammatory response is required in fracture healing, a timely resolution is necessary to

mitigate impaired fracture healing cases.[11] The fibrocartilaginous phase entails recruitment of MSCs derived from periosteum and endosteum, to the site of the fracture.[12] Concurrently, revascularization of the callus provides a supply of nutrients, oxygen and cells to the fracture site.[9] For endochondral ossification to proceed, MSCs give rise to chondrocytes, which transition to hypertrophic chondrocytes, highly angiogenic cell type.[9, 13] Hypertrophic chondrocytes have been found to transdifferentiate into osteoprogenitors and osteoblasts.[14-16] The final remodeling stage involves the replacement of trabecular bone with cortical bone, and is characterized by the resorption and remodeling of newly formed bone .[10]

Current approaches to augment fracture healing involve fracture reduction, surgical alignment of the fracture ends, and various fixation methods to achieve rigid stabilization.[17] In order for a fractured bone to heal properly, mechanical and biological factors at the facture site must be highly regulated. All tissues within the fracture have differing strain tolerances following mechanical load. Strain tolerances progressively decrease through each fracture stage until the strain decreases enough to facilitate bone formation.[18] For instance, granulation and fibrous tissues have the highest strain tolerances with reports up to 100%.[19] Remarked decreases in strain tolerance are found in cartilage and bone tissues of 10 and 2-5% respectively.[18, 19] Deformation of tissues outside of these levels fail to give rise to normal fracture healing. Surgical interventions, such as intermedullary nailing and internal and external fixation techniques are employed to maintain the mechanical environment within range to promote bone formation.[20-22]

Impaired fracture healing occurs due to a lack of sufficient mechanical factors, biological factors or a combination of the two in fractured tissue.[18] In fact, if strain levels fall outside of the strain thresholds, the fracture is at risk for impaired healing.[10, 17] For instance, the absence of strain surrounding the fracture gap results in inadequate mechanical stimulation of a callus and can contribute to atrophic nonunion.[22] Conversely, high strain conditions can increase callus size and often results in insufficient bridging between the fracture ends, leading to hypertrophic nonunion.[22] A clinical diagnosis of delayed fracture healing and non-union is made using radiographs. Delayed union is defined as a fracture which lacks radiographic progression and non-union is diagnosed when there is no radiographic sign of

union after 3 months.[17, 23] Clinical management of non-union includes repeated surgeries resulting in long recovery times. This has been associated with co-morbidities including increased frailty, depression, loss of independence, and, in some cases, a series of complications that ends in death.[7, 8]

Other than additional surgery, biologic solutions to facilitate fracture healing in non-union or delayed union cases are limited. Protein-based therapeutics, including the only FDA-approved osteoanabolic, recombinant human bone morphogenetic protein-2 (BMP-2), have been employed to augment fracture healing.[24-28] However, recombinant proteins must be delivered at supraphysiological doses and have been limited by short half-lives and low physiologic activity.[27, 29, 30] Furthermore, in order to sustain protein release when using BMP2 as a therapeutic, it must be delivered on an absorbable collagen sponge, necessitating surgical implantation.[28, 31, 32] Reported complication rates with recombinant BMP-2 remain unacceptably high, ranging from 20-70%.[30, 33] Adverse side effects associated with recombinant BMP-2 therapy include abnormal inflammatory responses, poor bone quality, heterotopic ossification, and osteolysis.[31, 33-35] Given the paucity of safe and effective therapeutics to accelerate fracture healing, there remains a clinical need to develop novel, and injectable-based therapies to accelerate fracture healing and minimize the incidence of delayed and non-union fractures and need for additional surgeries.

Mechanistic data has shown the canonical Wnt pathway to play a key role in this chondrocyte to osteoblast transdifferentiation and is a key molecular driver of endochondral ossification.[16] Due to canonical Wnt's integral role in bone formation, this pathway has served as a therapeutic target for bone repair.[36-38] However, direct activation of this pathway has been challenged with lipidation of Wnt ligands, which limit purification of the protein due to difficulty and expense.[36, 39] Current clinical approaches to target canonical Wnt involve targeting the inhibitors of the pathway with success for osteoporosis.[40, 41] Yet these indirect approaches have not been reported as efficacious for fracture healing applications.[42] Therapeutics using mRNA technology to activate canonical Wnt is proposed to facilitate

direct activation of this pathway, overcoming several limitations associated with Wnt proteins and Wnt activation.

The crosstalk between BMP/TGF-β signaling and canonical Wnt pathways lead to synergistic effects ultimately regulating bone repair. Several groups have found that BMPs promote bone growth through modulation of Wnt expression.[43, 44] Chen *et al.* reported that the expression of Wnt ligand, Wnt3a, and the downstream Wnt gene *runx2* are upregulated following BMP-2 treatment.[44] In fact, multiple studies found elevated levels of *runx2* following treatment with BMP-2, BMP-4, and/or BMP-7.[45-47] Conversely, Zhang *et al.* reported BMP-2 expression following activation of the canonical Wnt pathway.[48] Not only do these pathways activate similar downstream transcription factors, but these pathways were also reported to negatively regulate each other. While these pathways have a large amount of crosstalk in regulating osteoblast differentiation, it continues to remain unclear the extent to which these pathways directly interact with one another.[45]

Over the past few decades, increasing demand for biologic-based orthopaedic technologies to augment fracture healing has followed the substantial growth in orthopaedic surgeries being performed each year.[49] Of these emerging solutions, gene therapy has undergone significant advancements due to developments in delivery carriers and their capabilities to maximize gene stability, minimize off-target effects, and reduce immunogenicity.[50-56] Specifically, the considerable success and safety profile of the SARS-CoV-2 vaccine has catalyzed intense research efforts to develop additional mRNA-based technologies. [55, 57, 58] However, mRNA-based therapy in orthopedics remains a nascent field, specifically for fracture healing.[55, 59] Recently published work on an mRNA therapy to promote bone regeneration through coding for BMP2/9 has shown considerable promise, yet this approach uses a biomimetic scaffold requiring surgical implantation.[60-62] We propose that the ideal mRNA delivery platform to promote fracture repair would be a localized and injectable therapeutic, thus mitigating the need for additional surgeries in impaired fracture healing cases.

Effective mRNA delivery requires the use of carriers to protect the nucleic acids from degradation from nucleases.[63, 64] Conventional mRNA delivery mechanisms include liposomes, or phospholipid structures consisting of one or more bilayers.[65] Liposomes complexed with nucleic acids, termed lipoplexes, can induce immunogenic reactions and are rapidly cleared by the mononuclear phagocytic system (MPS) through the kidney, liver, and spleen.[63] Intravenous administration of lipid carriers can be recognized by toll-like receptors (TLR) and result in a strong immune reaction.[66] Recent advancements in liposomal technologies have led to the development of lipid nanoparticles (LNPs), or complex micelle-like structures comprised of phospholipids, sterols and hydrophilic polymers, to facilitate evasion of an immune reaction.[65] [67] These new advances have led to successful clinical translation of several novel and highly effective therapies, including FDA approved pharmaceuticals, like Onpattro and the SARS-CoV-2 vaccines.[66, 68]

mRNA delivery for therapeutic applications has been limited by mRNA instability, cytotoxicity and immunogenicity. Alternative strategies have been employed to mitigate these limitations. One such approach is the use of mineral coated microparticles (MCM) as a biomimetic and biocompatible system to deliver liposomes at the site of a fracture in a controlled manner.[69-73] While traditionally, MCM were developed for protein delivery, recent studies have shown enhanced transfection of mRNA both *in vitro* and *in vivo*.[74] The use of MCMs as a carrier for mRNA lipoplexes enhances mRNA transfection and mitigates cytotoxicity resulting from high *in vitro* mRNA concentrations.[69, 75, 76] While MCMs have recently shown improved transfection capacity as compared to protein delivery, they have only been tested *in vivo* using a rat spinal cord injury model and not for fracture healing. Of importance, endogenous protein expression from MCM-mRNA lipoplexes has been associated with higher bioactivity, prolonged protein expression and improved functional outcomes as compared to exogenous protein expression.[29, 77] Taken together, MCMs have the capacity to improve localization and cell uptake of mRNA at the fracture site addressing several challenges associated with mRNA delivery.

The overall goal of this thesis project was to develop and test an injectable mRNA- technology to activate canonical Wnt, a key molecular pathway driving endochondral ossification.[16] What follows in the ensuing chapters is the result of our extensive work to develop this novel approach. First, we review the body of knowledge regarding systemic and localized canonical Wnt activation for bone regeneration and identify knowledge gaps. We then report on our process to develop and optimize delivery systems for mRNA -base therapy for fracture healing. Finally, we describe how a novel sequence, non-destructive transcription factor, β-catenin mRNA transcript, was designed and shown to activate the canonical Wnt pathway and outline how this transcript was tested *in vitro* for bioactivity and *in vivo* efficacy to promote bone formation in a murine tibia fracture model.

References

1. Ekegren, C. L., Edwards, E. R., de Steiger, R., and Gabbe, B. J., *Incidence, Costs and Predictors of Non-Union, Delayed Union and Mal-Union Following Long Bone Fracture.* Int J Environ Res Public Health, 2018. **15**(12).
2. Cauley, J. A., *The global burden of fractures.* Lancet Healthy Longev, 2021. **2**(9): p. e535-e536.
3. Papakostidis, C., Kanakaris, N. K., Pretel, J., Faour, O., Morell, D. J., and Giannoudis, P. V., *Prevalence of complications of open tibial shaft fractures stratified as per the Gustilo-Anderson classification.* Injury, 2011. **42**(12): p. 1408-15.
4. Weiss, R. J., Montgomery, S. M., Ehlin, A., Al Dabbagh, Z., Stark, A., and Jansson, K. A., *Decreasing incidence of tibial shaft fractures between 1998 and 2004: information based on 10,627 Swedish inpatients.* Acta Orthop, 2008. **79**(4): p. 526-33.
5. Gaebler, C., Berger, U., Schandelmaier, P., Greitbauer, M., Schauwecker, H., Applegate, B., Zych, G., and Vecsei, V., *Rates and Odds Ratios for Complications in Closed and Open Tibial Fractures Treated With Unreamed, Small Diameter Tibial Nails: A Multicenter Analysis of 467 Cases.* Journal of Orthopaedic Trauma, 2001. **15**: p. 415-423.
6. Collaborators*, GBD 2019 Fracture, *Global, regional, and national burden of bone fractures in 204 countries and territories, 1990–2019: a systematic analysis from the Global Burden of Disease Study 2019.* The Lancet Healthy Longevity, 2021. **2**(9): p. E580-592.
7. Gruber, R., Koch, H., Doll, B. A., Tegtmeier, F., Einhorn, T. A., and Hollinger, J. O., *Fracture healing in the elderly patient.* Exp Gerontol, 2006. **41**(11): p. 1080-93.
8. Colón-Emeric, C., Saag, K., *Osteoporotic fractures in older adults.* Best Pract Res Clin Rheumatol, 2006. **20**(4): p. 695-706.
9. Bahney, C. S., Zondervan, R. L., Allison, P., Theologis, A., Ashley, J. W., Ahn, J., Miclau, T., Marcucio, R. S., and Hankenson, K. D., *Cellular biology of fracture healing.* J Orthop Res, 2019. **37**(1): p. 35-50.
10. Sheen, J. R., Mabrouk, A., and Garla, V. V., *Fracture Healing Overview*, in *StatPearls*. 2023, StatPearls Publishing Copyright © 2023, StatPearls Publishing LLC.: Treasure Island (FL).
11. Newman, H., Shih, Y. V., and Varghese, S., *Resolution of inflammation in bone regeneration: From understandings to therapeutic applications.* Biomaterials, 2021. **277**: p. 121114.
12. Knight, M. N. and Hankenson, K. D., *Mesenchymal Stem Cells in Bone Regeneration.* Adv Wound Care (New Rochelle), 2013. **2**(6): p. 306-316.
13. Hu, Diane P, Ferro, Federico, Yang, Frank, Taylor, Aaron J, Chang, Wenhan, Miclau, Theodore, Marcucio, Ralph S, and Bahney, Chelsea S, *Cartilage to bone transformation during fracture healing is coordinated by the invading vasculature and induction of the core pluripotency genes.* Development, 2017. **144**(2): p. 221-234.
14. Kodama, Joe, Wilkinson, Kevin J, Iwamoto, Masahiro, Otsuru, Satoru, and Enomoto-Iwamoto, Motomi, *The role of hypertrophic chondrocytes in regulation of the cartilage-to-bone transition in fracture healing.* Bone Reports, 2022: p. 101616.
15. Bahney, Chelsea S, Hu, Diane P, Taylor, Aaron J, Ferro, Federico, Britz, Hayley M, Hallgrimsson, Benedikt, Johnstone, Brian, Miclau, Theodore, and Marcucio, Ralph S, *Stem cell–derived endochondral cartilage stimulates bone healing by tissue transformation.* Journal of Bone and Mineral Research, 2014. **29**(5): p. 1269-1282.
16. Wong, Sarah Anne, Hu, Diane, Shao, Tiffany, Niemi, Erene, Barruet, Emilie, Morales, Blanca M, Boozarpour, Omid, Miclau, Theodore, Hsiao, Edward C, Nakamura, Mary, Bahney, Chelsea S, and Marcucio, Ralph S, *β-catenin Signaling Regulates Cell Fate Decisions at the Transition Zone of the Chondro-Osseous Junction During Fracture Healing.* bioRxiv, 2020: p. 2020.03.11.986141.

17. Schlickewei, C. W., Kleinertz, H., Thiesen, D. M., Mader, K., Priemel, M., Frosch, K. H., and Keller, J., *Current and Future Concepts for the Treatment of Impaired Fracture Healing.* Int J Mol Sci, 2019. **20**(22).
18. Elliott, D. S., Newman, K. J. H., Forward, D. P., Hahn, D. M., Ollivere, B., Kojima, K., Handley, R., Rossiter, N. D., Wixted, J. J., Smith, R. M., and Moran, C. G., *A unified theory of bone healing and nonunion.* The Bone & Joint Journal, 2016. **98-B**(7): p. 884-891.
19. Duan, Z. W. and Lu, H., *Effect of Mechanical Strain on Cells Involved in Fracture Healing.* Orthop Surg, 2021. **13**(2): p. 369-375.
20. Perren, SM, *Optimizing the degree of fixation stability based on the strain theory.* Der Orthopäde, 2010. **39**: p. 132-138.
21. Perren, SM, *Physical and biological aspects of fracture healing with special reference to internal fixation.* Clinical Orthopaedics and Related Research (1976-2007), 1979. **138**: p. 175-196.
22. Perren, SM, Fernandez, A, and Regazzoni, P, *Understanding fracture healing biomechanics based on the "strain" concept and its clinical applications.* Acta Chir Orthop Traumatol Cech, 2015. **82**(4): p. 253-60.
23. Calori, G. M., Mazza, E. L., Mazzola, S., Colombo, A., Giardina, F., Romanò, F., and Colombo, M., *Non-unions.* Clin Cases Miner Bone Metab, 2017. **14**(2): p. 186-188.
24. Dumic-Cule, I., Peric, M., Kucko, L., Grgurevic, L., Pecina, M., and Vukicevic, S., *Bone morphogenetic proteins in fracture repair.* Int Orthop, 2018. **42**(11): p. 2619-2626.
25. Tsuji, K., Bandyopadhyay, A., Harfe, B. D., Cox, K., Kakar, S., Gerstenfeld, L., Einhorn, T., Tabin, C. J., and Rosen, V., *BMP2 activity, although dispensable for bone formation, is required for the initiation of fracture healing.* Nat Genet, 2006. **38**(12): p. 1424-9.
26. Garrison KR, Shemilt I, Donell S, Ryder JJ, Mugford M, Harvey I, Song F, *Bone morphogenetic protein (BMP) for fracture healing in adults.* Cochrane Database ofSystematic Reviews, 2008(1).
27. Lissenberg-Thunnissen, S. N., de Gorter, D. J., Sier, C. F., and Schipper, I. B., *Use and efficacy of bone morphogenetic proteins in fracture healing.* Int Orthop, 2011. **35**(9): p. 1271-80.
28. Gillman, C. E. and Jayasuriya, A. C., *FDA-approved bone grafts and bone graft substitute devices in bone regeneration.* Mater Sci Eng C Mater Biol Appl, 2021. **130**: p. 112466.
29. Khalil, Andrew S., Yu, Xiaohua, Umhoefer, Jennifer M., Chamberlain, Connie S., Wildenauer, Linzie A., Diarra, Gaoussou M., Hacker, Timothy A., and Murphy, William L., *Single-dose mRNA therapy via biomaterial-mediated sequestration of overexpressed proteins.* Science Advances, 2020. **6**(27): p. eaba2422.
30. Shields, Lisa B. E., Raque, George H., Glassman, Steven D., Campbell, Mitchell, Vitaz, Todd, Harpring, John, and Shields, Christopher B., *Adverse Effects Associated With High-Dose Recombinant Human Bone Morphogenetic Protein-2 Use in Anterior Cervical Spine Fusion.* Spine, 2006. **31**(5): p. 542-547.
31. Durham, E. L., Howie, R. N., Hall, S., Larson, N., Oakes, B., Houck, R., Grey, Z., Steed, M., LaRue, A. C., Muise-Helmericks, R., and Cray, J., *Optimizing bone wound healing using BMP2 with absorbable collagen sponge and Talymed nanofiber scaffold.* J Transl Med, 2018. **16**(1): p. 321.
32. NE, Epstein, *Complications due to the use of BMP/INFUSE in spine surgery: The evidence continues to mount.* Surg Neurol Int., 2013. **4**(5): p. S343-352.
33. James, A. W., LaChaud, G., Shen, J., Asatrian, G., Nguyen, V., Zhang, X., Ting, K., and Soo, C., *A Review of the Clinical Side Effects of Bone Morphogenetic Protein-2.* Tissue Eng Part B Rev, 2016. **22**(4): p. 284-97.
34. Ramly, E. P., Alfonso, A. R., Kantar, R. S., Wang, M. M., Siso, J. R. D., Ibrahim, A., Coelho, P. G., and Flores, R. L., *Safety and Efficacy of Recombinant Human Bone Morphogenetic Protein-2 (rhBMP-2) in Craniofacial Surgery.* Plast Reconstr Surg Glob Open, 2019. **7**(8): p. e2347.
35. Simmonds, M., Brown, J., Heirs, M., Higgins, J., Mannion, R., Rodgers, M., Stewart, L., *Safety and Effectiveness of Recombinant Human Bone Morphogenetic Protein-2 for Spinal Fusion.* Annals of Internal Medicine, 2013(158): p. 877-889.

36. Liu, X. L., Li, C. C., Liu, K. J., Cui, C. Y., Zhang, Y. Z., and Liu, Y., *The influence of fluoride on the expression of inhibitors of Wnt/beta-catenin signaling pathway in rat skin fibroblast Cells.* Biol Trace Elem Res, 2012. **148**(1): p. 117-21.
37. Minear, S., Leucht, P., Jiang, J., Liu, B., Zeng, A., Fuerer, C., Nusse, R., and Helms, J. A., *Wnt proteins promote bone regeneration.* Sci Transl Med, 2010. **2**(29): p. 29ra30.
38. Xu, H., Duan, J., Ning, D., Li, J., Liu, R., Yang, R., Jiang, J. X., and Shang, P., *Role of Wnt signaling in fracture healing.* BMB Rep, 2014. **47**(12): p. 666-72.
39. Cadigan, K. M. and Liu, Y. I., *Wnt signaling: complexity at the surface.* J Cell Sci, 2006. **119**(Pt 3): p. 395-402.
40. Baron, R. and Rawadi, G., *Targeting the Wnt/beta-catenin pathway to regulate bone formation in the adult skeleton.* Endocrinology, 2007. **148**(6): p. 2635-43.
41. Krishnamurthy, N. and Kurzrock, R., *Targeting the Wnt/beta-catenin pathway in cancer: Update on effectors and inhibitors.* Cancer Treat Rev, 2018. **62**: p. 50-60.
42. Bhandari, M., Schemitsch, E. H., Karachalios, T., Sancheti, P., Poolman, R. W., Caminis, J., Daizadeh, N., Dent-Acosta, R. E., Egbuna, O., Chines, A., and Miclau, T., *Romosozumab in Skeletally Mature Adults with a Fresh Unilateral Tibial Diaphyseal Fracture: A Randomized Phase-2 Study.* J Bone Joint Surg Am, 2020. **102**(16): p. 1416-1426.
43. Song, D., He, G., Shi, Y., Ni, J., and Long, F., *Functional interaction between Wnt and Bmp signaling in periosteal bone growth.* Sci Rep, 2021. **11**(1): p. 10782.
44. Chen, Y., Whetstone, H. C., Youn, A., Nadesan, P., Chow, E. C., Lin, A. C., and Alman, B. A., *Beta-catenin signaling pathway is crucial for bone morphogenetic protein 2 to induce new bone formation.* J Biol Chem, 2007. **282**(1): p. 526-33.
45. McCarthy, T. L. and Centrella, M., *Novel links among Wnt and TGF-beta signaling and Runx2.* Mol Endocrinol, 2010. **24**(3): p. 587-97.
46. Ruan, Wendong, Xue, Yuan, Zong, Yaqi, and Sun, Chao, *Effect of BMPs and Wnt3a co-expression on the osteogenetic capacity of osteoblasts.* Mol Med Rep, 2016. **14**(5): p. 4328-4334.
47. Liu, D.D., Zhang, C.Y., Liu, Y., Li, J., Wang, Y.X., and Zheng, S.G., *RUNX2 Regulates Osteoblast Differentiation via the BMP4 Signaling Pathway.* Journal of Dental Research, 2022. **101**(10): p. 1227-1237.
48. Zhang, R., Oyajobi, B. O., Harris, S. E., Chen, D., Tsao, C., Deng, H. W., and Zhao, M., *Wnt/β-catenin signaling activates bone morphogenetic protein 2 expression in osteoblasts.* Bone, 2013. **52**(1): p. 145-56.
49. Su, Charles A., Vopat, Matthew L., Jildeh, Toufic R., Day, Hannah K., Philippon, Marc J., and Huard, Johnny, *Biologic Therapies in Orthopaedic Surgery.* Operative Techniques in Orthopaedics, 2022. **32**(2).
50. Zohra, F. T., Chowdhury, E. H., Tada, S., Hoshiba, T., and Akaike, T., *Effective delivery with enhanced translational activity synergistically accelerates mRNA-based transfection.* Biochem Biophys Res Commun, 2007. **358**(1): p. 373-8.
51. Sultana, N., Magadum, A., Hadas, Y., Kondrat, J., Singh, N., Youssef, E., Calderon, D., Chepurko, E., Dubois, N., Hajjar, R. J., and Zangi, L., *Optimizing Cardiac Delivery of Modified mRNA.* Mol Ther, 2017. **25**(6): p. 1306-1315.
52. Mockey, M., Goncalves, C., Dupuy, F. P., Lemoine, F. M., Pichon, C., and Midoux, P., *mRNA transfection of dendritic cells: synergistic effect of ARCA mRNA capping with Poly(A) chains in cis and in trans for a high protein expression level.* Biochem Biophys Res Commun, 2006. **340**(4): p. 1062-8.
53. Ramunas, J., Yakubov, E., Brady, J. J., Corbel, S. Y., Holbrook, C., Brandt, M., Stein, J., Santiago, J. G., Cooke, J. P., and Blau, H. M., *Transient delivery of modified mRNA encoding TERT rapidly extends telomeres in human cells.* FASEB J, 2015. **29**(5): p. 1930-9.
54. Mukherjee, S. and Thrasher, A. J., *Gene therapy for PIDs: progress, pitfalls and prospects.* Gene, 2013. **525**(2): p. 174-81.

55. Watson-Levings, R. S., Palmer, G. D., Levings, P. P., Dacanay, E. A., Evans, C. H., and Ghivizzani, S. C., *Gene Therapy in Orthopaedics: Progress and Challenges in Pre-Clinical Development and Translation.* Front Bioeng Biotechnol, 2022. **10**: p. 901317.
56. Shirley, J. L., de Jong, Y. P., Terhorst, C., and Herzog, R. W., *Immune Responses to Viral Gene Therapy Vectors.* Mol Ther, 2020. **28**(3): p. 709-722.
57. Altawalah, H., *Antibody Responses to Natural SARS-CoV-2 Infection or after COVID-19 Vaccination.* Vaccines (Basel), 2021. **9**(8).
58. Ward, H., Whitaker, M., Flower, B., Tang, S. N., Atchison, C., Darzi, A., Donnelly, C. A., Cann, A., Diggle, P. J., Ashby, D., Riley, S., Barclay, W. S., Elliott, P., and Cooke, G. S., *Population antibody responses following COVID-19 vaccination in 212,102 individuals.* Nat Commun, 2022. **13**(1): p. 907.
59. Evans, C. H., Ghivizzani, S. C., and Robbins, P. D., *Orthopaedic Gene Therapy: Twenty-Five Years On.* JBJS Rev, 2021. **9**(8).
60. Balmayor, E. R., Geiger, J. P., Aneja, M. K., Berezhanskyy, T., Utzinger, M., Mykhaylyk, O., Rudolph, C., and Plank, C., *Chemically modified RNA induces osteogenesis of stem cells and human tissue explants as well as accelerates bone healing in rats.* Biomaterials, 2016. **87**: p. 131-146.
61. Khorsand, B., Elangovan, S., Hong, L., Dewerth, A., Kormann, M. S., and Salem, A. K., *A Comparative Study of the Bone Regenerative Effect of Chemically Modified RNA Encoding BMP-2 or BMP-9.* Aaps j, 2017. **19**(2): p. 438-446.
62. De La Vega, Rodolfo E., van Griensven, Martijn, Zhang, Wen, Coenen, Michael J., Nagelli, Christopher V., Panos, Joseph A., Peniche Silva, Carlos J., Geiger, Johannes, Plank, Christian, Evans, Christopher H., and Balmayor, Elizabeth R., *Efficient healing of large osseous segmental defects using optimized chemically modified messenger RNA encoding BMP-2.* Science Advances. **8**(7): p. eabl6242.
63. Kowalski, P. S., Rudra, A., Miao, L., and Anderson, D. G., *Delivering the Messenger: Advances in Technologies for Therapeutic mRNA Delivery.* Mol Ther, 2019. **27**(4): p. 710-728.
64. Nitika, Wei, J., and Hui, A. M., *The Delivery of mRNA Vaccines for Therapeutics.* Life (Basel), 2022. **12**(8).
65. Nsairat, H., Khater, D., Sayed, U., Odeh, F., Al Bawab, A., and Alshaer, W., *Liposomes: structure, composition, types, and clinical applications.* Heliyon, 2022. **8**(5): p. e09394.
66. Lee, Kuo-Ming, Lin, Syh-Jae, Wu, Chung-Jung, and Kuo, Rei-Lin, *Race with virus evolution: The development and application of mRNA vaccines against SARS-CoV-2.* Biomedical Journal, 2023.
67. Tenchov, R., Bird, R., Curtze, A. E., and Zhou, Q., *Lipid Nanoparticles─From Liposomes to mRNA Vaccine Delivery, a Landscape of Research Diversity and Advancement.* ACS Nano, 2021. **15**(11): p. 16982-17015.
68. Rouge, Jessica, *RNA and nanocarriers: next generation drug and delivery platform take center stage.* Trends in Biotechnology, 2023.
69. Fontana, G., Martin, H. L., Lee, J. S., Schill, K., Hematti, P., and Murphy, W. L., *Mineral-Coated Microparticles Enhance mRNA-Based Transfection of Human Bone Marrow Cells.* Mol Ther Nucleic Acids, 2019. **18**: p. 455-464.
70. Choi, S. and Murphy, W. L., *Sustained plasmid DNA release from dissolving mineral coatings.* Acta Biomater, 2010. **6**(9): p. 3426-35.
71. Yu, X. and Murphy, W. L., *3-D Scaffold Platform for Optimized Non-viral Transfection of Multipotent Stem Cells.* J Mater Chem B, 2014. **2**(46): p. 8186-8193.
72. Alluri, R., Song, X., Bougioukli, S., Pannell, W., Vakhshori, V., Sugiyama, O., Tang, A., Park, S. H., Chen, Y., and Lieberman, J. R., *Regional gene therapy with 3D printed scaffolds to heal critical sized bone defects in a rat model.* J Biomed Mater Res A, 2019. **107**(10): p. 2174-2182.
73. Kang, H. P., Ihn, H., Robertson, D. M., Chen, X., Sugiyama, O., Tang, A., Hollis, R., Skorka, T., Longjohn, D., Oakes, D., Shah, R., Kohn, D., Jakus, A. E., and Lieberman, J. R., *Regional gene*

therapy for bone healing using a 3D printed scaffold in a rat femoral defect model. J Biomed Mater Res A, 2021. **109**(11): p. 2346-2356.

74. Khalil, Andrew S., Hellenbrand, Daniel, Reichl, Kaitlyn, Umhoefer, Jennifer, Filipp, Mallory, Choe, Joshua, Hanna, Amgad, and Murphy, William L., *A Localized Materials-Based Strategy to Non-Virally Deliver Chondroitinase ABC mRNA Improves Hindlimb Function in a Rat Spinal Cord Injury Model.* Advanced Healthcare Materials, 2022. **11**(19): p. 2200206.
75. Khalil, A. S., Yu, X., Xie, A. W., Fontana, G., Umhoefer, J. M., Johnson, H. J., Hookway, T. A., McDevitt, T. C., and Murphy, W. L., *Functionalization of microparticles with mineral coatings enhances non-viral transfection of primary human cells.* Sci Rep, 2017. **7**(1): p. 14211.
76. Dang, P. N., Dwivedi, N., Yu, X., Phillips, L., Bowerman, C., Murphy, W. L., and Alsberg, E., *Guiding Chondrogenesis and Osteogenesis with Mineral-Coated Hydroxyapatite and BMP-2 Incorporated within High-Density hMSC Aggregates for Bone Regeneration.* ACS Biomater Sci Eng, 2016. **2**(1): p. 30-42.
77. Khalil, A. S., Hellenbrand, D., Reichl, K., Umhoefer, J., Filipp, M., Choe, J., Hanna, A., and Murphy, W. L., *A Localized Materials-Based Strategy to Non-Virally Deliver Chondroitinase ABC mRNA Improves Hindlimb Function in a Rat Spinal Cord Injury Model.* Adv Healthc Mater, 2022. **11**(19): p. e2200206.

CHAPTER I: STRATEGIES TO ACTIVATE CANONICAL WNT[1]

I.1 Introduction

Three Wnt signaling pathways have been described: the canonical Wnt pathway (β-catenin-dependent) and two non-canonical (β-catenin-independent) pathways, including, the Wnt-Planar Cell Polarity (PCP) pathway and the Wnt/Ca2+ pathway.[1] The canonical Wnt pathway is a highly conserved pathway which plays a central role in tissue development, regeneration and serves as a key anabolic regulator of bone repair and homeostasis.[2-4] Canonical Wnt signaling modulates cytosolic transcription factor β-catenin to activate genes involved in osteoblast differentiation and bone matrix maintenance.[5, 6] Canonical Wnt pathway reduces osteoclast differentiation through secretion of osteoclast receptor antagonist, osteoprotegerin.[7, 8] While some studies have indicated that bone healing is also modulated by the non-canonical Wnt pathways, it is unknown if these pathways serve as positive or negative modulators.[6] Due to its established role in osteogenesis, activation of the canonical Wnt pathway is a promising approach to promote bone regeneration or accelerate bone healing.

A total of 19 Wnt ligands (secreted glycoproteins which activate Wnt) which target 10 different receptors in the frizzled (Fzd) protein family with multiple co-receptors required to activate a downstream response.[9, 10] Each Wnt ligand may stimulate different Wnt pathways depending on the receptor and co-receptor combination, yet there are several ligands strongly associated with canonical Wnt (Wnt1, Wnt3a).[9, 10] Wnt ligands undergo extensive post translational modifications with one of the most significant modifications to these proteins being lipidation. Due to canonical Wnt's involvement in stem cell maintenance, stem cells require an excess supply of the enzymes catalyzing fatty acylation.[1] In fact,

[1]This dissertation includes data from the published manuscript listed below. I have gained permission from all co-authors and publishers to use this work. Further, copies of all copyright permissions are in Appendix B of this document.

Nelson AL, Fontana G, Miclau E, Rongstad M, Murphy W, Huard J, Ehrhart N, Bahney C. Therapeutic approaches to activate the canonical Wnt pathway for bone regeneration. Journal of Tissue Engineering and Regenerative Medicine. 2022 Nov;16(11):961-76.

dysregulations in the fatty acyl chains of Wnts are associated with various embryonic developmental abnormalities.[11, 12] Lipid modifications serve to anchor the Wnt ligands to the ER membrane, prevent misfolding, regulate signal transduction and facilitate long range signaling.[1] While essential for function, the hydrophobic nature of the Wnt proteins makes them difficult to engineer and deliver therapeutically using conventional strategies.

The canonical Wnt pathway is stimulated through binding of a Wnt ligand to the Fzd receptor, a seven transmembrane-span receptor, and the low density lipoprotein receptor-related proteins (LRP5/6) co-receptor.[13-15] (**FIGURE 1A**) Once the ligand binds to the receptor complex, the cytoplasmic tail of the LRP5/6 co-receptor is phosphorylated, opening a binding site for Axin.[16, 17] This co-cluster of proteins (LRP5/6, frizzled and Dishevelled (Dsh/Dvl)) recruit Axin and GSK3 complex to form the destruction complex, which is key in regulating the stability of β-catenin.[18-20] Following Axin's recruitment, the destruction complex is disassembled and β-catenin enters the nucleus to stimulate transcription of targeted genes.[21, 22] Specifically, β-catenin modulates the TCF/LEF-1 family of transcription factors regulating multiple pathways associated with proliferation and differentiation.[23-25] Relative to bone formation, target genes that are activated upon stimulation of canonical Wnt include transcriptional cascade RUNX2 (runt-related transcription factor 2) and OSX (Osterix), which have been shown to transcribe osteoblast markers Collagen 1 (COL1), Osteopontin (OPN), Osteocalcin (OCN) and Alkaline phosphatase (ALP).[26] In the absence of Wnt ligands, β-catenin is phosphorylated and sent to the proteosome for proteolytic degradation.[27, 28]

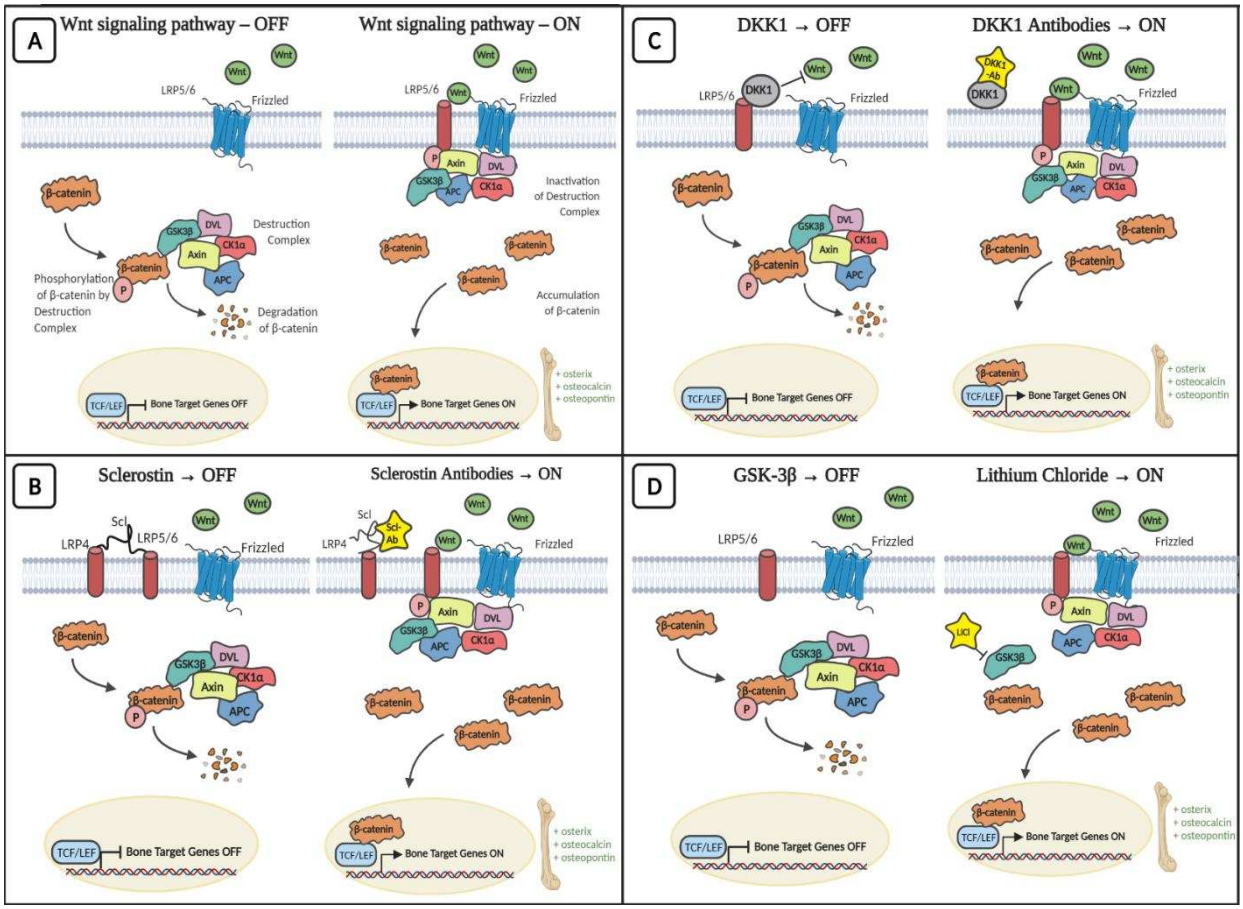

Figure 1. Schematic of the canonical Wnt signaling pathway and mechanistic approaches of how various bioactive agents target the canonical Wnt pathway. ***A)*** *In the absence of Wnt ligands, beta-catenin is phosphorylated, triggering ubiquitination by the destruction complex. In the presence of Wnt ligands, destruction complex disassembles. This allows for beta-catenin to accumulate in the cytoplasm and translocate to the nucleus, stimulating transcription of target genes.* ***B)*** *Antibodies targeting Sclerostin, an inhibitor of Wnt, allow for Wnt ligands to bind and activate the pathway.* ***C)*** *Dkk1 binds to the LRP receptor inhibiting Wnt ligands from activating the pathway. Antibodies specific to Dkk1 allow for Wnt ligands to bind to the LRP receptor and stimulate the pathway.* ***D)*** *Lithium Chloride, an inhibitor of GSK-3β, facilitates disassembly of the destruction complex.*

β-catenin also serves as an important role in cell adhesion as it is an integral structural component of cadherin-based adherens junctions. Following synthesis of β-catenin, membrane-bound β-catenin colocalizes with the LRP6 receptor which further acts as a transcriptional regulator.[29, 30] Sequentially, membrane-bound β-catenin is then recruited as a component of adherens junctions, which interact with actin cytoskeleton and regulate cell-cell adhesions.[30, 31] As β-catenin plays dual functional roles in cell signaling and cell adhesion, coordination between these two roles may be required.[32] The location of

β-catenin has reported to depend on tissue type and stiffness of tissue.[33] Specifically in bone, β-catenin plays a significant role in signaling and activation of canonical Wnt transcription cascade as opposed to cell adhesion.[34]

Given the canonical Wnt pathway's central role in promoting bone formation, it is an attractive therapeutic target for bone regeneration.[35-37] However, there are several challenges associated with therapeutic activation of the Wnt pathway, predominantly with the lipid modifications of Wnt ligands that make isolating and purifying the protein difficult and expensive.[35, 38] Currently available clinical interventions target the inhibitors of the canonical Wnt pathway in age-related diseases, such as osteoporosis and cancer.[39, 40] Although there is more recent evidence that demonstrates an antibody-based treatment modality can improve bone formation[41], this review highlights a broader range of strategies to activate the canonical Wnt pathway using engineering approaches.

Dysregulation within the canonical Wnt signaling pathway has been associated with various age-related conditions. Age-associated aberrations within Wnt/β-catenin signaling pathway are tissue dependent. For example, an increase in Wnt/β-catenin signaling has been associated with age-related pathology of muscle, specifically sarcopenia.[42] Conversely, a decrease in Wnt/β-catenin signaling is correlated with age-related disorders of bone, such as osteoporosis.[43] Dysregulation of Wnt signaling pathways in age-related diseases will need to be further studied to understand effects of systemic and local Wnt activation therapies across the lifespan in order to elucidate best practices for clinical use.

I.2 WNT Activating Therapeutics

In terms of specificity and therapeutic potential, protein delivery is typically superior to small molecule drugs. However, proteins have low stability in physiological environments.[44] For this reason, therapeutic efficacy in protein delivery is usually achieved by delivering supraphysiological doses of proteins, causing several side-effects.[45] This hampers the clinical translation of protein delivery and is the main reason why the vast majority of FDA-approved drugs for clinical use are small molecule drugs

instead.[46] Moreover, specific to the Wnt pathway, since the ligand is lipidated, unmodified therapeutic delivery of this protein is ineffective. As such, alternative approaches have been tested to achieve targeted activation of canonical Wnt signaling. Re-purposing some of these compounds to target the Wnt pathway could accelerate clinical translation. In this section, we discuss bioactive agents which have been used in pre-clinical and clinical studies to activate Wnt and stimulate bone regeneration. In the following section, we assess tissue engineering strategies to deliver these bioactive agents.

I.2.1 Sclerostin Antibodies

Sclerostin is a well-defined inhibitor of the canonical Wnt signaling pathway. Sclerostin is a small glycoprotein transcribed from the SOST gene secreted by osteocytes. Sclerostin binds to the LRP5/6 co-receptor on the cell surface of osteoblasts preventing association with the Frz receptor and thereby inhibiting canonical Wnt pathway activation (**FIGURE 1B**).[19, 47] Sclerostin antibodies activate canonical Wnt signaling by inhibiting the inhibitor of the Wnt pathway to enhance bone formation and are one of the most translational strategies to date. Their use has been shown in several preclinical and clinical studies for the treatment of osteoporosis and is elegantly reviewed by Clarke.[47-54]

Romosozumab (EVENITY™) is an FDA-approved monoclonal antibody that inhibits sclerostin. EVENITY™ is approved for the treatment of severe osteoporosis in postmenopausal women at high risk of fracture in 37 countries, including the U.S., Japan, and Canada.[49] The approved EVENITY™ dose is 210 mg administered subcutaneously once a month for 12 months. In addition to a systemic effect in osteoporosis, the sclerostin antibody has also been tested as a bioactive approach to improve fracture healing. As recently reviewed, most preclinical studies suggest that systemic administration of EVENITY™ enhances bone formation and may accelerate fracture healing.[55-57] Based on these pre-clinical successes, an international, Phase-2, randomized and placebo-controlled clinical trial tested the efficacy of EVENITY™ on fracture patients with open reduction and internal fixation of intertrochanteric or femoral neck hip fractures. No significant differences were found in the median time to radiographic evidence of fracture healing between EVENITY™ and placebo treated groups.[58] Similarly, in a study

evaluating the effect of EVENITY™ on tibial diaphyseal fractures, radiographic evaluation after 6 months revealed no significant differences in the time to radiographic and clinical healing between treatment groups.[59] EVENITY™ is considered an osteoanabolic treatment yet it has been reported to only have transient effects on increasing bone formation.[60] Thus, it has been proposed that the therapeutic efficacy derives from its anti-resorptive properties, which result in decreased bone turnover rate and an increase in bone density.[60] Taken together, these data suggest systemic delivery of sclerostin antibodies are effective in building bone to treat osteoporosis, but this therapeutic approach is not effective for bone repair applications.

I.2.2 Other Antibody-based Approaches to Modulate Wnt

Based on the translational success of EVENITY™, multiple other antibodies to Wnt pathway inhibitors have been tested for treating osteoporosis or as a fracture healing therapeutic. Here, we focus on summarizing data utilizing these antibodies for bone repair. One approach utilizes an antibody to Dickkopf-related protein 1 (Dkk1), which, like sclerostin, is a soluble protein that binds to LRP5/LRP6 co-receptor to inhibit canonical Wnt signaling (**FIGURE 1C**). As Dkk1 overexpressing mice are characterized with osteopenia, preclinical models have shown that the inhibition of Dkk1 with anti-Dkk1 antibodies has increased bone mass.[61, 62] Other studies analyzing levels of Dkk1 in cells surrounding a fracture callus report elevated levels in human nonunion fractures.[63] To test the use of anti-Dkk1 antibodies as a potential anabolic agent in fracture healing, murine fracture models were treated with anti-Dkk1 antibodies and showed radiographic evidence of enhanced callus formation.[64] Dkk1 treatment appears to necessitate a critical window for administration to enhance fracture healing, with studies showing that treatment is not effective unless started immediately post-fracture.[65] Importantly, osteoanabolic effects of Dkk1-inhibition through treatment with anti-Dkk1 antibodies only results in bone formation when Sclerostin is deactivated.[66] Using this information, groups have tested therapeutic potential using combinatorial treatments of Wnt inhibitors, Dkk1 and Sclerostin.[67] Choi *et al.* determined significantly enhanced therapeutic efficacy using this dual antibody treatment on cancellous bone, but not for cortical bone.[67]

Additional approaches for targeting Wnt/β-catenin pathway inhibitors using antibody-based therapeutics include targeting the growth factor midkine or secreted frizzled-receptor 1 (sFRP1). Antagonizing midkine, which targets LRP family of receptors, has helped accelerate fracture healing in mice by increasing bone volume density, bone formation, and osteoblast activity.[68, 69] However, more research is needed to determine whether midkine represents a viable bioactive target to enhance fracture healing. sFRP1 is a glycoprotein that negatively modulates Wnt signaling through binding and inhibition of Wnt ligands.[3] Mice deficient in sFRP1 resulted in slower age-related bone loss and decreased apoptosis in osteoblasts.[70, 71] sFRP1 antagonists could serve as an additional therapeutic target for osteoporosis and its ability to mitigate its progression is currently being studied preclinically.[72] Additionally, it has been reported that the loss of sFRP1 expression improves fracture healing *in vivo*.[37, 73] While antibody-based therapeutics show promising results in increasing bone mass, further tests on the dosing, timing, and route of delivery of these antibodies for fracture repair need to be executed in both pre-clinical and clinical studies.

The four R-spondin proteins, derived from roof-plate specific spondin (Rspo) gene, are implicated in various biological functions including skeletal repair.[74, 75] Within the last decade, there have been several breakthroughs in R-spondin signaling and stimulation of canonical Wnt pathway activation.[75-77] Specifically, several groups reported that R-spondins amplify Wnt activation when co-delivered with Wnt ligands.[76, 78] The mechanism of how R-spondins synergistically activate the canonical Wnt pathway has yet to be elucidated, yet it is generally thought that R-spondins do not bind directly with Fzd receptor.[78, 79] Despite limited mechanistic details, many groups show that R-spondins synergistically stimulate bone repair through enhanced osteoblast differentiation following treatment with R-spondin1 and Wnt3a *in vitro*.[80-82] Additionally, R-spondin1 disrupted osteoclast expansion, reduced bone erosion, and enhanced cartilage integrity following intraarticular injections into an osteoarthritic mouse model.[83] R-spondin2 has also been shown to promote osteoblastogenesis during skeletal repair by modulating BMP signaling.[84, 85] Despite these published roles in potentiating Wnt activity, fundamental details addressing

R-spondins role in activating canonical Wnt and bone repair are still needed to effectively harness its therapeutic potential.[79, 86]

I.2.3 Synthetic Wnts

Recent interest has been geared towards developing surrogate Wnt ligands for the activation of canonical Wnt pathway.[87, 88] Janda *et al.* generated synthetic Wnt surrogates to be non-lipidated, water-soluble Wnt ligands which induce Fzd-LRP5/6 receptor heterodimerization, identified as a key molecular regulator for canonical Wnt pathway activation. Treatment of synthetic Wnt surrogates resulted in accumulation of nuclear β-catenin and upregulation of ALP, suggesting activation of canonical Wnt, in a murine hepatomegaly model.[88] Despite these advances in generating synthetic Wnt surrogates, many groups have questioned the surrogate specificity for activating the Fzd pathway since Wnt ligands are cross-reactive for multiple receptors.[89] To combat this selectivity concern, Tao *et al.* has developed tetravalent synthetic antibodies specific for any Fzd receptor. Further, they reported that activation of both binding sites within LRP6 resulted in greater intracellular signaling.[89] Future directions in synthetic Wnt development entail elucidating the specific mechanisms involved in Wnt receptor activation and determining the therapeutic capacity of synthetic Wnts for bone repair applications.

I.2.4 Lithium Chloride

In addition to extracellular modulation of the Wnt pathway with antibodies to Wnt inhibitors, Wnt pathway activation can be modulated at the intracellular level by targeting the destruction complex. Lithium is a chemical element that has been compounded with salts and given orally as a psychoactive medication to treat bipolar disorder by increasing mTOR phosphorylation.[90, 91] Dysregulation of mTOR pathway has been found in patients who suffer from bipolar disorder and once mTOR signaling is activated, the production of synaptic proteins and inhibition of autophagy result in nerve growth and synaptic transmission.[92] Interestingly, the pleiotropic effects from lithium was shown through its change in patient bone mineral density and was subsequently discovered that lithium activates canonical Wnt signaling.

Lithium specifically inhibits GSK-3β in the destruction complex, enabling β-catenin to stimulate Wnt-responsive genes (**FIGURE 1D**).[93, 94] Numerous preclinical studies confirm that lithium has significantly enhanced fracture healing by improving bone mass, volume, and formation when administered several days after fracture.[95] Due to its success preclinically, a double blind, randomized controlled clinical trial has begun evaluating the clinical efficacy of lithium treatment in long-bone fractures, but have yet to report any conclusions.[96]

I.2.5 Fluoride

Fluoride is the ion of the highly reactive element fluorine and it can influence the Wnt signaling pathway by inhibiting the destruction complex.[97, 98] Specifically, fluoride stimulates phosphorylation of Akt and GSK-3β, thereby blocking activity of the destruction complex and increasing nuclear localization of β-catenin.[98] Additionally, exposure to fluoride was shown to decrease the secretion of other inhibitors of the WNT pathway, such as Dkk-1 and SOST, in a time and concentration-dependent manner.[35] In murine models, fluoride increased the enzymatic activity of alkaline phosphatase and decreased activity of osteoclast-derived serum tartrate-resistant acid phosphatase (TRAP), indicating enhanced osteoblastic differentiation and reduced bone resorption.[99] However, fluoride has displayed adverse effects, including potentially dangerous levels of toxicity and decreased gene expression levels of bone morphogenetic protein 2 (BMP-2) and type I collagen (COL1A1) when treated at high doses.[97, 99] Additionally, fluoride has been shown to have pleiotropic effects and it has been characterized to suppress mTOR pathway, significantly downregulating mTOR related genes, inhibiting cell proliferation and increasing autophagy when delivered at high doses.[100, 101] While fluoride demonstrates a promising approach to enhancing bone formation both *in vitro* and *in vivo*, there has been no published research evaluating its effects on fracture repair.[97]

I.2.6 Strontium

It has been found that strontium can substitute calcium in bone, increasing bone formation.[102] Mechanistically, strontium substitution serves as an osteoanabolic by promoting osteoblastic differentiation[103] and proliferation,[104] increasing ALP activity,[105, 106] promoting angiogenesis[107], and increasing calcium deposition[108] and mineralization.[109, 110] Strontium also enhances osteoblast activity through calcium-sensing receptors (CaSRs) which activate the Ras/MAPK signaling pathway and trigger cell replication.[111] Furthermore, strontium acts directly on the Wnt pathway by decreasing the expression of sclerostin[112] and increasing the expression of Wnt11 and Wnt3a.[113, 114] Independent studies have demonstrated links between strontium and the Wnt pathway, showing that strontium-induced osteogenesis were managed by the canonical Wnt pathway through regulation of sFRP1 and DKK1.[113, 115] Strontium ranelate (StRan), PROTELOS®, is a newly-approved drug for lowering the risk of vertebral fracture in postmenopausal women. In addition to treating osteoporosis, preclinical studies have shown that StRan can promote bone repair by accelerating osteogenesis and improving bone formation in a calvarial defect.[50] Similarly, in an ovariectomized rat model of osteoporotic fractures, two months of treatment with StRan increased bone volume within the fracture callus[107] and improved callus strength.[116] While clinical trials of StRan report its efficacy in reducing the risk of new vertebral fractures in postmenopausal women, no clinical data has shown a benefit in fracture repair.[117]

I.2.7 Other Wnt modifiers

Several other families of Wnt modulators have recently been determined to antagonize and deactivate Wnt proteins, such as Tiki, while other modulators serve as an agonist of canonical Wnt pathway, like Porcupine. Tiki proteins have been found to act as metalloproteases by cleaving and deactivating Wnt ligands.[118] These glycosylphosphatidylinositol-anchored proteins (GPI-Aps) are localized to the plasma-membrane through the GPI moiety and inhibit canonical Wnt ligands.[119] Porcupine is another protein which post-translationally modifies Wnt proteins through catalyzing their lipidation, imperative for Wnt

ligand secretion.[120] Specifically, both Wnt1 and Wnt3a have been found to be lipidated through porcupine, promoting their Wnt activity.[121] While these proteins have been implicated in the canonical Wnt pathway, few studies have determined their therapeutic efficacy in bone repair. As porcupine inhibitors have been studied for use as a cancer treatment, Funck-Brentano *et al.* examined potential adverse effects on bone health finding deleterious amounts of bone loss and bone resorption.[122, 123]

I.3 Tissue Engineering Strategies to Achieve Delivery

The two main obstacles that drug delivery strategies must overcome to ensure therapeutic efficacy are: (i) the stability of the cargo and (ii) targeting the area of interest. While some of the molecular modulators of the Wnt pathway discussed above have demonstrated pharmaceutical benefits for treatment of osteoporosis (e.g. increased bone density following EVENITY™ treatment), few of these modulators have been tested in fracture repair. Although systemic approaches are often simple, the non-selective nature of their delivery results in variable concentrations delivered to the region of interest. As an example, the systemic delivery of strontium ranelate without proper targeting strategies results in biodistribution of less than 1% of the drug to the bone.[45] Due to the vast nature of cellular responses in which Wnt plays a role, systemic administration of bioactive agents targeting Wnt to enhance bone formation poses the risk of off-target effects.[40] For example, lithium has been shown to enhance bone mass through the inhibition of GSK-3β enzymes, but studies now reveal that its long-term usage is associated with elevated incidence ratios of renal cancer.[124] Even sclerostin monoclonal antibodies, like the newly approved EVENITY™, have reported adverse events such as injection-site erythema, hemorrhage, headaches, and arthralgia.[125] While these therapies can be further designed to circumvent adverse events, side effects are an inherent risk with systemic delivery.

To circumvent the limitations associated with systemic delivery, including poor biodistribution and aberrant side effects, there is a need to engineer more effective approaches to activate the Wnt pathway at a local level. An overview of the potential applications for systemic versus localized Wnt-activation strategies can be found in **FIGURE 2**.[126] Localized delivery of a bioactive agent involves integrating the

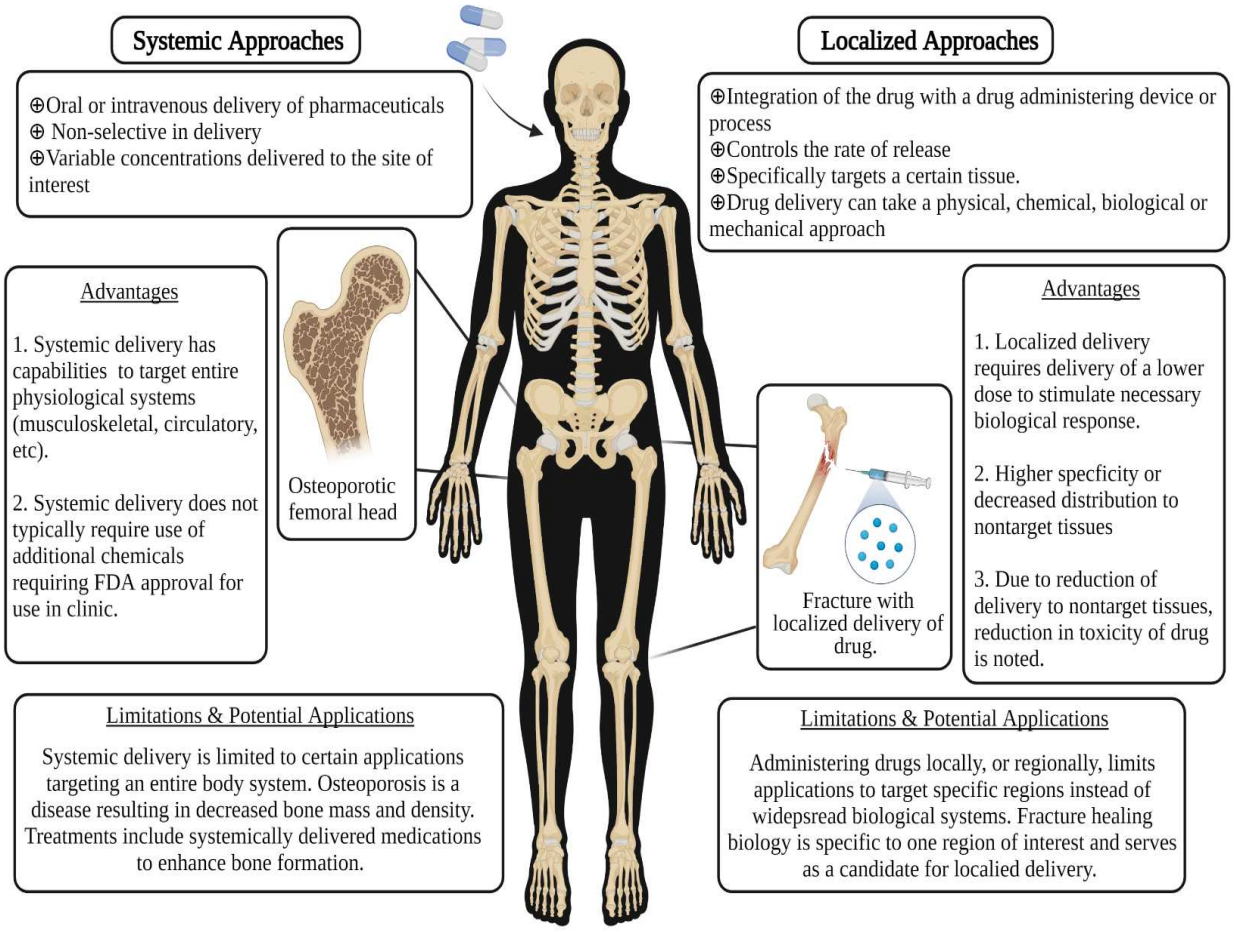

Figure 2. Clinical overview of systemic versus localized drug or small molecule delivery approaches.[126]

drug with a drug administering device or process to control the rate of release and target a specific tissue type. Various approaches have been used to activate canonical Wnt pathway locally, including embedding bioactive agent into a delivery carrier, using bioactive agents as a dopant for scaffolds, or incorporating them in hydrogel platforms. A schematic of these tissue engineered approaches to deliver Wnt-activating therapeutics is shown in **FIGURE 3**. While these approaches have been successful *in vitro* and *in vivo* applications, they have yet to be translated to the clinic. This section highlights local approaches for targeting canonical Wnt pathway.

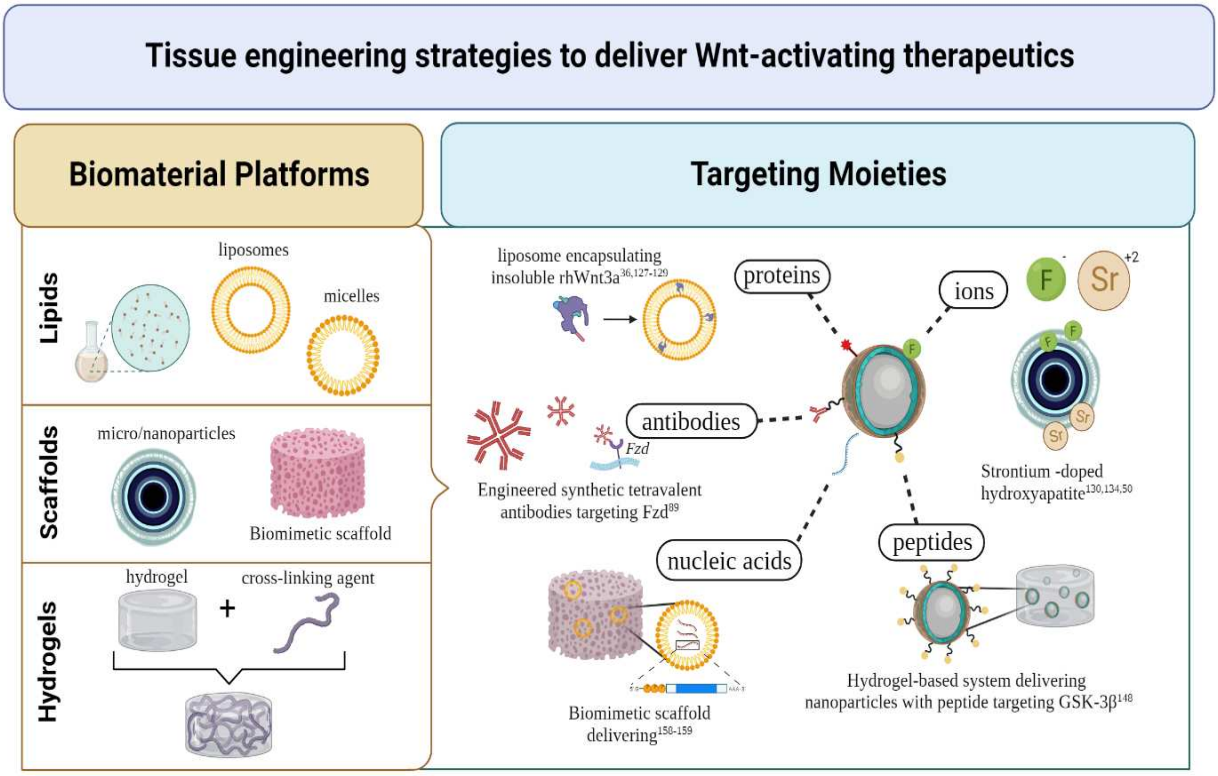

Figure 3. Tissue engineering strategies to achieve delivery of Wnt-activating therapeutics. *Localized, engineered approaches frequently involve the use of biomaterial platforms to deliver targeted therapeutics. This schematic depicts tissue engineering strategies integrating biomaterial platforms and targeting moieties which are reviewed in this manuscript.*

I.3.1 Liposomes

The most direct pathway to locally activate canonical Wnt signaling would be through delivery of the ligand. Lipid nanoparticles, inspired by the lipid bilayer of liposomes, can be an effective delivery vehicle to circumvent the limitations of delivering hydrophobic Wnt proteins. Liposomal Wnt-ligand therapies serve as a promising clinically translatable approach due to its preclinical successes.[127, 128] In one embodiment, Chen *et al*. sought to transiently activate Wnt in murine bone grafts by adding a liposomal Wnt3a formulation.[129] Following treatment, the cells in the bone graft showed elevated Wnt signaling, increased cell proliferation and reduced apoptosis, resulting in three-fold increase in bone formation as compared to bone grafts alone.[129] Similarly, other studies have reported that liposomal Wnt delivery injected into skeletal defects enhanced bone regeneration three times more than the control.[36] Leucht *et*

al. has highlighted the therapeutic potential for transiently upregulating canonical Wnt in patients with reduced skeletal healing potential, such as an aged demographic.[36, 127]

I.3.2 Scaffold Dopants

A promising approach to deliver ions is to use them as a dopant in biomaterials. This approach enables the local delivery of small Wnt-activating ions, such as strontium or fluoride, while utilizing the biomaterial scaffold to interact with the adjacent tissues. Mineralization of biomaterials, typically through the addition of synthetic hydroxyapatite or calcium phosphate, is a common procedure used to increase scaffold strength and promote osseointegration with the surrounding microenvironment.[130-135] Moreover, mineralization of metal-based implants obtained through coating with hydroxyapatite or bioglass was found to alleviate inflammation caused by the corrosion of the implant.[136]

Strontium is one of the most used dopants in mineralized biomaterials and strontium-doped biomaterials consistently promote improved osteogenic effects *in vitro* and *in vivo*.[107, 137, 138] For example, strontium-doped hydroxyapatite induced osteogenic differentiation of MSCs through upregulation of β-catenin expression to produce new bone formation both *in vitro* and *in vivo*.[50, 134, 136] Based on the successes of these strontium-doped hydroxyapatite systems, Kavitha *et al.* has studied the synthesis parameters of strontium doped hydroxyapatite powder for the purpose of scaling up the process to maintain desired powder characteristics and optimal strontium concentrations to fabricate in bulk.[130] Similarly, bioactive borate glass cement containing strontium was also found to enhance osteogenesis *in vivo* and *in vitro* models.[136] Another strontium containing cement comprised of calcium phosphate was reported to have new bone formation and enhanced osseointegration at the bone-implant area of the cements *in vivo* as compared to the strontium-free bone cements.[139, 140] While there only a few published studies for the use of strontium-doped materials *in vivo*, they have promising results for the treatment of osteoporotic-related fractures.[141]

As with strontium, biomaterials can be doped with fluoride to enhance osteogenesis. Cooper *et al.* studied fluoride's capabilities in accentuating osseointegration of sandblasted titanium implants.[142] They

found that fluoride modified titanium implants resulted in increased osteoblast differentiation capacity *in vitro* and twice as much bone formation on the implant *in vivo*.[143] Hydroxyapatite scaffolds have also been engineered to release fluoride ions at a controlled rate, increasing proliferation and osteogenesis of MC3T3 cells *in vitro*.[143] Similarly, titanium containing fluoride-doped phosphate nanobioglasses enhanced osteogenesis *in vitro* resulting in higher amounts of bone formation *in vivo*.[144]

I.3.3 Hydrogels

Hydrogels, networks of hydrophilic polymers, have been used in a large number of studies to target bone repair as they can be absorbable, integrated with adjacent tissues and do not require surgical removal.[145, 146] Hydrogels can be synthesized from natural or synthetic materials and have a wide range of applications due to their flexibility and potential for injectability.[147] Many studies have employed hydrogel systems to deliver growth factors and/or cells for the promotion of bone regeneration, but few have used this approach specifically to activate Wnt signaling.[145, 146, 148] Alaohali *et al.* used a hyaluronic acid-based hydrogel to deliver a GSK-3 inhibitor to promote bone formation in dental applications.[148] In this application, the hydrogel was injected into a murine molar defect, crosslinked using UV light to facilitate drug encapsulation, and the drug was control released through degradation, stimulating dentine formation.[148] Similarly, Wang *et al.* utilized a hydrogel-based system to deliver bone targeting nanoparticles with a peptide targeting GSK-3β, showing that fracture healing was accelerated in a murine fracture model.[149] Other groups utilized a thermo-responsive hydrogel platform as a scalable, cost-effective strategy to enhance the production of Wnt3a protein.[150]

I.4 Future Directions

There remains an unmet clinical need developing strategies to activate the canonical Wnt pathway in bone repair and bone regeneration. Emerging technologies, such as mRNA-based therapeutics, have had exciting developments leading to clinical translation. However, few of these technologies have been applied

to activating canonical Wnt pathway or fracture healing. We postulate that mRNA based approaches could successfully circumvent the limitations reported with other Wnt-activating therapeutics.

I.4.1 mRNA Delivery

Delivery of mRNA is an attractive new bioactive approach as it does not require genomic integration.[151, 152] Protein expression through mRNA delivery is sustained for a limited time which is ideal to stimulate bone formation and minimize adverse events for application to fracture healing.[153] Until recently, the use of mRNA as a therapeutic has been limited due to challenges associated with mRNA stability, cytotoxicity of the delivery platform, and induction of innate inflammation.[151, 154-156] New technology to mitigate these undesirable effects through modification of mRNA constructs and delivery platforms has recently led to the successful mRNA COVID-19 vaccines.[46, 157] Recent work pioneering mRNA therapies to promote bone regeneration through coding for BMP2/9 has shown promise, yet all studies use a biomimetic scaffold which requires surgical implantation.[158, 159] One attractive locally injectable alternative would be to use microparticles as an injectable delivery vehicle for therapeutic mRNA. Recent studies have shown that delivering mRNA via mineral-coated microparticles increased transfection and cell survival *in vitro*[160] and *in vivo*.[161] Using mRNA-based approaches to target the Wnt pathway will circumvent the solubility challenges encountered when delivering Wnt proteins and capitalize on the endogenous cellular machinery to add the post-translational modifications essential to ligand function.

I.4.2 CRISPR Gene Editing

As with mRNA strategies, gene editing technology has vast potential in tissue engineering. The newest of the genome editing technologies, CRISPR/Cas9, has accelerated translation from bench to clinic. Many groups have proposed various methods for leveraging this technology for the regeneration of bone, yet this approach has yet to be fully explored. While CRISPR genome editing has been used to develop osteoporotic murine models[162-164], several investigators are currently exploring the therapeutic capacity

of using CRISPR technology in therapies. The most current clinically effective CRISPR-Cas9 applications involve genetic engineering of cells *ex vivo*. One group recently used CRISPR/Cas9 and single guide RNAs (sgRNAs) as a platform to restore the expression of type I collagen to combat osteogenesis imperfecta, a genetic disorder characterized by bone fragility and repeat fractures.[165] Another group has employed CRISPR technology to engineer stem cells as an alternative therapeutic approach to combat osteoarthritis.[166] Brunger *et al.* engineered stem cells to maintain resistance towards IL-1-induced degradation and inflammation. This approach implies that when cells are inserted in diseased or injured tissues the host inflammatory response may compromise the therapeutic potential of the implant. Importantly, *ex vivo* CRISPR gene therapy has now moved into human clinical trials as an immunotherapy treatment and these trials will help to establish safety and efficacy of this technology.[167-169]

The RNA targeting CRISPR-Cas technologies may be the most promising *in vivo* therapeutic approach for bone repair and/or trauma. The RNA-targeting Cas9 platform (RCas9) works by cleaving ssDNA strands, and can also be designed to specifically target RNA sequences using sgRNAs.[170, 171] Therapies aiming to reduce expression of toxic or potentially lethal RNAs have been employed in patient cells *ex vivo*.[172] While RCas9 shows promise in treating nongenetic derived injuries, it has yet to be employed for use in bone repair but could be possibly be used to silence inhibitors of Wnt/β-catenin.

Despite the most clinically effective CRISPR-Cas9 applications involving genetic engineering of cells *ex vivo*, the first human clinical trials using *in vivo* genome editing have recently been performed to treat various genetic diseases.[173, 174] Further studies utilizing *in vivo* CRISPR technologies need to establish a robust safety profile of the developed therapies and their capacity in acquiring off-target effects in order to employ *in vivo* technologies using CRISPR-based platforms.[166, 170]

I.5 Conclusions

While the canonical Wnt signaling proves to be a complex pathway to target therapeutically, this review presents promising engineering approaches to circumvent limitations in activating Wnt specifically for bone regeneration. First, we reviewed Wnt-activating therapeutics designed to stimulate canonical Wnt

when delivered systemically. Systemic delivery of bioactive agents requires targeting the entire skeletal system, limiting the clinical application to diseases like osteoporosis. We subsequently discussed strategies to deliver bioactive molecules and ions locally, which may be a preferable strategy for bone regeneration and fracture repair applications. Local delivery approaches, including liposomes, scaffold doping, and hydrogel-based systems show promise, but these strategies have not yet been translated clinically. In addition to these approaches, several emerging methods should be considered as novel strategies to activate the canonical Wnt pathway.

I.6 References

1. Hosseini, V., Dani, C., Geranmayeh, M. H., Mohammadzadeh, F., Nazari Soltan Ahmad, S., and Darabi, M., *Wnt lipidation: Roles in trafficking, modulation, and function.* J Cell Physiol, 2019. **234**(6): p. 8040-8054.
2. Kirstetter, P., Anderson, K., Porse, B. T., Jacobsen, S. E., and Nerlov, C., *Activation of the canonical Wnt pathway leads to loss of hematopoietic stem cell repopulation and multilineage differentiation block.* Nat Immunol, 2006. **7**(10): p. 1048-56.
3. Komiya, Y. and Habas, R., *Wnt signal transduction pathways.* Organogenesis, 2008. **4**(2): p. 68-75.
4. Wang, J. and Wynshaw-Boris, A., *The canonical Wnt pathway in early mammalian embryogenesis and stem cell maintenance/differentiation.* Curr Opin Genet Dev, 2004. **14**(5): p. 533-9.
5. Manolagas, S. C., *Wnt signaling and osteoporosis.* Maturitas, 2014. **78**(3): p. 233-7.
6. Schupbach, D., Comeau-Gauthier, M., Harvey, E., and Merle, G., *Wnt modulation in bone healing.* Bone, 2020. **138**: p. 115491.
7. Lacey DL, Timms E, Tan HL, Kelley MJ, Dunstan CR, Burgess T, Elliott R, Colombero A, Elliott G, Scully S, Hsu H, Sullivan J, Hawkins N, Davy E, Capparelli C, Eli A, Qian YX, Kaufman S, Sarosi I, Shalhoub V, Senaldi G, Guo J, Delaney J, Boyle WJ., *Osteoprotegerin Ligand Is a Cytokine that Regulates Osteoclast Differentiation and Activation.* Cell, 1998. **93**(2): p. 165-176.
8. Yasuda, H., Shima, N., Nakagawa, N., Yamaguchi, K., Kinosaki, M., Mochizuki, S., Tomoyasu, A., Yano, K., Goto, M., Murakami, A., Tsuda, E., Morinaga, T., Higashio, K., Udagawa, N., Takahashi, N., and Suda, T., *Osteoclast differentiation factor is a ligand for osteoprotegerin/osteoclastogenesis-inhibitory factor and is identical to TRANCE/RANKL.* Proc Natl Acad Sci U S A, 1998. **95**(7): p. 3597-602.
9. Siman-Tov, R., Zelikson, N., Caspi, M., Levi, Y., Perry, C., Khair, F., Stauber, H., Sznitman, J., and Rosin-Arbesfeld, R., *Circulating Wnt Ligands Activate the Wnt Signaling Pathway in Mature Erythrocytes.* Arterioscler Thromb Vasc Biol, 2021. **41**(5): p. e243-e264.
10. Kim, J. H., Liu, X., Wang, J., Chen, X., Zhang, H., Kim, S. H., Cui, J., Li, R., Zhang, W., Kong, Y., Zhang, J., Shui, W., Lamplot, J., Rogers, M. R., Zhao, C., Wang, N., Rajan, P., Tomal, J., Statz, J., Wu, N., Luu, H. H., Haydon, R. C., and He, T. C., *Wnt signaling in bone formation and its therapeutic potential for bone diseases.* Ther Adv Musculoskelet Dis, 2013. **5**(1): p. 13-31.
11. Ng, L. F., Kaur, P., Bunnag, N., Suresh, J., Sung, I. C. H., Tan, Q. H., Gruber, J., and Tolwinski, N. S., *WNT Signaling in Disease.* Cells, 2019. **8**(8).
12. Nile, A. H. and Hannoush, R. N., *Fatty acylation of Wnt proteins.* Nat Chem Biol, 2016. **12**(2): p. 60-9.
13. Andreas Wodarz and Nusse, Roel, *MECHANISMS OF WNT SIGNALING IN DEVELOPMENT.* Cell Dev. Biol., 1998. **14**: p. 59-88.
14. Brown, S. D., Twells, R. C., Hey, P. J., Cox, R. D., Levy, E. R., Soderman, A. R., Metzker, M. L., Caskey, C. T., Todd, J. A., and Hess, J. F., *Isolation and characterization of LRP6, a novel member of the low density lipoprotein receptor gene family.* Biochem Biophys Res Commun, 1998. **248**(3): p. 879-88.
15. Kato, M., Patel, M. S., Levasseur, R., Lobov, I., Chang, B. H., Glass, D. A., 2nd, Hartmann, C., Li, L., Hwang, T. H., Brayton, C. F., Lang, R. A., Karsenty, G., and Chan, L., *Cbfa1-independent decrease in osteoblast proliferation, osteopenia, and persistent embryonic eye vascularization in mice deficient in Lrp5, a Wnt coreceptor.* J Cell Biol, 2002. **157**(2): p. 303-14.
16. Tamai, K., Zeng, X., Liu, C., Zhang, X., Harada, Y., Chang, Z., & He, X., *A Mechanism for Wnt Coreceptor Activation.* Molecular Cell, 2004. **13**(1): p. 149-156.

17. Zeng, X., Tamai, K., Doble, B., Li, S., Huang, H., Habas, R., Okamura, H., Woodgett, J., and He, X., *A dual-kinase mechanism for Wnt co-receptor phosphorylation and activation.* Nature, 2005. **438**(7069): p. 873-7.
18. Rana Dajani, Elizabeth Fraser, S.Mark Roe, Maggie Yeo, Valerie M.Good, Vivienne Thompson, Trevor C.Dale and Laurence H.Pearl, *Structural basis for recruitment of glycogen synthase kinase 3˜ to the axin±APC scaffold complex.* The EMBO Journal, 2003. **22**(3): p. 494-501.
19. He, X., Semenov, M., Tamai, K., and Zeng, X., *LDL receptor-related proteins 5 and 6 in Wnt/beta-catenin signaling: arrows point the way.* Development, 2004. **131**(8): p. 1663-77.
20. Mao J, Wang J, Liu B, Pan W, Farr GH 3rd, Flynn C, Yuan H, Takada S, Kimelman D, Li L, Wu D., *Low-Density Lipoprotein Receptor-Related Protein-5 Binds to Axin and Regulates the Canonical Wnt Signaling Pathway.* Molecular Cell, 2001. **7**(4): p. 801-809.
21. Satoshi Ikeda, Michiko Kishida, Yoshiharu Matsuura, Usui, Hirofumi, and Kikuchi, Akira, *GSK-3b-dependent phosphorylation of adenomatous polyposis coli gene product can be modulated by b-catenin and protein phosphatase 2A complexed with Axin.* Oncogene, 2000. **19**: p. 537-545.
22. Xing, Y., Clements, W. K., Kimelman, D., and Xu, W., *Crystal structure of a beta-catenin/axin complex suggests a mechanism for the beta-catenin destruction complex.* Genes Dev, 2003. **17**(22): p. 2753-64.
23. Tolwinski, N. S. and Wieschaus, E., *A nuclear function for armadillo/beta-catenin.* PLoS Biol, 2004. **2**(4): p. E95.
24. Bienz, M. and Clevers, H., *Armadillo/beta-catenin signals in the nucleus--proof beyond a reasonable doubt?* Nat Cell Biol, 2003. **5**(3): p. 179-82.
25. Cong, F., Schweizer, L., Chamorro, M., and Varmus, H., *Requirement for a nuclear function of beta-catenin in Wnt signaling.* Mol Cell Biol, 2003. **23**(23): p. 8462-70.
26. Felber, K., Elks, P. M., Lecca, M., and Roehl, H. H., *Expression of osterix Is Regulated by FGF and Wnt/β-Catenin Signalling during Osteoblast Differentiation.* PLoS One, 2015. **10**(12): p. e0144982.
27. Hermann Aberle, Andreas Bauer, Jorg Stappert, Kispert, Andreas, and Kemler, Rolf, *β-catenin is a target for the ubiquitin–proteasome pathway.* EMBO Journal, 1997. **16**(13): p. 3797–3804.
28. Orford, K., Crockett, C., Jensen, J. P., Weissman, A. M., and Byers, S. W., *Serine phosphorylation-regulated ubiquitination and degradation of beta-catenin.* J Biol Chem, 1997. **272**(40): p. 24735-8.
29. Hendriksen, Jolita, Jansen, Marnix, Brown, Carolyn M., van der Velde, Hella, van Ham, Marco, Galjart, Niels, Offerhaus, G. Johan, Fagotto, Francois, and Fornerod, Maarten, *Plasma membrane recruitment of dephosphorylated β-catenin upon activation of the Wnt pathway.* Journal of Cell Science, 2008. **121**(11): p. 1793-1802.
30. Azbazdar, Y., Karabicici, M., Erdal, E., and Ozhan, G., *Regulation of Wnt Signaling Pathways at the Plasma Membrane and Their Misregulation in Cancer.* Front Cell Dev Biol, 2021. **9**: p. 631623.
31. Brembeck, F. H., Rosário, M., and Birchmeier, W., *Balancing cell adhesion and Wnt signaling, the key role of beta-catenin.* Curr Opin Genet Dev, 2006. **16**(1): p. 51-9.
32. Bienz, M., *beta-Catenin: a pivot between cell adhesion and Wnt signalling.* Curr Biol, 2005. **15**(2): p. R64-7.
33. Amit, Chatterjee, Padmanabhan, Prema, and Narayanan, Janakiraman, *Deciphering the mechanoresponsive role of β-catenin in Keratoconus epithelium.* bioRxiv, 2019: p. 603738.
34. Santarelli, A., Colella, G., Carinci, F., Pannone, G., Rubini, R., Lo Russo, L., Polimeni, A., Sgaramella, N., Annibali, S., Spinelli, G., and Lo Muzio, L., *Expression of β-Catenin and γ-Catenin in Maxillary Bone Regeneration.* International Journal of Immunopathology and Pharmacology, 2011. **24**(2_suppl): p. 107-111.
35. Liu, X. L., Li, C. C., Liu, K. J., Cui, C. Y., Zhang, Y. Z., and Liu, Y., *The influence of fluoride on the expression of inhibitors of Wnt/beta-catenin signaling pathway in rat skin fibroblast Cells.* Biol Trace Elem Res, 2012. **148**(1): p. 117-21.

36. Minear, S., Leucht, P., Jiang, J., Liu, B., Zeng, A., Fuerer, C., Nusse, R., and Helms, J. A., *Wnt proteins promote bone regeneration.* Sci Transl Med, 2010. **2**(29): p. 29ra30.
37. Xu, H., Duan, J., Ning, D., Li, J., Liu, R., Yang, R., Jiang, J. X., and Shang, P., *Role of Wnt signaling in fracture healing.* BMB Rep, 2014. **47**(12): p. 666-72.
38. Cadigan, K. M. and Liu, Y. I., *Wnt signaling: complexity at the surface.* J Cell Sci, 2006. **119**(Pt 3): p. 395-402.
39. Baron, R. and Rawadi, G., *Targeting the Wnt/beta-catenin pathway to regulate bone formation in the adult skeleton.* Endocrinology, 2007. **148**(6): p. 2635-43.
40. Krishnamurthy, N. and Kurzrock, R., *Targeting the Wnt/beta-catenin pathway in cancer: Update on effectors and inhibitors.* Cancer Treat Rev, 2018. **62**: p. 50-60.
41. Haffner-Luntzer, M., *Experimental agents to improve fracture healing: utilizing the WNT signaling pathway.* Injury, 2021. **52 Suppl 2**: p. S44-S48.
42. Andrew S. Brack, Michael J. Conboy, Sudeep Roy, Mark Lee, Calvin J. Kuo, Charles Keller, and Rando, Thomas A., *Increased Wnt Signaling During Aging Alters Muscle Stem Cell Fate and Increases Fibrosis.* Science, 2007. **317**: p. 807-810.
43. Shun-ichi Harada and Rodan, Gideon A., *Control of osteoblast function and regulation of bone mass.* Nature, 2003. **423**: p. 349-355.
44. Boraiah, S., Paul, O., Hawkes, D., Wickham, M., and Lorich, D. G., *Complications of recombinant human BMP-2 for treating complex tibial plateau fractures: a preliminary report.* Clin Orthop Relat Res, 2009. **467**(12): p. 3257-62.
45. Yuchen Wang, Maureen R. Newman, and Benoit, Danielle S.W., *Development of Controlled Drug Delivery Systems for Bone Fracture-Targeted Therapeutic Delivery: A Review.* Eur J Pharm Biopharm, 2018. **127**: p. 223-236.
46. Pilishvili, T., Gierke, R., Fleming-Dutra, K. E., Farrar, J. L., Mohr, N. M., Talan, D. A., Krishnadasan, A., Harland, K. K., Smithline, H. A., Hou, P. C., Lee, L. C., Lim, S. C., Moran, G. J., Krebs, E., Steele, M. T., Beiser, D. G., Faine, B., Haran, J. P., Nandi, U., Schrading, W. A., Chinnock, B., Henning, D. J., Lovecchio, F., Lee, J., Barter, D., Brackney, M., Fridkin, S. K., Marceaux-Galli, K., Lim, S., Phipps, E. C., Dumyati, G., Pierce, R., Markus, T. M., Anderson, D. J., Debes, A. K., Lin, M. Y., Mayer, J., Kwon, J. H., Safdar, N., Fischer, M., Singleton, R., Chea, N., Magill, S. S., Verani, J. R., Schrag, S. J., and Vaccine Effectiveness among Healthcare Personnel Study, Team, *Effectiveness of mRNA Covid-19 Vaccine among U.S. Health Care Personnel.* N Engl J Med, 2021. **385**(25): p. e90.
47. Li, X., Zhang, Y., Kang, H., Liu, W., Liu, P., Zhang, J., Harris, S. E., and Wu, D., *Sclerostin binds to LRP5/6 and antagonizes canonical Wnt signaling.* J Biol Chem, 2005. **280**(20): p. 19883-7.
48. Clarke, B. L., *Anti-sclerostin antibodies: utility in treatment of osteoporosis.* Maturitas, 2014. **78**(3): p. 199-204.
49. Markham, A., *Romosozumab: First Global Approval.* Drugs, 2019. **79**(4): p. 471-476.
50. Yang, F., Yang, D., Tu, J., Zheng, Q., Cai, L., and Wang, L., *Strontium enhances osteogenic differentiation of mesenchymal stem cells and in vivo bone formation by activating Wnt/catenin signaling.* Stem Cells, 2011. **29**(6): p. 981-91.
51. McClung, M. R., Grauer, A., Boonen, S., Bolognese, M. A., Brown, J. P., Diez-Perez, A., Langdahl, B. L., Reginster, J. Y., Zanchetta, J. R., Wasserman, S. M., Katz, L., Maddox, J., Yang, Y. C., Libanati, C., and Bone, H. G., *Romosozumab in postmenopausal women with low bone mineral density.* N Engl J Med, 2014. **370**(5): p. 412-20.
52. Becker, C. B., *Sclerostin inhibition for osteoporosis--a new approach.* N Engl J Med, 2014. **370**(5): p. 476-7.
53. Ominsky, M. S., Boyd, S. K., Varela, A., Jolette, J., Felx, M., Doyle, N., Mellal, N., Smith, S. Y., Locher, K., Buntich, S., Pyrah, I., and Boyce, R. W., *Romosozumab Improves Bone Mass and Strength While Maintaining Bone Quality in Ovariectomized Cynomolgus Monkeys.* J Bone Miner Res, 2017. **32**(4): p. 788-801.

54. Li, X., Ominsky, M. S., Warmington, K. S., Morony, S., Gong, J., Cao, J., Gao, Y., Shalhoub, V., Tipton, B., Haldankar, R., Chen, Q., Winters, A., Boone, T., Geng, Z., Niu, Q. T., Ke, H. Z., Kostenuik, P. J., Simonet, W. S., Lacey, D. L., and Paszty, C., *Sclerostin antibody treatment increases bone formation, bone mass, and bone strength in a rat model of postmenopausal osteoporosis.* J Bone Miner Res, 2009. **24**(4): p. 578-88.
55. Alaee, F., Virk, M. S., Tang, H., Sugiyama, O., Adams, D. J., Stolina, M., Dwyer, D., Ominsky, M. S., Ke, H. Z., and Lieberman, J. R., *Evaluation of the effects of systemic treatment with a sclerostin neutralizing antibody on bone repair in a rat femoral defect model.* J Orthop Res, 2014. **32**(2): p. 197-203.
56. Ke, H. Z., Richards, W. G., Li, X., and Ominsky, M. S., *Sclerostin and Dickkopf-1 as therapeutic targets in bone diseases.* Endocr Rev, 2012. **33**(5): p. 747-83.
57. Cui, L., Cheng, H., Song, C., Li, C., Simonet, W. S., Ke, H. Z., and Li, G., *Time-dependent effects of sclerostin antibody on a mouse fracture healing model.* J Musculoskelet Neuronal Interact, 2013. **13**(2): p. 178-84.
58. Schemitsch, E. H., Miclau, T., Karachalios, T., Nowak, L. L., Sancheti, P., Poolman, R. W., Caminis, J., Daizadeh, N., Dent-Acosta, R. E., Egbuna, O., Chines, A., Maddox, J., Grauer, A., and Bhandari, M., *A Randomized, Placebo-Controlled Study of Romosozumab for the Treatment of Hip Fractures.* J Bone Joint Surg Am, 2020. **102**(8): p. 693-702.
59. Bhandari, M., Schemitsch, E. H., Karachalios, T., Sancheti, P., Poolman, R. W., Caminis, J., Daizadeh, N., Dent-Acosta, R. E., Egbuna, O., Chines, A., and Miclau, T., *Romosozumab in Skeletally Mature Adults with a Fresh Unilateral Tibial Diaphyseal Fracture: A Randomized Phase-2 Study.* J Bone Joint Surg Am, 2020. **102**(16): p. 1416-1426.
60. Chavassieux, P., Chapurlat, R., Portero-Muzy, N., Roux, J. P., Garcia, P., Brown, J. P., Libanati, C., Boyce, R. W., Wang, A., and Grauer, A., *Bone-Forming and Antiresorptive Effects of Romosozumab in Postmenopausal Women With Osteoporosis: Bone Histomorphometry and Microcomputed Tomography Analysis After 2 and 12 Months of Treatment.* J Bone Miner Res, 2019. **34**(9): p. 1597-1608.
61. Pinzone, J. J., Hall, B. M., Thudi, N. K., Vonau, M., Qiang, Y. W., Rosol, T. J., and Shaughnessy, J. D., Jr., *The role of Dickkopf-1 in bone development, homeostasis, and disease.* Blood, 2009. **113**(3): p. 517-25.
62. Yaccoby, S., Ling, W., Zhan, F., Walker, R., Barlogie, B., and Shaughnessy, J. D., Jr., *Antibody-based inhibition of DKK1 suppresses tumor-induced bone resorption and multiple myeloma growth in vivo.* Blood, 2007. **109**(5): p. 2106-11.
63. Jin, H., Wang, B., Li, J., Xie, W., Mao, Q., Li, S., Dong, F., Sun, Y., Ke, H. Z., Babij, P., Tong, P., and Chen, D., *Anti-DKK1 antibody promotes bone fracture healing through activation of β-catenin signaling.* Bone, 2015. **71**: p. 63-75.
64. Bajada, S., Marshall, M. J., Wright, K. T., Richardson, J. B., and Johnson, W. E., *Decreased osteogenesis, increased cell senescence and elevated Dickkopf-1 secretion in human fracture non union stromal cells.* Bone, 2009. **45**(4): p. 726-35.
65. Komatsu, D. E., Mary, M. N., Schroeder, R. J., Robling, A. G., Turner, C. H., and Warden, S. J., *Modulation of Wnt signaling influences fracture repair.* J Orthop Res, 2010. **28**(7): p. 928-36.
66. Witcher, P. C., Miner, S. E., Horan, D. J., Bullock, W. A., Lim, K. E., Kang, K. S., Adaniya, A. L., Ross, R. D., Loots, G. G., and Robling, A. G., *Sclerostin neutralization unleashes the osteoanabolic effects of Dkk1 inhibition.* JCI Insight, 2018. **3**(11).
67. Choi, R. B., Bullock, W. A., Hoggatt, A. M., Loots, G. G., Genetos, D. C., and Robling, A. G., *Improving Bone Health by Optimizing the Anabolic Action of Wnt Inhibitor Multitargeting.* JBMR Plus, 2021. **5**(5): p. e10462.
68. Haffner-Luntzer, M., Heilmann, A., Rapp, A. E., Roessler, R., Schinke, T., Amling, M., Ignatius, A., and Liedert, A., *Antagonizing midkine accelerates fracture healing in mice by enhanced bone formation in the fracture callus.* Br J Pharmacol, 2016. **173**(14): p. 2237-49.

69. Liedert, A., Schinke, T., Ignatius, A., and Amling, M., *The role of midkine in skeletal remodelling.* Br J Pharmacol, 2014. **171**(4): p. 870-8.
70. Ohnaka, K., Yamamoto, K., Nakamura, K., Adachi, M., Kawate, H., Kono, S., and Takayanagi, R., *Association of single nucleotide polymorphisms in secreted frizzled-related protein 1 gene with bone mineral density in Japanese women.* Geriatr Gerontol Int, 2009. **9**(3): p. 304-9.
71. Yao, W., Cheng, Z., Shahnazari, M., Dai, W., Johnson, M. L., and Lane, N. E., *Overexpression of secreted frizzled-related protein 1 inhibits bone formation and attenuates parathyroid hormone bone anabolic effects.* J Bone Miner Res, 2010. **25**(2): p. 190-9.
72. Bodine, P. V., Stauffer, B., Ponce-de-Leon, H., Bhat, R. A., Mangine, A., Seestaller-Wehr, L. M., Moran, R. A., Billiard, J., Fukayama, S., Komm, B. S., Pitts, K., Krishnamurthy, G., Gopalsamy, A., Shi, M., Kern, J. C., Commons, T. J., Woodworth, R. P., Wilson, M. A., Welmaker, G. S., Trybulski, E. J., and Moore, W. J., *A small molecule inhibitor of the Wnt antagonist secreted frizzled-related protein-1 stimulates bone formation.* Bone, 2009. **44**(6): p. 1063-8.
73. Gaur, T., Wixted, J. J., Hussain, S., O'Connell, S. L., Morgan, E. F., Ayers, D. C., Komm, B. S., Bodine, P. V., Stein, G. S., and Lian, J. B., *Secreted frizzled related protein 1 is a target to improve fracture healing.* J Cell Physiol, 2009. **220**(1): p. 174-81.
74. Kamata, T., Katsube, K., Michikawa, M., Yamada, M., Takada, S., and Mizusawa, H., *R-spondin, a novel gene with thrombospondin type 1 domain, was expressed in the dorsal neural tube and affected in Wnts mutants.* Biochim Biophys Acta, 2004. **1676**(1): p. 51-62.
75. Kazanskaya, O., Glinka, A., del Barco Barrantes, I., Stannek, P., Niehrs, C., and Wu, W., *R-Spondin2 is a secreted activator of Wnt/beta-catenin signaling and is required for Xenopus myogenesis.* Dev Cell, 2004. **7**(4): p. 525-34.
76. Binnerts, M.E., Kim, K.A., Bright, J.M., Patel, S.M., Tran, K., Zhou, M., Leung, J.M., Liu, Y., Lomas III, W.E., Dixon, M., Hazell, S.A., *R-Spondin1 regulates Wnt signaling by inhibiting internalization of LRP6.* PNAS, 2007. **104**(37): p. 14700–14705.
77. Nam, J. S., Turcotte, T. J., Smith, P. F., Choi, S., and Yoon, J. K., *Mouse cristin/R-spondin family proteins are novel ligands for the Frizzled 8 and LRP6 receptors and activate beta-catenin-dependent gene expression.* J Biol Chem, 2006. **281**(19): p. 13247-13257.
78. Wei, Q., Yokota, C., Semenov, M. V., Doble, B., Woodgett, J., and He, X., *R-spondin1 is a high affinity ligand for LRP6 and induces LRP6 phosphorylation and beta-catenin signaling.* J Biol Chem, 2007. **282**(21): p. 15903-11.
79. Jin, Y. R. and Yoon, J. K., *The R-spondin family of proteins: emerging regulators of WNT signaling.* Int J Biochem Cell Biol, 2012. **44**(12): p. 2278-87.
80. Lu, W., Kim, K. A., Liu, J., Abo, A., Feng, X., Cao, X., and Li, Y., *R-spondin1 synergizes with Wnt3A in inducing osteoblast differentiation and osteoprotegerin expression.* FEBS Lett, 2008. **582**(5): p. 643-50.
81. Nagano, K., *R-spondin signaling as a pivotal regulator of tissue development and homeostasis.* Jpn Dent Sci Rev, 2019. **55**(1): p. 80-87.
82. Sharma, A. R., Choi, B. S., Park, J. M., Lee, D. H., Lee, J. E., Kim, H. S., Yoon, J. K., Song, D. K., Nam, J. S., and Lee, S. S., *Rspo 1 promotes osteoblast differentiation via Wnt signaling pathway.* Indian J Biochem Biophys, 2013. **50**(1): p. 19-25.
83. Kronke, G., Uderhardt, S., Kim, K. A., Stock, M., Scholtysek, C., Zaiss, M. M., Surmann-Schmitt, C., Luther, J., Katzenbeisser, J., David, J. P., Abdollahi-Roodsaz, S., Tran, K., Bright, J. M., Binnerts, M. E., Akhmetshina, A., Bohm, C., Distler, J. H., Joosten, L. A., Schett, G., and Abo, A., *R-spondin 1 protects against inflammatory bone damage during murine arthritis by modulating the Wnt pathway.* Arthritis Rheum, 2010. **62**(8): p. 2303-12.
84. Friedman, M. S., Oyserman, S. M., and Hankenson, K. D., *Wnt11 promotes osteoblast maturation and mineralization through R-spondin 2.* J Biol Chem, 2009. **284**(21): p. 14117-25.
85. Knight, M. N., Karuppaiah, K., Lowe, M., Mohanty, S., Zondervan, R. L., Bell, S., Ahn, J., and Hankenson, K. D., *R-spondin-2 is a Wnt agonist that regulates osteoblast activity and bone mass.* Bone Res, 2018. **6**: p. 24.

86. Knight, M. N. and Hankenson, K. D., *R-spondins: novel matricellular regulators of the skeleton.* Matrix Biol, 2014. **37**: p. 157-61.
87. Chen, H., Lu, C., Ouyang, B., Zhang, H., Huang, Z., Bhatia, D., Lee, S. J., Shah, D., Sura, A., Yeh, W. C., and Li, Y., *Development of Potent, Selective Surrogate WNT Molecules and Their Application in Defining Frizzled Requirements.* Cell Chem Biol, 2020. **27**(5): p. 598-609 e4.
88. Janda, C. Y., Dang, L. T., You, C., Chang, J., de Lau, W., Zhong, Z. A., Yan, K. S., Marecic, O., Siepe, D., Li, X., Moody, J. D., Williams, B. O., Clevers, H., Piehler, J., Baker, D., Kuo, C. J., and Garcia, K. C., *Surrogate Wnt agonists that phenocopy canonical Wnt and beta-catenin signalling.* Nature, 2017. **545**(7653): p. 234-237.
89. Tao, Y., Mis, M., Blazer, L., Ustav, M. Jnr, Steinhart, Z., Chidiac, R., Kubarakos, E., O'Brien, S., Wang, X., Jarvik, N., Patel, N., Adams, J., Moffat, J., Angers, S., and Sidhu, S. S., *Tailored tetravalent antibodies potently and specifically activate Wnt/Frizzled pathways in cells, organoids and mice.* Elife, 2019. **8**.
90. Xiao, Y., Fan, M., Jin, W., Li, W. A., Jia, Y., Dong, Y., Jiang, X., Xu, J., Meng, N., and Lv, P., *Lithium chloride ameliorated spatial cognitive impairment through activating mTOR phosphorylation and inhibiting excessive autophagy in the repeated cerebral ischemia-reperfusion mouse model.* Exp Ther Med, 2020. **20**(5): p. 109.
91. O'Connell, R. A., Mayo, J. A., Flatow, L., Cuthbertson, B., and O'Brien, B. E., *Outcome of bipolar disorder on long-term treatment with lithium.* Br J Psychiatry, 1991. **159**: p. 123-9.
92. Park, S. W., Seo, M. K., Webster, M. J., Lee, J. G., and Kim, S., *Differential expression of gene co-expression networks related to the mTOR signaling pathway in bipolar disorder.* Transl Psychiatry, 2022. **12**(1): p. 184.
93. Philippe Clement-Lacroix, Minrong Ai, Frederic Morvan, Sergio Roman-Roman, Be´ atrice Vayssie` re, Cecille Belleville, Kenneth Estrera, Matthew L. Warman, Roland Baron, and Rawadi, and Georges, *Lrp5-independent activation of Wnt signaling by lithium chloride increases bone formation and bone mass in mice.* PNAS, 2005. **102**(48): p. 17406–17411.
94. Klein, P. S. and Melton, D. A., *A molecular mechanism for the effect of lithium on development.* Proc Natl Acad Sci U S A, 1996. **93**(16): p. 8455-9.
95. Chen, Y., Whetstone, H. C., Lin, A. C., Nadesan, P., Wei, Q., Poon, R., and Alman, B. A., *Beta-catenin signaling plays a disparate role in different phases of fracture repair: implications for therapy to improve bone healing.* PLoS Med, 2007. **4**(7): p. e249.
96. Nam, D., Balasuberamaniam, P., Milner, K., Kunz, M., Vachhani, K., Kiss, A., and Whyne, C., *Lithium for Fracture Treatment (LiFT): a double-blind randomised control trial protocol.* BMJ Open, 2020. **10**(1): p. e031545.
97. Grynpas, Marc D., Chachra, Debbie, and Limeback, Hardy, *The action of fluoride on bone*, in *The Osteoporosis Primer*. 2000. p. 318-330.
98. Pan, L., Shi, X., Liu, S., Guo, X., Zhao, M., Cai, R., and Sun, G., *Fluoride promotes osteoblastic differentiation through canonical Wnt/beta-catenin signaling pathway.* Toxicol Lett, 2014. **225**(1): p. 34-42.
99. Li, Yan-yan, Bian, Shengtai, Wang, Jinming, and Wanga, Jundong. *EFFECTS OF FLUORIDE AND CHITOSAN ON THE GENE EXPRESSIONS OF BONE MORPHOGENIC PROTEIN 2 AND COLLAGEN TYPE-1 ALPHA 1 CHAIN IN THE MOUSE FEMUR*. 2014.
100. Kuang, , Ping, Deng, , Huidan, Huan Liu, Cui, , Hengmin, Jing Fang, Zhicai Zuo, Junliang Deng, Yinglun Li, Xun Wang, and Zhao, Ling, *Sodium fluoride induces splenocyte autophagy via the mammalian targets of rapamycin (mTOR) signaling pathway in growing mice.* Aging, 2018. **10**(7).
101. Ma, L., Zhang, R., Li, D., Qiao, T., and Guo, X., *Fluoride regulates chondrocyte proliferation and autophagy via PI3K/AKT/mTOR signaling pathway.* Chem Biol Interact, 2021. **349**: p. 109659.

102. J. BUEHLER, P. CHAPPUIS, J.L. SAFFAR, Y. TSOUDEROS, and VIGNERY, A., *Strontium Ranelate Inhibits Bone Resorption While Maintaining Bone Formation in Alveolar Bone in Monkeys (Macaca fascicularis).* Bone, 2001. **29**(2): p. 176-179.
103. Stefanic, M., Peroglio, M., Stanciuc, A. M., Machado, G. C., Campbell, I., Kržmanc, M. Maček, Alini, M., and Zhang, X., *The influence of strontium release rate from bioactive phosphate glasses on osteogenic differentiation of human mesenchymal stem cells.* Journal of the European Ceramic Society, 2018. **38**(3): p. 887-897.
104. Jun, Wu, Peng, Wang, Dianming, Jiang, Hong, Li, Cong, Luo, Xing, Liu, Xiangyang, Qu, Yujiang, Cao, and Ming, Li, *In vitroandin vivocharacterization of strontium-containing calcium sulfate/poly(amino acid) composite as a novel bioactive graft for bone regeneration.* RSC Advances, 2017. **7**(86): p. 54306-54312.
105. Khan, P. K., Mahato, A., Kundu, B., Nandi, S. K., Mukherjee, P., Datta, S., Sarkar, S., Mukherjee, J., Nath, S., Balla, V. K., and Mandal, C., *Influence of single and binary doping of strontium and lithium on in vivo biological properties of bioactive glass scaffolds.* Sci Rep, 2016. **6**: p. 32964.
106. Moghanian, Amirhossein, Firoozi, Sadegh, and Tahriri, Mohammadreza, *Characterization, in vitro bioactivity and biological studies of sol-gel synthesized SrO substituted 58S bioactive glass.* Ceramics International, 2017. **43**(17): p. 14880-14890.
107. Al Qaysi, M., Walters, N. J., Foroutan, F., Owens, G. J., Kim, H. W., Shah, R., and Knowles, J. C., *Strontium- and calcium-containing, titanium-stabilised phosphate-based glasses with prolonged degradation for orthopaedic tissue engineering.* J Biomater Appl, 2015. **30**(3): p. 300-10.
108. Su, W. T., Wu, P. S., and Huang, T. Y., *Osteogenic differentiation of stem cells from human exfoliated deciduous teeth on poly(epsilon-caprolactone) nanofibers containing strontium phosphate.* Mater Sci Eng C Mater Biol Appl, 2015. **46**: p. 427-34.
109. Ehret, C., Aid-Launais, R., Sagardoy, T., Siadous, R., Bareille, R., Rey, S., Pechev, S., Etienne, L., Kalisky, J., de Mones, E., Letourneur, D., and Amedee Vilamitjana, J., *Strontium-doped hydroxyapatite polysaccharide materials effect on ectopic bone formation.* PLoS One, 2017. **12**(9): p. e0184663.
110. Sato, M., Chen, P., Tsutsumi, Y., Shiota, M., Hanawa, T., and Kasugai, S., *Effect of strontium ions on calcification of preosteoblasts cultured on porous calcium- and phosphate-containing titanium oxide layers formed by micro-arc oxidation.* Dent Mater J, 2016. **35**(4): p. 627-34.
111. Songlin Peng, Guangqian Zhou, Keith D.K. Luk, Kenneth M.C Cheung, Zhaoyang Li, Wing Moon Lam, Zhongjun Zhou, and Lu, William W., *Strontium Promotes Osteogenic Differentiation of Mesenchymal Stem Cells Through the Ras/MAPK Signaling Pathway.* Cellular Physiology and Biochemistry, 2009. **23**: p. 165-174.
112. Rybchyn, M. S., Slater, M., Conigrave, A. D., and Mason, R. S., *An Akt-dependent increase in canonical Wnt signaling and a decrease in sclerostin protein levels are involved in strontium ranelate-induced osteogenic effects in human osteoblasts.* J Biol Chem, 2011. **286**(27): p. 23771-9.
113. Fromigue, O., Hay, E., Barbara, A., and Marie, P. J., *Essential role of nuclear factor of activated T cells (NFAT)-mediated Wnt signaling in osteoblast differentiation induced by strontium ranelate.* J Biol Chem, 2010. **285**(33): p. 25251-8.
114. Saidak, Z. and Marie, P. J., *Strontium signaling: molecular mechanisms and therapeutic implications in osteoporosis.* Pharmacol Ther, 2012. **136**(2): p. 216-26.
115. Wang, B., Guo, H., Geng, T., Sun, K., Zhang, L., Lu, Z., and Jin, Q., *The effect of strontium ranelate on titanium particle-induced periprosthetic osteolysis regulated by WNT/beta-catenin signaling in vivo and in vitro.* Biosci Rep, 2021. **41**(1).
116. Habermann, B., Kafchitsas, K., Olender, G., Augat, P., and Kurth, A., *Strontium ranelate enhances callus strength more than PTH 1-34 in an osteoporotic rat model of fracture healing.* Calcif Tissue Int, 2010. **86**(1): p. 82-9.

117. Emma D. Deeks and Dhillon, Sohita, *Spotlight on Strontium Ranelate: In Postmenopausal Osteoporosis*, in *Drugs Aging*. 2010. p. 771-773.
118. Zhang, X., MacDonald, B. T., Gao, H., Shamashkin, M., Coyle, A. J., Martinez, R. V., and He, X., *Characterization of Tiki, a New Family of Wnt-specific Metalloproteases.* J Biol Chem, 2016. **291**(5): p. 2435-43.
119. Li, M., Zheng, J., He, X., and Zhang, X., *Tiki proteins are glycosylphosphatidylinositol-anchored proteases.* FEBS Lett, 2022. **596**(8): p. 1037-1046.
120. Proffitt, K. D. and Virshup, D. M., *Precise regulation of porcupine activity is required for physiological Wnt signaling.* J Biol Chem, 2012. **287**(41): p. 34167-78.
121. Galli, L. M., Barnes, T. L., Secrest, S. S., Kadowaki, T., and Burrus, L. W., *Porcupine-mediated lipid-modification regulates the activity and distribution of Wnt proteins in the chick neural tube.* Development, 2007. **134**(18): p. 3339-48.
122. Funck-Brentano, T., Nilsson, K. H., Brommage, R., Henning, P., Lerner, U. H., Koskela, A., Tuukkanen, J., Cohen-Solal, M., Moverare-Skrtic, S., and Ohlsson, C., *Porcupine inhibitors impair trabecular and cortical bone mass and strength in mice.* J Endocrinol, 2018. **238**(1): p. 13-23.
123. Hsuan Lung, Tania Moody, Kelly Wentworth, Misun Kang, Sunita Ho, and Hsiao, Edward, *Global Wnt Inhibition With a Porcupine Inhibitor Decreases Established Trabecular Bone in a Mouse Model of Fibrous Dysplasia.* Journal of the Endocrine Society 2022: p. 234.
124. Kahn, M., *Can we safely target the WNT pathway?* Nat Rev Drug Discov, 2014. **13**(7): p. 513-32.
125. Padhi, D., Jang, G., Stouch, B., Fang, L., and Posvar, E., *Single-dose, placebo-controlled, randomized study of AMG 785, a sclerostin monoclonal antibody.* J Bone Miner Res, 2011. **26**(1): p. 19-26.
126. Erdine, S. and De Andrés, J., *Drug delivery systems.* Pain Pract, 2006. **6**(1): p. 51-7.
127. Leucht, P., Jiang, J., Cheng, D., Liu, B., Dhamdhere, G., Fang, M. Y., Monica, S. D., Urena, J. J., Cole, W., Smith, L. R., Castillo, A. B., Longaker, M. T., and Helms, J. A., *Wnt3a reestablishes osteogenic capacity to bone grafts from aged animals.* J Bone Joint Surg Am, 2013. **95**(14): p. 1278-88.
128. Popelut, A., Rooker, S. M., Leucht, P., Medio, M., Brunski, J. B., and Helms, J. A., *The acceleration of implant osseointegration by liposomal Wnt3a.* Biomaterials, 2010. **31**(35): p. 9173-81.
129. Chen, T., Li, J., Cordova, L. A., Liu, B., Mouraret, S., Sun, Q., Salmon, B., and Helms, J., *A WNT protein therapeutic improves the bone-forming capacity of autografts from aged animals.* Sci Rep, 2018. **8**(1): p. 119.
130. Kavitha, M., Subramanian, R., Vinoth, K. Somasundara, Narayanan, R., Venkatesh, G., and Esakkiraja, N., *Optimization of process parameters for solution combustion synthesis of Strontium substituted Hydroxyapatite nanocrystals using Design of Experiments approach.* Powder Technology, 2015. **271**: p. 167-181.
131. Kim, Hyun-Woo and Kim, Young-Jin, *Fabrication of strontium-substituted hydroxyapatite scaffolds using 3D printing for enhanced bone regeneration.* Journal of Materials Science, 2020. **56**(2): p. 1673-1684.
132. Lee, J., Byun, H., Madhurakkat Perikamana, S. K., Lee, S., and Shin, H., *Current Advances in Immunomodulatory Biomaterials for Bone Regeneration.* Adv Healthc Mater, 2019. **8**(4): p. e1801106.
133. Liu, Dinghua, Nie, Wei, Li, Dejian, Wang, Weizhong, Zheng, Lixia, Zhang, Jingtian, Zhang, Jiulong, Peng, Chen, Mo, Xiumei, and He, Chuanglong, *3D printed PCL/SrHA scaffold for enhanced bone regeneration.* Chemical Engineering Journal, 2019. **362**: p. 269-279.
134. Muller, W. E. G., Tolba, E., Ackermann, M., Neufurth, M., Wang, S., Feng, Q., Schroder, H. C., and Wang, X., *Fabrication of amorphous strontium polyphosphate microparticles that induce mineralization of bone cells in vitro and in vivo.* Acta Biomater, 2017. **50**: p. 89-101.

135. Park, So Yeon, Kim, Kyung-Il, Park, Sung Pyo, Lee, Jung Heon, and Jung, Hyun Suk, *Aspartic Acid-Assisted Synthesis of Multifunctional Strontium-Substituted Hydroxyapatite Microspheres.* Crystal Growth & Design, 2016. **16**(8): p. 4318-4326.
136. Cui, X., Zhang, Y., Wang, J., Huang, C., Wang, Y., Yang, H., Liu, W., Wang, T., Wang, D., Wang, G., Ruan, C., Chen, D., Lu, W. W., Huang, W., Rahaman, M. N., and Pan, H., *Strontium modulates osteogenic activity of bone cement composed of bioactive borosilicate glass particles by activating Wnt/beta-catenin signaling pathway.* Bioact Mater, 2020. **5**(2): p. 334-347.
137. Meka, S. R., Jain, S., and Chatterjee, K., *Strontium eluting nanofibers augment stem cell osteogenesis for bone tissue regeneration.* Colloids Surf B Biointerfaces, 2016. **146**: p. 649-56.
138. Weng, L., Boda, S. K., Teusink, M. J., Shuler, F. D., Li, X., and Xie, J., *Binary Doping of Strontium and Copper Enhancing Osteogenesis and Angiogenesis of Bioactive Glass Nanofibers while Suppressing Osteoclast Activity.* ACS Appl Mater Interfaces, 2017. **9**(29): p. 24484-24496.
139. Pina, S., Vieira, S. I., Rego, P., Torres, P. M., da Cruz e Silva, O. A., da Cruz e Silva, E. F., and Ferreira, J. M., *Biological responses of brushite-forming Zn- and ZnSr- substituted beta-tricalcium phosphate bone cements.* Eur Cell Mater, 2010. **20**: p. 162-77.
140. Thormann, U., Ray, S., Sommer, U., Elkhassawna, T., Rehling, T., Hundgeburth, M., Henss, A., Rohnke, M., Janek, J., Lips, K. S., Heiss, C., Schlewitz, G., Szalay, G., Schumacher, M., Gelinsky, M., Schnettler, R., and Alt, V., *Bone formation induced by strontium modified calcium phosphate cement in critical-size metaphyseal fracture defects in ovariectomized rats.* Biomaterials, 2013. **34**(34): p. 8589-98.
141. Schumacher, M. and Gelinsky, M., *Strontium modified calcium phosphate cements - approaches towards targeted stimulation of bone turnover.* J Mater Chem B, 2015. **3**(23): p. 4626-4640.
142. Cooper, L. F., Zhou, Y., Takebe, J., Guo, J., Abron, A., Holmen, A., and Ellingsen, J. E., *Fluoride modification effects on osteoblast behavior and bone formation at TiO2 grit-blasted c.p. titanium endosseous implants.* Biomaterials, 2006. **27**(6): p. 926-36.
143. Borkowski, L., Przekora, A., Belcarz, A., Palka, K., Jozefaciuk, G., Lubek, T., Jojczuk, M., Nogalski, A., and Ginalska, G., *Fluorapatite ceramics for bone tissue regeneration: Synthesis, characterization and assessment of biomedical potential.* Mater Sci Eng C Mater Biol Appl, 2020. **116**: p. 111211.
144. Sankaralingam, Pugalanthi Pandian, Sakthivel, Poornimadevi, Andinadar Subbiah, Priscilla, Rahumathulla, Jenifabegum, and Chinnaswamy Thangavel, Vijayakumar, *Preparation and physical-biological characterization on titanium doped fluorophosphate nanobioglass: Bone implants.* International Journal of Ceramic Engineering & Science, 2021. **3**(1): p. 37-48.
145. Bai, X., Gao, M., Syed, S., Zhuang, J., Xu, X., and Zhang, X. Q., *Bioactive hydrogels for bone regeneration.* Bioact Mater, 2018. **3**(4): p. 401-417.
146. Gresham, R. C. H., Bahney, C. S., and Leach, J. K., *Growth factor delivery using extracellular matrix-mimicking substrates for musculoskeletal tissue engineering and repair.* Bioact Mater, 2021. **6**(7): p. 1945-1956.
147. Ahmed, E. M., *Hydrogel: Preparation, characterization, and applications: A review.* J Adv Res, 2015. **6**(2): p. 105-21.
148. Alaohali, A., Salzlechner, C., Zaugg, L. K., Suzano, F., Martinez, A., Gentleman, E., and Sharpe, P. T., *GSK3 Inhibitor-Induced Dentinogenesis Using a Hydrogel.* J Dent Res, 2022. **101**(1): p. 46-53.
149. Wang, Y., Newman, M. R., Ackun-Farmmer, M., Baranello, M. P., Sheu, T. J., Puzas, J. E., and Benoit, D. S. W., *Fracture-Targeted Delivery of β-Catenin Agonists via Peptide-Functionalized Nanoparticles Augments Fracture Healing.* ACS Nano, 2017. **11**(9): p. 9445-9458.
150. Li, Q., Wang, Q., Wang, O., Shao, K., Lin, H., and Lei, Y., *A simple and scalable hydrogel-based system for culturing protein-producing cells.* PLoS One, 2018. **13**(1): p. e0190364.
151. Zohra, F. T., Chowdhury, E. H., Tada, S., Hoshiba, T., and Akaike, T., *Effective delivery with enhanced translational activity synergistically accelerates mRNA-based transfection.* Biochem Biophys Res Commun, 2007. **358**(1): p. 373-8.

152. Mukherjee, S. and Thrasher, A. J., *Gene therapy for PIDs: progress, pitfalls and prospects.* Gene, 2013. **525**(2): p. 174-81.
153. Agholme, F., Li, X., Isaksson, H., Ke, H. Z., and Aspenberg, P., *Sclerostin antibody treatment enhances metaphyseal bone healing in rats.* J Bone Miner Res, 2010. **25**(11): p. 2412-8.
154. Mockey, M., Gonçalves, C., Dupuy, F. P., Lemoine, F. M., Pichon, C., and Midoux, P., *mRNA transfection of dendritic cells: synergistic effect of ARCA mRNA capping with Poly(A) chains in cis and in trans for a high protein expression level.* Biochem Biophys Res Commun, 2006. **340**(4): p. 1062-8.
155. Ramunas, J., Yakubov, E., Brady, J. J., Corbel, S. Y., Holbrook, C., Brandt, M., Stein, J., Santiago, J. G., Cooke, J. P., and Blau, H. M., *Transient delivery of modified mRNA encoding TERT rapidly extends telomeres in human cells.* Faseb j, 2015. **29**(5): p. 1930-9.
156. Sultana, N., Magadum, A., Hadas, Y., Kondrat, J., Singh, N., Youssef, E., Calderon, D., Chepurko, E., Dubois, N., Hajjar, R. J., and Zangi, L., *Optimizing Cardiac Delivery of Modified mRNA.* Mol Ther, 2017. **25**(6): p. 1306-1315.
157. Roy, B., *Effects of mRNA Modifications on Translation: An Overview.* Methods Mol Biol, 2021. **2298**: p. 327-356.
158. Balmayor, E. R., Geiger, J. P., Aneja, M. K., Berezhanskyy, T., Utzinger, M., Mykhaylyk, O., Rudolph, C., and Plank, C., *Chemically modified RNA induces osteogenesis of stem cells and human tissue explants as well as accelerates bone healing in rats.* Biomaterials, 2016. **87**: p. 131-146.
159. Khorsand, B., Elangovan, S., Hong, L., Dewerth, A., Kormann, M. S., and Salem, A. K., *A Comparative Study of the Bone Regenerative Effect of Chemically Modified RNA Encoding BMP-2 or BMP-9.* Aaps j, 2017. **19**(2): p. 438-446.
160. Fontana, G., Martin, H. L., Lee, J. S., Schill, K., Hematti, P., and Murphy, W. L., *Mineral-Coated Microparticles Enhance mRNA-Based Transfection of Human Bone Marrow Cells.* Mol Ther Nucleic Acids, 2019. **18**: p. 455-464.
161. Khalil, A. S., Yu, X., Umhoefer, J. M., Chamberlain, C. S., Wildenauer, L. A., Diarra, G. M., Hacker, T. A., and Murphy, W. L., *Single-dose mRNA therapy via biomaterial-mediated sequestration of overexpressed proteins.* Sci Adv, 2020. **6**(27).
162. Lambert, L. J., Challa, A. K., Niu, A., Zhou, L., Tucholski, J., Johnson, M. S., Nagy, T. R., Eberhardt, A. W., Estep, P. N., Kesterson, R. A., and Grams, J. M., *Increased trabecular bone and improved biomechanics in an osteocalcin-null rat model created by CRISPR/Cas9 technology.* Dis Model Mech, 2016. **9**(10): p. 1169-1179.
163. Liu, Y., Wang, J., Liu, S., Kuang, M., Jing, Y., Zhao, Y., Wang, Z., and Li, G., *A novel transgenic murine model with persistently brittle bones simulating osteogenesis imperfecta type I.* Bone, 2019. **127**: p. 646-655.
164. Ubels, J. L., Diegel, C. R., Foxa, G. E., Ethen, N. J., Lensing, J. N., Madaj, Z. B., and Williams, B. O., *Low-Density Lipoprotein Receptor-Related Protein 5-Deficient Rats Have Reduced Bone Mass and Abnormal Development of the Retinal Vasculature.* Crispr j, 2020. **3**(4): p. 284-298.
165. Jung, H., Rim, Y. A., Park, N., Nam, Y., and Ju, J. H., *Restoration of Osteogenesis by CRISPR/Cas9 Genome Editing of the Mutated COL1A1 Gene in Osteogenesis Imperfecta.* J Clin Med, 2021. **10**(14).
166. Brunger, J. M., Zutshi, A., Willard, V. P., Gersbach, C. A., and Guilak, F., *CRISPR/Cas9 Editing of Murine Induced Pluripotent Stem Cells for Engineering Inflammation-Resistant Tissues.* Arthritis Rheumatol, 2017. **69**(5): p. 1111-1121.
167. Khalaf, K., Janowicz, K., Dyszkiewicz-Konwinska, M., Hutchings, G., Dompe, C., Moncrieff, L., Jankowski, M., Machnik, M., Oleksiewicz, U., Kocherova, I., Petitte, J., Mozdziak, P., Shibli, J. A., Izycki, D., Jozkowiak, M., Piotrowska-Kempisty, H., Skowronski, M. T., Antosik, P., and Kempisty, B., *CRISPR/Cas9 in Cancer Immunotherapy: Animal Models and Human Clinical Trials.* Genes (Basel), 2020. **11**(8).

168. Uddin, F., Rudin, C. M., and Sen, T., *CRISPR Gene Therapy: Applications, Limitations, and Implications for the Future.* Front Oncol, 2020. **10**: p. 1387.
169. Hsu, M. N., Huang, K. L., Yu, F. J., Lai, P. L., Truong, A. V., Lin, M. W., Nguyen, N. T. K., Shen, C. C., Hwang, S. M., Chang, Y. H., and Hu, Y. C., *Coactivation of Endogenous Wnt10b and Foxc2 by CRISPR Activation Enhances BMSC Osteogenesis and Promotes Calvarial Bone Regeneration.* Mol Ther, 2020. **28**(2): p. 441-451.
170. Pickar-Oliver, Adrian and Gersbach, Charles A., *The next generation of CRISPR–Cas technologies and applications.* Nature Reviews Molecular Cell Biology, 2019. **20**(8): p. 490-507.
171. O'Connell, Mitchell R., Oakes, Benjamin L., Sternberg, Samuel H., East-Seletsky, Alexandra, Kaplan, Matias, and Doudna, Jennifer A., *Programmable RNA recognition and cleavage by CRISPR/Cas9.* Nature, 2014. **516**(7530): p. 263-266.
172. Batra, R., Nelles, D. A., Pirie, E., Blue, S. M., Marina, R. J., Wang, H., Chaim, I. A., Thomas, J. D., Zhang, N., Nguyen, V., Aigner, S., Markmiller, S., Xia, G., Corbett, K. D., Swanson, M. S., and Yeo, G. W., *Elimination of Toxic Microsatellite Repeat Expansion RNA by RNA-Targeting Cas9.* Cell, 2017. **170**(5): p. 899-912.e10.
173. Maeder, Morgan L., Stefanidakis, Michael, Wilson, Christopher J., Baral, Reshica, Barrera, Luis Alberto, Bounoutas, George S., Bumcrot, David, Chao, Hoson, Ciulla, Dawn M., DaSilva, Jennifer A., Dass, Abhishek, Dhanapal, Vidya, Fennell, Tim J., Friedland, Ari E., Giannoukos, Georgia, Gloskowski, Sebastian W., Glucksmann, Alexandra, Gotta, Gregory M., Jayaram, Hariharan, Haskett, Scott J., Hopkins, Bei, Horng, Joy E., Joshi, Shivangi, Marco, Eugenio, Mepani, Rina, Reyon, Deepak, Ta, Terence, Tabbaa, Diana G., Samuelsson, Steven J., Shen, Shen, Skor, Maxwell N., Stetkiewicz, Pam, Wang, Tongyao, Yudkoff, Clifford, Myer, Vic E., Albright, Charles F., and Jiang, Haiyan, *Development of a gene-editing approach to restore vision loss in Leber congenital amaurosis type 10.* Nature Medicine, 2019. **25**(2): p. 229-233.
174. Frangoul, Haydar, Altshuler, David, Cappellini, M. Domenica, Chen, Yi-Shan, Domm, Jennifer, Eustace, Brenda K., Foell, Juergen, de la Fuente, Josu, Grupp, Stephan, Handgretinger, Rupert, Ho, Tony W., Kattamis, Antonis, Kernytsky, Andrew, Lekstrom-Himes, Julie, Li, Amanda M., Locatelli, Franco, Mapara, Markus Y., de Montalembert, Mariane, Rondelli, Damiano, Sharma, Akshay, Sheth, Sujit, Soni, Sandeep, Steinberg, Martin H., Wall, Donna, Yen, Angela, and Corbacioglu, Selim, *CRISPR-Cas9 Gene Editing for Sickle Cell Disease and β-Thalassemia.* New England Journal of Medicine, 2020. **384**(3): p. 252-260.

CHAPTER II: MINERAL COATED MICROPARTICLES AS MRNA DELIVERY PLATFORMS FOR FRACTURE HEALING

II.1 Introduction

As an alternative to traditional protein-based therapeutics, gene therapy has emerged as a promising approach to accelerate bone healing. Genes encoding growth factors, transcription factors, and hormones involved in osteogenesis have been explored.[1-3] De la Vega *et al.* has thoroughly reviewed the delivery of bone morphogenetic protein-2 (BMP-2) cDNA using viral vector systems, such as adenovirus and lentivirus.[3] Viral platforms to deliver gene encoding BMP-2 have been shown to be associated with an immune response resulting in impeded bone healing when tested *in vivo*.[4-7] New gene therapy strategies for bone regeneration involve use of mRNA, yet this approach is still challenged with short-half life and immunogenicity.[8, 9] To combat these challenges, other approaches have focused on modifying the mRNA sequence to maximize transfection while minimizing an immune reaction.[9, 10] The use of liposomes to encapsulate chemically modified BMP-2 mRNA loaded on a collagen sponge has also been studied.[11, 12] Thus, mRNA therapies for fracture healing that result in effective transfection, promotion of bone formation and minimal immunogenicity show great promise, but have yet to be thoroughly explored.

Effective mRNA delivery to cells requires the use of carriers that will protect the nucleic acids from degradation from nucleases.[13, 14] Currently, liposomal complexes (lipoplexes) are the most commonly utilized delivery vehicles for mRNA based therapeutics, and include lipid nanoparticles and liposomes.[13, 14] However, lipoplexes can induce immunogenic reactions and are rapidly cleared by the mononuclear phagocytic system (MPS).[13] Alternative strategies have been employed to mitigate limitations seen with liposomal delivery and to effectively transport genes for bone repair. These include the use of β-tricalcium phosphate biomaterials and mineral coated microparticles (MCM).[15-17] MCM consist of a bioresorbable core material that become coated with calcium phosphate when bathed in biomimetic fluid, resulting in

microparticles 5-8 μm in diameter with a thin, flaky mineral coating.[17-19] MCM show promise for fracture healing applications, due to the fact that they are highly tunable and compatible with local injection delivery thereby negating the need for an open approach. In fact, MCMs have been used *in vivo* to effectively sustain release of vascular endothelial growth factor (VEGF) and BMP-2 protein to treat impaired fracture healing and have resulted in improved bone volume composition.[20, 21] Although the majority of publications focus on MCMs to deliver proteins in a controlled-release manner, recent work has focused on the controlled release dynamics of lipoplexes using MCMs.[17, 22] *In vitro* studies have demonstrated that MCMs enhance mRNA transfection and diminish cytotoxic impacts from high mRNA concentrations as tested in mesenchymal stem cells (MSCs) amongst other cell lineages.[17, 23, 24] In these studies, a single-dose method to deliver MCM-lipoplexes with a functional mRNA sequence has been resulted in successful local expression of the target protein.[25] Importantly, protein expression through delivery of MCM-mRNA lipoplexes has reported higher bioactivity, prolonged protein expression and improved functional outcomes as compared to delivery of recombinant proteins.[25, 26]

We hypothesized that using MCM complexes to locally deliver lipoplexes enhances transfection potential, reduces immunogenicity, and does not interfere with fracture healing as compared to delivery of lipoplexes alone in a murine fracture model. To test this hypothesis, we explored MCM-mRNA complexes and sought to identify an effective MCM composition to deliver a reporter mRNA in a fracture setting (**FIGURE 4**). The biomimetic mineral coating enhances the delivery of lipoplexes to cells in various *in vitro* applications, yet have only effectively delivered lipoplexes in a rat spinal cord injury model to date.[17, 23, 25, 26] The use of MCMs to improve localization and cell uptake of mRNA at the fracture site would address several limitations, including the cytotoxicity associated with liposomal carriers. Here we show that mRNA transfection is enhanced, prolonged, and does not interfere with fracture healing or modulate inflammation when using MCMs as a transfection platform in a murine tibial fracture healing model.

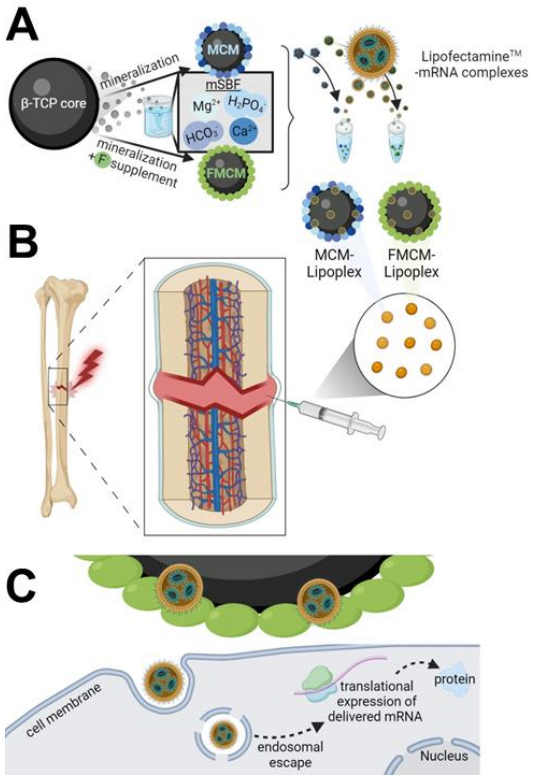

Figure 4. *Schematic of MCM and FMCM synthesis, delivery, cell interactions and characterization of microparticles.* ***A).*** *Schematic of MCM and FMCM synthesis and lipoplex interaction.* ***B).*** *Delivery of test article and controls were localized at the site of the fracture callus,* ***C).*** *where MCM-LPX-FLuc and FMCM-LPX-FLuc are not endocytosed by the cells.*

II.2 Methods & Materials

II.2.1 Synthesis of MCM and FMCM

Mineral coated microparticles were made from β-tricalcium phosphate (β-TCP) 2 µm powder (Cambioceramics, Amsterdam, Netherlands) as the microparticle core and incubated in modified simulated body fluid (mSBF) at 1 mg/mL for 7 days. The mSBF was prepared by using 141 mM NaCl, 4 mM KCl, 0.5 mM MgSO4, 1 mM MgCl2, 4.2 mM NaHCO3, 20 mM HEPES, 5 mM CaCl2, and 2 mM KH2PO4. To synthesize fluoride-doped MCM (FMCM) we introduced 1 mM NaF to the standard mSBF. All microparticles were maintained in suspension at 37˚C with rotation. The microparticles were centrifuged at 2,000 x g for 5 minutes every 24 hours over 7 days. The supernatant was discarded and replenished with

fresh mSBF. Post 7 days, the MCMs were rinsed three times using 50mL deionized water and filtered using a 40µm pore cell strainer. Finally, the MCMs were concentrated and subjected them to lyophilization for 48 hours.[17] Dry MCMs were placed on carbon tape and sputter coated with 10 nm of platinum (ACE600, Leica Microsystems, Morrisville, NC, USA). MCMs were imaged at 5.0 KV using a Gemini 450 scanning electron microscope (Zeiss, Jena, Germany).

II.2.2 MCM and FMCM formulations with lipoplexes for *in vitro* experiments

MCM and FMCM were used to deliver lipid vesicles encapsulating mRNA to ATDC5 cells *in vitro*. To determine transfection protocols and concentrations for effective delivery of mRNA, firefly luciferase (FLuc) mRNA was used as a reporter transcript (TriLink Biotech, Cat# L-7202) for all experiments. Lipoplexes (LPX), liposomes complexed with mRNA, were generated using Lipofectamine™ MessengerMAX (ThermoFisher, Cat# LMRNA001) and firefly luciferase mRNA according to manufacturer's protocol. To combine the LPXs with MCM and FMCM, the LPX solution was added to MCM or FMCM in OPTI-MEM for *in vitro* studies, with shaking for 30 minutes at RT. All *in vitro* experiments used 0.25 µg of firefly luciferase mRNA/well, 2 µL of Lipofectamine™/well, and 100 µg of MCM or FMCM per well. Firefly luciferase expression in MCM-Lipofectamine™-FLuc mRNA platform (MCM-LPX-FLuc) and FMCM-Lipofectamine™-FLuc mRNA (FMCM-LPX-FLuc) was compared to the luciferase expression from Lipofectamine™-FLuc mRNA (LPX-FLuc).

II.2.3 Testing MCM and FMCM cytotoxicity *in vitro*

The chondrogenic cell line (ATDC5, Sigma Aldrich, Cat # 99072806) was used for all *in vitro* studies. Cells were used at passage 5 and under for all experiments. ATDC5 cells were maintained using media DMEM/F12 (Thermo Fisher, Cat# 11320033), 5 % fetal bovine serum (FBS, Thermo Fisher, Cat# 16000044) and 1 % penicillin/streptomycin (P/S, Thermo Fisher, Cat# 15140122). For all *in vitro* experiments, ATDC5 cells were plated at 20,000 cells/well in 12 well plates. Prior to transfection

experiments, chondrocytes underwent serum starvation using basal media OPTI-MEM (Thermo Fisher, Cat# 31985070) 0.5 % FBS and 1 % P/S for 24 hours. All transfection protocols were executed using serum-free media, OPTI-MEM supplemented with 1 % P/S. The cytotoxic effects were assessed using PrestoBlue™ Cell Viability Reagent (Thermo Fisher, Cat# A13261) according to the manufacturer's protocol. To quantify the number of metabolically active cells, a standard curve of ATDC5 cells was created and the absorbance values were related back to the number of cells for quantitation. The plate was read at 570 nm with a reference wavelength at 600 nm using a plate reader (TECAN infinite M200 Pro).

II.2.4 Testing immunogenicity and osteogenesis *in vitro*

To further examine the potential impacts of MCM and FMCM on chondrocytes *in vitro*, immunogenic and osteogenic markers were measured using qRT-PCR. Analysis of MCM-LPX, FMCM-LPX and LPXs alone were measured *in vitro* after collecting RNA at 3, 6, 24 and 48 hours after treatments. RNA was isolated using TRIzol™ Reagent (ThermoFisher, Cat# 15596026) according to the manufacturer's guidelines. RNA was then quantified by reading the absorbance values at 260 and 280 nm. 1 µg of RNA was then synthesized into cDNA using qScript cDNA SuperMix (QuantaBio, Cat# 95048-025). Primers were designed and are listed in **TABLE 1**. Quality measurements were used to confirm primer specificity and appropriate reaction temperatures by running PCR using DreamTaq Green PCR Master Mix (2X) (ThermoFisher, Cat# K1081) using a 3-step method with denaturation at 95°C for 30 sec, annealing at 60°C for 30 secs and extension at 72°C for 1 minute. The bands were analyzed on a 1.5 % agarose gel with 2 µL GelStar Nucleic Acid Stain (Lonza, Cat # 50535) run at 150V for 25 minutes. Quantitative real-time PCR was run using SYBR Green Master Mix (Bio-Rad, Cat#1725270) to detect the amplified DNA. qRT-PCR was performed on a StepOnePlus™ instrument (Applied Biosystems). To analyze the output Ct values, the reference housekeeping gene (*β-2-modulin*) was used to determine ΔCt values. The value of $2^{-(\Delta\Delta Ct)}$ was calculated for all graphs and to determine statistical significance. All $2^{(-\Delta\Delta Ct)}$ values less than 1.0, were calculated as $-1/(2^{(-\Delta\Delta Ct)})$ as followed and described in Schmittgen *et al.*[27]

Table 1. *Primer sequences validated for use in qRT-PCR specifically for ATDC5 samples.*

Gene	**Forward**	**Reverse**
β-2-modulin	ATACGCCTGCAGAGTTAAGCA	TCACATGTCTCGATCCCAGT
axin2	GTGAGCTGGTTGTCACCTACTT	GCAAATTCGTCACTCGCCTTC
osteocalcin (ocn)	CGCTCTGTCTCTCTGACCTC	TCACAAGCAGGGTTAAGCTC
interleukin-1β (il-1β)	TGGACCTTCCAGGATGAGGACA	GTTCATCTCGGAGCCTGTAGTG
interleukin-4 (il-4)	GGTCTCAACCCCCAGCTAGT	GCCGATGATCTCTCTCAAGTGAT
firefly luciferase (fluc)	GTGGTGTGCAGCGAGAATAG	CGCTCGTTGTAGATGTCGTTAG

II.2.5 Murine tibia fracture and stabilization model

In vivo experiments were approved by and conducted in compliance with the Institutional Animal Care and Use Committee at Colorado State University (CSU). Mid-shaft tibial fractures were created in adult (12-14 weeks), male C57BL/6J mice (Charles River # 027). All animals received a pre-surgical analgesic, Buprenorphine SR (ZooPharm), at a dose of 0.6-1.0 mg/kg. Mice were placed under general anesthesia using inhaled 1-5 % isoflurane to effect. Left hind limbs were shaved and sterilely prepared using 70 % alcohol wipes and Chlorhexidine surgical scrub solution, repeated for a total of 3 times. Lubrication was provided for the eyes of each mouse using artificial tears ointment (Bausch & Lomb) and mice were then transferred to a heated operating table. Using aseptic technique, an incision was made along the tibia, and a hole was made at the top of the tibial plateau using a 23-gauge needle. An intermedullary pin (sterilized insect pin) was inserted through the hole made from the tibial plateau through the tibial cavity and into the distal tibia. One small hole was created in the mid-shaft of the tibia using a Dremel and pressure was applied to both proximal and distal ends to fracture the tibia.[28, 29] The surgical incision was then sutured using 5-0 Biosyn Sutures (Covidien, Cat #5687) and one surgical skin staple was applied over the skin incision to protect against chewing. A local anesthetic, 0.25% Bupivicaine Hydrochloride (NovaPlus, cat # RL-7562), was applied topically after the initial staple was placed. Mice were then allowed to recover individually in a heated cage before being transferred back to their original cage. Mice were socially housed throughout the in-life period, and permitted free ambulation. Mice were closely monitored for pain and

signs of infections for 72 hours following the surgery. All treatments were suspended in 25 µL sterile PBS and vortexed before injecting. All experimental and control groups were injected on day 6 post-fracture into the fracture callus using a Hamilton syringe 1800 series (Sigma Aldrich, Cat # 21397). Localized treatments consisted of experimental groups (MCM-LPX and FMCM-LPX), negative and positive control groups (PBS and LPX respectively). Serum was collected 2 days following treatment via tail vein blood draw and lastly at time of harvest using a cardiac puncture. Animals were sacrificed according to approved euthanasia protocols after 2 or 8 days following localized treatments. At euthanasia, serum, fractured tibia, kidneys, liver, spleen and lung were harvested for analysis. Harvested tibias were either fixed in 4 % paraformaldehyde for histological analysis or flash-frozen in liquid nitrogen for RNA analysis. Tissues and serum were flash frozen by immediately placing in liquid nitrogen and stored at -80°C.

II.2.6 Localized MCM and FMCM injections

All treatments were injected into the fracture callous 6 days following fracture. *In vivo* analysis of transfection reagents used firefly luciferase mRNA at a concentration of 10 µg/mouse, Lipofectamine™ at 15 µL/mouse, and MCM/FMCM at 100 µg/mouse. Following the generation of lipoplexes as described in II.2.2, the MCM/FMCM solutions were added to the lipoplex formulations and incubated for 30 minutes at RT with moderate shaking. *In vivo* studies used sterile filtered 1X phosphate buffer solution (PBS, Thermo Fisher, Cat # 10010023) as the solvent to produce the various solutions. Negative control groups included a sterile-filtered phosphate buffered saline (PBS) group with a total volume of injections to be 25 µL/mouse. Firefly luciferase expression in MCM-Lipofectamine™-FLuc mRNA platform (MCM-LPX-FLuc) and FMCM-Lipofectamine™-FLuc mRNA (FMCM-LPX-FLuc) was compared to the luciferase expression from Lipofectamine™-FLuc mRNA (LPX-FLuc). The following n-values can be found in the table listed below for each experiment and for each time point (**TABLE 2**).

Table 2. *The n-values associated with reported experiments for each treatment group.*

Group	Day 2	Day 8	
	Histology	RNA	Histology
PBS	4	3	6
LPX	5	5	4
MCM-LPX	5	4	6
FMCM-LPX	5	6	7

II.2.7 Transfection efficacy and kinetics *in vivo*

Transfection efficacy and kinetics were measured through use of reporter gene, firefly luciferase mRNA, and quantification of luminescence using IVIS imaging (manufacturer, town, state). IVIS imaging was performed daily to assess the magnitude and duration of luciferase expression from the time of delivery of reporter mRNA until signal dissipated. All mice were anesthetized using inhaled isoflurane and injected with 100 µL of firefly luciferase substrate, D-luciferin, subcutaneously at 10 mg/mL in PBS. Isoflurane Anestheisa was maintained using inhaled isoflurane at 1-5 % to effect and mice were imaged 5 minutes following subcutaneous injection of D-luciferin. Bioluminescence was acquired using the 'Auto' setting and regions of interest were measured for bioluminescence using LivingImage software (PerkinElmer, version). Percent retention was calculated using the following equation for each animal:

$$\% \text{ Retention} = 100 \% - [((A - B_x)/A) \times 100\%],$$

where A = bioluminescence intenstiy at day 1, and B_x = biolumescence intensity at day x.

II.2.8 *In vivo* immunogenicity and osteogenic testing

Mice were humanely euthanized at day 8 post-treatment. All fractured limbs were harvested, immediately placed in liquid nitrogen and stored at -80°C. To isolate the RNA from the fracture callus, the fracture callus was dissected and removed, minced and placed in 1 mL of TRIzol. The tissues were homogenized using IKA Tissue Homogenizer (IKA, Cat# 0003737001) using a speed of 5 for 3 minutes, or until all large chunks were broken down. RNA was then quantified by reading the absorbance values at

260 and 280 nm. 1 µg of RNA was then synthesized into cDNA using qScript cDNA SuperMix. Primers were designed and are listed in **TABLE 3** and qRT-PCR was performed as described in Section II.2.4.

Table 3. *Primer sequences validated for use in qRT-PCR for use in a murine fracture model.*

Gene	Forward	Reverse
β-2-modulin	ATACGCCTGCAGAGTTAAGCA	TCACATGTCTCGATCCCAGT
collagen 10a1 (colX)	TTCTGCTGCTAATGTTCTTGACC	GGGATGAAGTATTGTGTCTTGGG
axin2	GTGAGCTGGTTGTCACCTACTT	GCAAATTCGTCACTCGCCTTC
runt-related transcription factor 2 (runx2)	ACTCTTCTGGAGCCGTTTATG	GTGAATCTGGCCATGTTTGTG
osterix (osx)	TGCGCCAGGAGTAAAGAATAG	CCTGACCCGTCATCATAACTTAG
osteocalcin (ocn)	CGCTCTGTCTCTCTGACCTC	TCACAAGCAGGGTTAAGCTC
interleukin-1β (il-1β)	TGGACCTTCCAGGATGAGGACA	GTTCATCTCGGAGCCTGTAGTG
interleukin-4 (il-4)	GGTCTCAACCCCCAGCTAGT	GCCGATGATCTCTCTCAAGTGAT
firefly luciferase (fluc)	GTGGTGTGCAGCGAGAATAG	CGCTCGTTGTAGATGTCGTTAG

To analyze treatment groups for immunogenicity and osteogenesis, RNA was first isolated from the fracture callus 8 days after injection. To measure *in vivo* immune responses, qRT-PCR was used to probe for the pro-inflammatory marker, *interleukin-1β (il-1β),* and anti-inflammatory marker, *interleukin-4 (il-4).* Local inflammatory response was measured using qRT-PCR and histopathology while systemic inflammation was tested using a C-Reactive Protein (CRP) ELISA kit (R&D Systems, Cat# MCRP00) according to manufacturer's instructions on the serum collected at day 2 and 8 post-treatment.[30] Osteostimulatory characterization was determined by using qRT-PCR for osteogenic markers *osterix* (*osx*), *osteocalcin (ocn*), *collagen 10a1* (*colX*) and downstream canonical Wnt markers, *axis inhibition protein 2* (*axin2)* and *runt-related transcription factor* (*runx2).*

II.2.9 Histology, histopathologic scoring and histomorphometric methodology

Fractured tibias were collected 2 and 8 days post treatment, fixed in 4 % paraformaldehyde, and decalcified using 19 % ethylenediaminetetraacetic acid (EDTA). The tissues were then processed in increased ethanol solutions (50%, 70%, 95% and 100%), processed in xylene (x2) and then placed in

paraffin for 1.5 hours each. Samples were embedded in paraffin, sectioned at 8 μm thickness, and mounted onto glass slides. Two serial sections of each sample were cut and stained with hematoxylin and eosin using routine methods. Semiquantitative histopathologic analysis was performed by a board-certified veterinary pathologist (D.P.R.) who was blinded to the treatment arm. For analysis, slides were scanned on low magnification and the fracture callus region-of-interest identified and histological scoring performed based on the qualitative cell population across this callus region-of-interest. Semi-quantitative scoring was performed using a modification of ISO10993-6 Annex E: Biological evaluation of medical devices – Part 6: Tests for local effects after implantation (**SUPPLEMENTAL TABLE 1**). Inflammatory response was determined by categorizing inflammatory cell type (polymorphonuclear cells (PMNs), lymphocytes (lymphs), plasma cells, macrophages, and giant cells,) Host tissue response analysis included categorical measures of necrosis, edema, hemorrhage, neovascularization and fibrosis. Responses were scored based on a 0-4 scale where 0 represents "none", 1 represents "rare/minimal", 2 represents "mild", 3 represents "heavy infiltrate/moderate" and 4 represents "packed/severe."

Immunohistochemistry (IHC) was performed to identify cells expressing Fluc within the fracture callus using previously published methods.[29, 31] Antigen labeling was performed using a primary anti-luciferase (Novus Biologicals, Cat# NM600-307) antibody. Negative control mouse IgG monoclonal antibody (ThermoFisher, Cat# 10400C) was used in replace of firefly luciferase antibody to determine non-specific stain. Cell morphology was used as the primary tool to identify specific immunopositive cell types, using Hall Brundt's Quadruple (HBQ) stain on adjacent slides, or the slide immediately following IHC stained sections.[32] The following kits were used for IHC detection: Mouse on Mouse Immunodetection Kit (Vector Laboratories, Cat# BMK2202), VectaStain Elite ABC-HRP Kit (Vector Laboratories, Cat# PK-6200) and DAB Substrate Kit, Peroxidase (HRP) (Vector Laboratories, Cat# SK-4100). All kits were used according to manufacturer's protocol. Sections were counterstained using Hematoxylin, dehydrated and mounted in a xylene-based mounting medium.

To perform quantitative histomorphometry, serial sections were obtained using the first section beginning in the fracture callus and every 10^{th} section afterwards. Standard histomorphometry principles were used as previously described and quantification of the fracture callus components including bone and cartilage tissues were determined.[29, 33] HBQ stain was used to identify the dense collagenous fibrils of bone, stained red by direct red, and proteoglycans in the cartilage matrix , stained by alcian blue. Quantification of callus composition was determined using the Trainable Weka Segmentation2 add-on in Fiji ImageJ (version 1.54f; NIH, Maryland, USA).[34] Volume of specific tissue types (bone, cartilage, fibrous) was determined by summing the individual component compositions relative to the whole fracture callus compositions. Tissues were imaged using a Nikon Eclipse Ti microscope. Additionally, photoshop (version 24.7.0, Adobe) was used to isolate fractured tissue from the adjacent muscle and skin tissues.

II.2.10 Statistics

Animal sample size was determined *a priori* using the mean and standard deviation from our preliminary data, where a power analysis was conducted using R Studio to determine that 5 mice/group/time are required for IVIS outputs (total flux) to achieve a power level >80% with an effect size η^2=0.99 and a significance level of 5% (**SUPPLEMENTAL FIGURE 2**). Statistical analysis was performed using Graph Pad Prism 8. Log10 transformation was performed on all IVIS outputs and all statistics was executed on log transformed values. Data were plotted so that each sample represented a single dot on each graph. The bar indicates the mean with error bars representing standard deviation. Statistical difference was determined by ANOVAs and all post-hoc comparison performed using Tukey's HSD test.

II.3 FMCM enhances transfection, promotes bone and minimizes immunogenicity *in vitro*

To determine the transfection efficacy of MCM-LPX, two different formulations of MCM were prepared. Fluoride was chosen as a dopant for MCM as it has been associated with stimulating the canonical Wnt pathway (as noted in Section I.2.5). MCM and FMCM were characterized using scanning electron

microscopy (SEM) to visualize the outer morphology of the microparticles (**FIGURE 5A**). MCM were found to have a plate-like outer coating where FMCM had a more needle-like structure. The cytotoxic effects of the microparticles were evaluated and were found to have no significant *in vitro* chondrocyte cytotoxicity at any dose tested (12.5 μg- 250 μg) (**FIGURE 5B**). Based on these data, 100 μg of MCM or FMCM was chosen to use in all *in vitro* experiments, as this concentration did not promote cytotoxic effects when tested in chondrocytes *in vitro.*

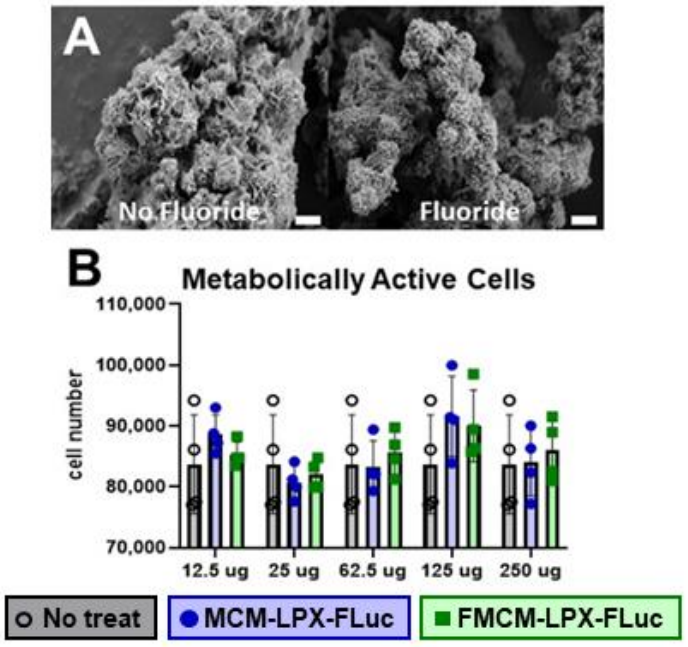

Figure 5. A). *SEM imaging of MCM (left) and FMCM (right). Scale bars represent 2 μm.* ***B).*** *Metabolic activity was measured to determine cytotoxicity of MCM-LPX-FLuc and FMCM-LPX-FLuc.*

Transfection efficacy of each delivery platform was measured by evaluating firefly luciferase gene expression through qRT-PCR. FMCM-LPX-FLuc was found to significantly enhance transfection to chondrocytes *in vitro* at 3 and 6 hours following treatment compared to both LPX-FLuc and MCM-LPX-FLuc groups (**FIGURE 6A**). FMCM-LPX-FLuc was found to have significantly less *il-1β* at all time points tested compared to the LPX-FLuc group alone, whereas MCM-LPX-FLuc was found to have significantly less *il-1β* at only the 48 hour timepoint compared to LPX-(**FIGURE 6B**). Additionally, FMCM-LPX-FLuc

had significantly lower *il-1β* measurements than MCM-LPX-FLuc at all earlier time points, yet MCM-LPX-FLuc had significantly lower at 48 hours. MCM-LPX-FLuc was found to have significantly more *il-4* at all time points as compared to both LPX-FLuc and FMCM-LPX-FLuc groups (**FIGURE 6C**).

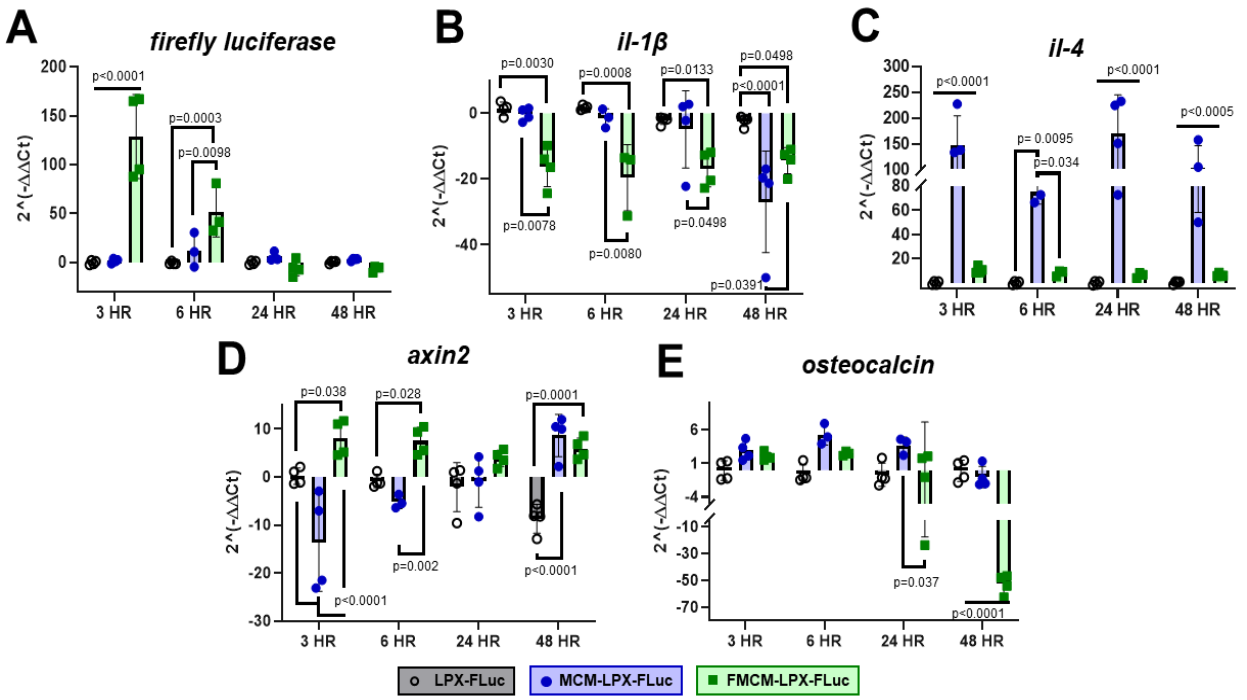

Figure 6. *In vitro transfection analysis of the three delivery platforms, Lipofectamine alone, MCM-Lipofectamine and FMCM-Lipofectamine. All transfections were performed using reporter mRNA, firefly luciferase, and RNA was isolated following 3, 6, 24 and 48 hours following transfection. qRT-PCR was performed to quantify various markers of* ***A).*** *transfection by probing for firefly luciferase, and markers of inflammatory responses by probing for* ***B).*** *pro-inflammatory marker, il-1b, and* ***C).*** *anti-inflammatory marker, il-4. Osteogenesis was measured through measuring* ***D).*** *osteocalcin, and* ***E).*** *downstream canonical Wnt gene, axin2.*

We tested whether there was any osteostimulatory effect in chondrocytes by probing for osteogenic markers *in vitro*. MCM-LPX-FLuc was found to have higher trends of *ocn* expression at all time points tested when compared to FMCM-LPX-FLuc (**FIGURE 6E**), but only showed significantly more *ocn* expression at 24 and 48 hours following treatment. FMCM-LPX-FLuc had significantly more *axin2* expression at earlier time points, specifically at 3 and 6 hours as compared to MCM-LPX-FLuc groups (**FIGURE 6D**). The upregulation seen in axin2 expression with FMCM is consistent with previous observations that fluoride activates the canonical Wnt pathway.[35]

We used a mineral coated microparticle (MCM) based platform to deliver mRNA encapsulated liposomes to chondrocytes and tested their ability to result in protein expression. Our data reveals that using FMCM-LPX-FLuc as a platform to deliver lipoplexes significantly enhanced transfection in chondrocytes without causing a pro-inflammatory response. While MCM-LPX-FLuc did not augment transfection, it resulted in a more favorable inflammatory response when compared to the LPX-FLuc group alone as evidenced through lower pro-inflammatory and higher anti-inflammatory markers in the MCM treated groups. Additionally, Both MCM-LPX-FLuc and FMCM-LPX-FLuc activated osteogenic genes in chondrocytes.

II.4 FMCM prolongs transfection without altering fracture healing in a murine model

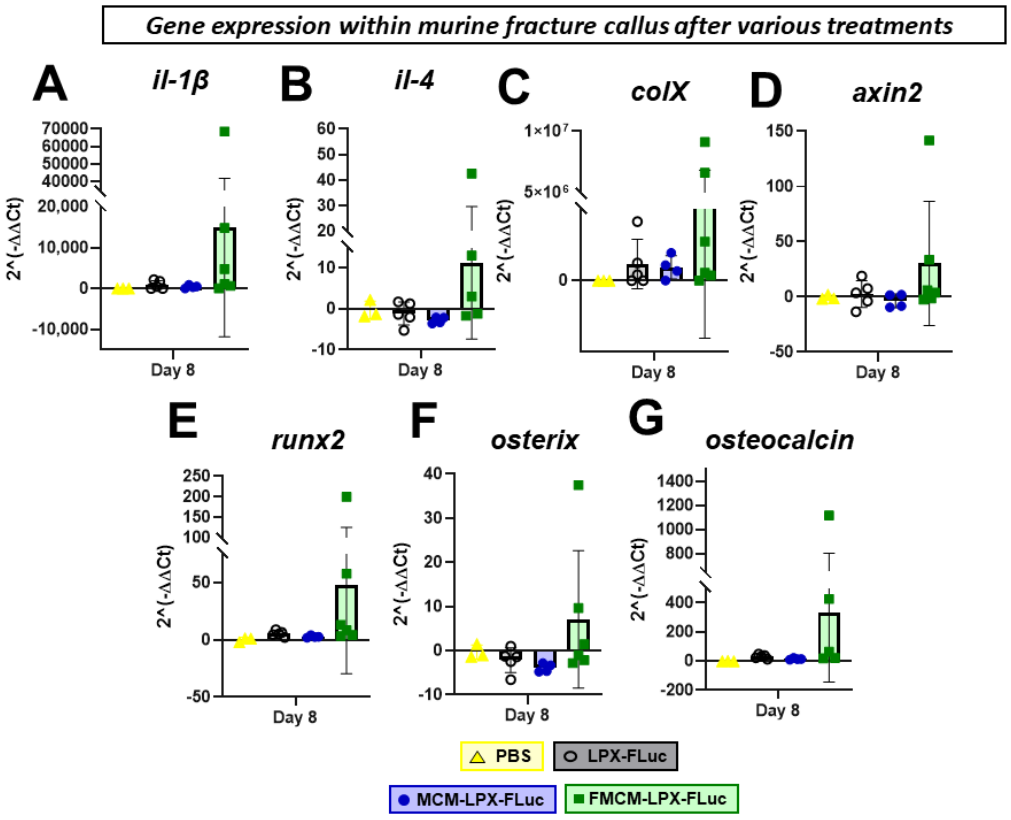

Figure 7. *Gene expression analysis within the fracture callus following 8 days post treatments. Markers of* ***A)*** *pro- and* ***B)*** *anti- inflammatory responses,* ***C-E)*** *early osteogenic genes, and* ***F-G)*** *late osteogenic genes were tested.*

Given the promising *in vitro* results described in Section II.2, the MCM-LPX-FLuc and FMCM-LPX-FLuc platforms were evaluated for their effect on osteogenesis, inflammatory response, bone and transfection efficacy in a murine fracture model. Within the tibia fracture callus, both early osteogenic genes, *collagen 10a1*, *axin2* and *runx2,* and late osteogenic genes, *osterix* and *osteocalcin,* were tested for a more robust analysis of MCM-LPX-FLuc and FMCM-LPX-FLuc osteogenic potential. While no statistical significance was found *in vivo*, we observed that higher expression of osteogenic genes was associated with the FMCM-LPX-FLuc group (**FIGURE 7 C-G**).

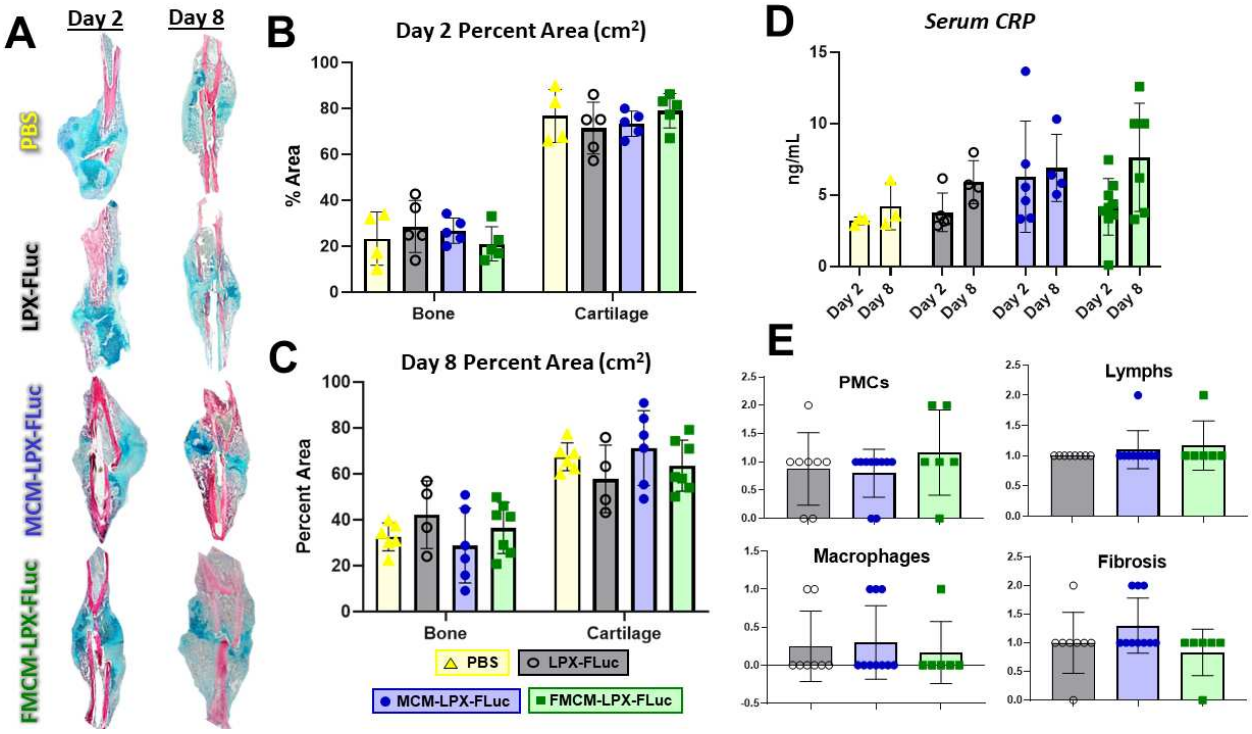

Figure 8. A). *Histomorphometric principles were used to* ***B-C).*** *quantify bone and cartilage.* ***D).*** *Systemic inflammation was measured through C-reactive protein (CRP) analysis in serum samples.* ***E).*** *Histopathology results from H&E slides 2 days after treatments.*

We next aimed to test local and systemic inflammatory responses following treatments with MCM-LPX-FLuc and FMCM-LPX-Fluc *in vivo*. While no significance was found, modulation of inflammatory markers *in vivo* showed FMCM-LPX-FLuc to trend higher in *il-1β* and *il-4* as compared to both MCM-LPX-FLuc and LPX-FLuc groups (**FIGURE 7A-B**). Additionally, systemic inflammation, measured

through C- Reactive protein (CRP) expression, revealed no significant differences found between any group in CRP values on either of the days tested (**FIGURE 8D**). H&E slides 2 days following injections were scored by a blinded pathologist for peripheral mononuclear cells, lymphocytes, macrophages and fibrosis, to reveal no differences between any of the groups nor within any inflammatory cell type (**FIGURE 8E**).

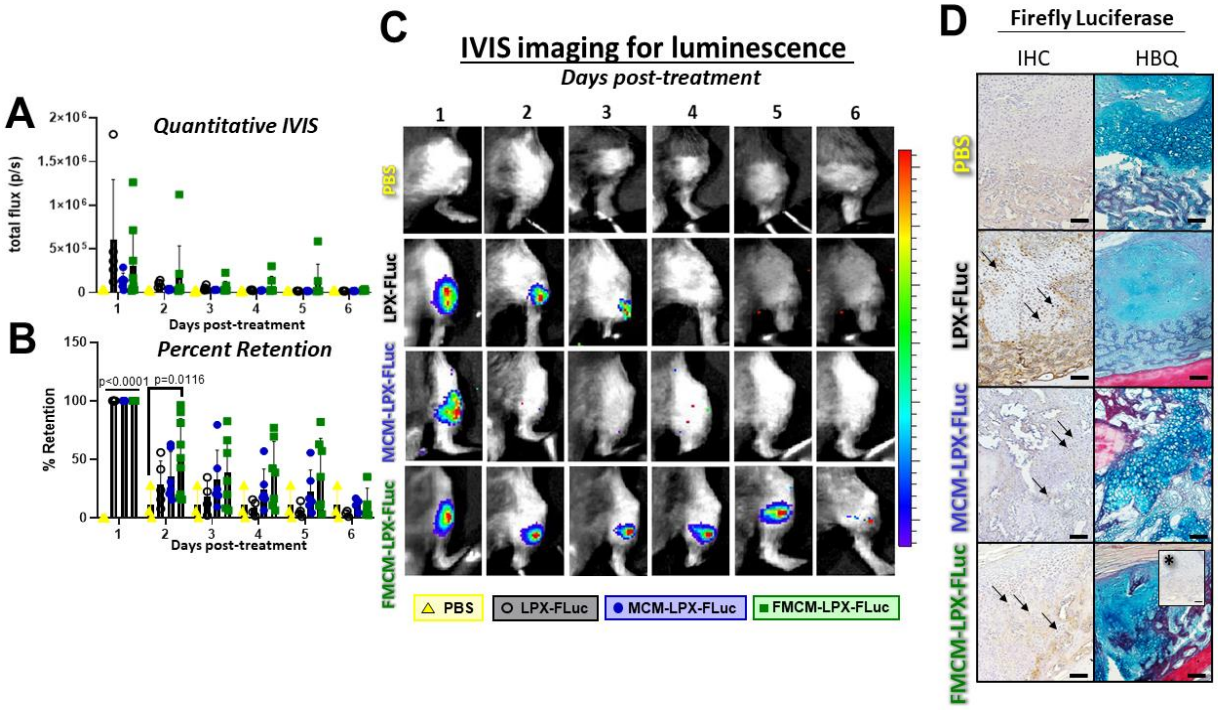

Figure 9. *IVIS images were taken daily following initial treatment locally into the fracture callus.* ***A).*** *IVIS images were then quantified and* ***B).*** *percent retention of signal was then calculated from* ***C).*** *daily IVIS images.* ***D).*** *Immunohistochemistry for firefly luciferase was performed in mice 2 days following treatment to determine cell type expressing mRNA.*

No significant differences were found between any of the groups tested in bone or cartilage tissue composition within the fracture callus at day 2 (**FIGURE 8B**) or day 8 (**FIGURE 8C**) following treatment. Interestingly, while FMCM-LPX-FLuc had the highest amount of luciferase expression *in vitro*, LPX-FLuc had the highest luciferase signal on the first day following treatment *in vivo* yet was not significant (**FIGURE 9A**). At 2 days after injection, FMCM-LPX-FLuc maintained significantly more luciferase expression than PBS, whereas all other treatment groups lost significant luciferase expression levels (**FIGURE 9 B,C**). For qualitative assessment, immunohistochemistry revealed firefly luciferase expression

within cartilage, and specifically within hypertrophic chondrocytes, and mesenchyme or fibrous tissues (**FIGURE 9D**). Arrows show examples of cells positive for expressing firefly luciferase.

II.5 Conclusions

The series of experiments characterized the ability of mineral coated microparticle (MCM) platforms to deliver mRNA encapsulated liposomes to a fracture site, showing prolonged mRNA delivery without promoting inflammation or inhibiting bone healing. FMCM-LPX-FLuc was found to prolong mRNA expression, without provoking immunogenicity or interfering with fracture repair. Protein expression following transient transfection with mRNA is sustained for only a limited time, making it an ideal platform for bone repair, as fracture healing requires a temporal upregulation of osteogenesis.[36] Further, gene expression necessitates the enhancement of mRNA stability from endonuclease-mediated decay.[37] Until recently, the use of mRNA therapeutic platforms have been limited due to challenges associated with mRNA stability, cytotoxicity of the delivery platform, and induction of innate inflammation.[38-41] Cationic lipid vesicles such as Lipofectamine™, are frequently used *in vitro* to enhance mRNA stability, yet the cytotoxicity associated with this reagent limits clinical translation.[42, 43] MCMs are comprised of calcium phosphate and biomimetic fluids, creating a mineral coating originally designed for controlled and localized delivery of growth factors.[18, 23, 24] Recently, MCM lipoplexes have been utilized to enhance mRNA and cDNA stability *in vitro*, resulting in an increased transfection efficiency, enhanced cell internalization, and reduced cytotoxicity seen as compared with cationic lipid vectors.[17] Additionally, it has previously been shown that mineral coatings may enhance osteostimulatory effects, and can enhance transfection of plasmid DNA in bone marrow stem cells.[18, 44]

We evaluated the effect of the chemical dopant fluoride on the MCM platform for mRNA delivery, Incorporating fluoride in the mineral coating has previously been shown to decelerate mineral dissolution which subsequently affected the protein binding and release kinetics for BMP2.[19, 23] Fluoride has also shown to activate of the canonical Wnt pathway, a critical pathway in bone formation.[35, 45, 46] Further,

fluoride prevents the destruction complex from sending β-catenin to be proteolytically degraded, thereby increasing the nuclear localization of β-catenin.[35] The transcription factor β-catenin modulates the expression of bone-associated genes, specifically *runt-related transcription factor 2* (*Runx2*) and *Osterix* (*Osx*).[47, 48] Importantly, while fluoride has frequently been tested as a treatment for osteoporosis and to enhance osseointegration, there is little known about fluoride's effect in fracture repair.[49-51] Our work has shown that fluoride does upregulate many known bone regulating pathways, including canonical Wnt. These promising *in vitro* results necessitate further optimization when testing for bone upregulation in an *in vivo* model for bone repair.

We evaluated the effect of FMCM-LPX on canonical Wnt activation and osteogenic gene expression by probing for bone-related genes *Axin2*, *Runx2*, *Osx* and *Ocn* following treatment. Although FMCM-LPX significantly activated the canonical Wnt pathway *in vitro*, there was no significant upregulation of Wnt *in vivo*. While fluoride has been heavily implicated in therapies that enhance bone mass, an adverse and deleterious effect at high doses (>8 mg/day) has been observed with chronic exposure.[52, 53] Thus, only moderate amounts of FMCM-LPX-FLuc were tested in this study *in vitro,* showing no cytotoxic effect on metabolic activity at any of the concentrations tested. Additionally, the concentration chosen for *in vivo* studies was previously used in a murine spinal cord injury model and was shown to not only effectively deliver mRNA, but also improve motor function.[26] Thus, further studies should be performed to analyze a dose response of chemical dopant, fluoride, in promoting bone volume.

Viral delivery of the BMP-2 gene has been found to impede fracture healing due to an immunogenic response. De la Vega *et al.* reported elevated levels of both pro-and anti-inflammatory cytokines in animals treated with synthetic RNA, yet were not elevated in animals treated with sham or protein groups.[11] Therefore we wanted to determine the immunogenic effect of MCM-LPX-FLuc and FMCM-LPX-FLuc.[3, 7] *In vitro* testing suggested no significant differences in inflammatory cytokines following treatment with MCM-LPX-FLuc and FMCM-LPX-FLuc as compared to PBS. *In vivo* testing of localized and systemic inflammation revealed that neither MCM-LPX-FLuc or FMCM-LPX-FLuc did not provoked a significant

immunogenic response. This lack of immunogenicity may be due in part to a modest amount of mRNA being delivered (10 μg) in comparison to other reports (50 μg).[11] Taken together, this set of experiments highlight the therapeutic potential of using FMCM to deliver LPX-FLuc as prolonged luciferase expression was found. Additionally, when using this biomaterial-based platform as a delivery mechanism, the FMCM-LPX-FLuc system did not interfere with fracture healing nor enhance an immune response in a murine tibia fracture healing model.

II.6 Limitations and Future Directions

This study had several limitations including use of Lipofectamine™ at various times within the shelf-life range, which impacts the transfection potency of cells as the reagent diminishes in potency with increased time on the shelf. Additionally, only one concentration of MCM-LPX-FLuc and FMCM-LPX-FLuc was tested *in vivo*. To fully elucidate the osteostimulatory responses of biomaterial platforms, MCM and FMCM, further *in vivo* studies should focus on optimizing the dose-response. Further, as this dose was selected based upon prior published *in vivo* studies in a rat spinal cord injury model, this dose was not optimized for use in a fracture healing model. By increasing the concentration of both biomaterial platforms, MCM and FMCM, and keeping the concentration of LPX-FLuc consistent, further osteostimulatory effects can be determined.

Future studies should also explore the delivery of a functional mRNA sequence involved in promoting bone, such as BMP2 or BMP7.[54, 55] Prior work using biomaterial-mediated protein delivery through MCM and FMCM platforms have shown prolonged expression of protein BMP-2 and enhanced bone volume when tested *in vivo*.[20, 24] Thus, delivering a sequence which encodes a bone-modulating protein, like BMP2, would further enhance the osteostimulatory effects seen with MCM and FMCM biomaterial delivery. Biomaterials specific for the delivery of mRNA therapeutics should maximize mRNA stability while enhancing functional outcomes. These data signify the need to further explore

osteostimulatory effects of MCM and FMCM platforms, as this can potentially reduce concentration of mRNA needed to promote bone.

II.7 References

1. Watson-Levings, R. S., Palmer, G. D., Levings, P. P., Dacanay, E. A., Evans, C. H., and Ghivizzani, S. C., *Gene Therapy in Orthopaedics: Progress and Challenges in Pre-Clinical Development and Translation.* Front Bioeng Biotechnol, 2022. **10**: p. 901317.
2. Evans, C. H., Ghivizzani, S. C., and Robbins, P. D., *Orthopaedic Gene Therapy: Twenty-Five Years On.* JBJS Rev, 2021. **9**(8).
3. De la Vega, R. E., Atasoy-Zeybek, A., Panos, J. A., M, V. A. N. Griensven, Evans, C. H., and Balmayor, E. R., *Gene therapy for bone healing: lessons learned and new approaches.* Transl Res, 2021. **236**: p. 1-16.
4. Müller, Christian W, Hildebrandt, Kristin, Gerich, Torsten, Krettek, Christian, Van Griensven, Martijn, and Rosado Balmayor, Elizabeth, *BMP-2-transduced human bone marrow stem cells enhance neo-bone formation in a rat critical-sized femur defect.* Journal of Tissue Engineering and Regenerative Medicine, 2017. **11**(4): p. 1122-1131.
5. Lieberman, Jay R, Le, Lu Q, Wu, Lilly, Finerman, Gerald AM, Berk, Arnie, Witte, Owen N, and Stevenson, Sharon, *Regional gene therapy with a BMP-2-producing murine stromal cell line induces heterotopic and orthotopic bone formation in rodents.* Journal of Orthopaedic Research, 1998. **16**(3): p. 330-339.
6. Musgrave, DS, Bosch, P, Ghivizzani, S, Robbins, PD, Evans, CH, and Huard, J, *Adenovirus-mediated direct gene therapy with bone morphogenetic protein-2 produces bone.* Bone, 1999. **24**(6): p. 541-547.
7. Egermann, Marcus, Lill, CA, Griesbeck, K, Evans, CH, Robbins, PD, Schneider, E, and Baltzer, AW, *Effect of BMP-2 gene transfer on bone healing in sheep.* Gene therapy, 2006. **13**(17): p. 1290-1299.
8. Balmayor, E. R., *Bringing gene therapy to regenerative medicine.* Mol Ther Methods Clin Dev, 2023. **30**: p. 81-82.
9. Balmayor, E. R., *Synthetic mRNA - emerging new class of drug for tissue regeneration.* Curr Opin Biotechnol, 2022. **74**: p. 8-14.
10. Zhang, Wen, De La Vega, Rodolfo E, Coenen, Michael J, Müller, Sebastian A, Peniche Silva, Carlos J, Aneja, Manish K, Plank, Christian, Van Griensven, Martijn, Evans, Christopher H, and Balmayor, Elizabeth R, *An improved, chemically modified RNA encoding BMP-2 enhances osteogenesis in vitro and in vivo.* Tissue Engineering Part A, 2019. **25**(1-2): p. 131-144.
11. De La Vega, Rodolfo E., van Griensven, Martijn, Zhang, Wen, Coenen, Michael J., Nagelli, Christopher V., Panos, Joseph A., Peniche Silva, Carlos J., Geiger, Johannes, Plank, Christian, Evans, Christopher H., and Balmayor, Elizabeth R., *Efficient healing of large osseous segmental defects using optimized chemically modified messenger RNA encoding BMP-2.* Science Advances. **8**(7): p. eabl6242.
12. Geng, Yingnan, Duan, Huichuan, Xu, Liang, Witman, Nevin, Yan, Bingqian, Yu, Zheyuan, Wang, Huijing, Tan, Yao, Lin, Liqin, and Li, Dong, *BMP-2 and VEGF-A modRNAs in collagen scaffold synergistically drive bone repair through osteogenic and angiogenic pathways.* Communications Biology, 2021. **4**(1): p. 82.
13. Kowalski, P. S., Rudra, A., Miao, L., and Anderson, D. G., *Delivering the Messenger: Advances in Technologies for Therapeutic mRNA Delivery.* Mol Ther, 2019. **27**(4): p. 710-728.
14. Nitika, Wei, J., and Hui, A. M., *The Delivery of mRNA Vaccines for Therapeutics.* Life (Basel), 2022. **12**(8).
15. Alluri, R., Song, X., Bougioukli, S., Pannell, W., Vakhshori, V., Sugiyama, O., Tang, A., Park, S. H., Chen, Y., and Lieberman, J. R., *Regional gene therapy with 3D printed scaffolds to heal critical sized bone defects in a rat model.* J Biomed Mater Res A, 2019. **107**(10): p. 2174-2182.
16. Kang, H. P., Ihn, H., Robertson, D. M., Chen, X., Sugiyama, O., Tang, A., Hollis, R., Skorka, T., Longjohn, D., Oakes, D., Shah, R., Kohn, D., Jakus, A. E., and Lieberman, J. R., *Regional gene*

therapy for bone healing using a 3D printed scaffold in a rat femoral defect model. J Biomed Mater Res A, 2021. **109**(11): p. 2346-2356.
17. Fontana, G., Martin, H. L., Lee, J. S., Schill, K., Hematti, P., and Murphy, W. L., *Mineral-Coated Microparticles Enhance mRNA-Based Transfection of Human Bone Marrow Cells.* Mol Ther Nucleic Acids, 2019. **18**: p. 455-464.
18. Choi, S. and Murphy, W. L., *Sustained plasmid DNA release from dissolving mineral coatings.* Acta Biomater, 2010. **6**(9): p. 3426-35.
19. Yu, X. and Murphy, W. L., *3-D Scaffold Platform for Optimized Non-viral Transfection of Multipotent Stem Cells.* J Mater Chem B, 2014. **2**(46): p. 8186-8193.
20. Orth, M, Kruse, NJ, Braun, BJ, Scheuer, C, Holstein, JH, Khalil, A, Yu, X, Murphy, WL, Pohlemann, T, and Laschke, MW, *BMP-2-coated mineral coated microparticles improve bone repair in atrophic non-unions.* Eur Cell Mater, 2017. **33**: p. 1-12.
21. Orth, Marcel, Shenar, Amira K, Scheuer, Claudia, Braun, Benedikt J, Herath, Steven C, Holstein, Jörg H, Histing, Tina, Yu, Xiaohua, Murphy, William L, and Pohlemann, Tim, *VEGF-loaded mineral-coated microparticles improve bone repair and are associated with increased expression of epo and RUNX-2 in murine non-unions.* Journal of Orthopaedic Research®, 2019. **37**(4): p. 821-831.
22. Martin, Hannah, Choe, Joshua, Baurceanu, Iris, and Murphy, William, *1127 Calcium phosphate biomaterials enhance immunotherapeutic mRNA delivery in melanoma*. 2022, BMJ Specialist Journals.
23. Khalil, A. S., Yu, X., Xie, A. W., Fontana, G., Umhoefer, J. M., Johnson, H. J., Hookway, T. A., McDevitt, T. C., and Murphy, W. L., *Functionalization of microparticles with mineral coatings enhances non-viral transfection of primary human cells.* Sci Rep, 2017. **7**(1): p. 14211.
24. Dang, P. N., Dwivedi, N., Yu, X., Phillips, L., Bowerman, C., Murphy, W. L., and Alsberg, E., *Guiding Chondrogenesis and Osteogenesis with Mineral-Coated Hydroxyapatite and BMP-2 Incorporated within High-Density hMSC Aggregates for Bone Regeneration.* ACS Biomater Sci Eng, 2016. **2**(1): p. 30-42.
25. Khalil, Andrew S., Yu, Xiaohua, Umhoefer, Jennifer M., Chamberlain, Connie S., Wildenauer, Linzie A., Diarra, Gaoussou M., Hacker, Timothy A., and Murphy, William L., *Single-dose mRNA therapy via biomaterial-mediated sequestration of overexpressed proteins.* Science Advances, 2020. **6**(27): p. eaba2422.
26. Khalil, A. S., Hellenbrand, D., Reichl, K., Umhoefer, J., Filipp, M., Choe, J., Hanna, A., and Murphy, W. L., *A Localized Materials-Based Strategy to Non-Virally Deliver Chondroitinase ABC mRNA Improves Hindlimb Function in a Rat Spinal Cord Injury Model.* Adv Healthc Mater, 2022. **11**(19): p. e2200206.
27. Schmittgen, T. D. and Livak, K. J., *Analyzing real-time PCR data by the comparative C(T) method.* Nat Protoc, 2008. **3**(6): p. 1101-8.
28. Wong, Sarah Anne, Hu, Diane, Shao, Tiffany, Niemi, Erene, Barruet, Emilie, Morales, Blanca M., Boozarpour, Omid, Miclau, Theodore, Hsiao, Edward C., Nakamura, Mary, Bahney, Chelsea S., and Marcucio, Ralph S., *Beta-catenin Signaling Regulates Cell Fate Decisions at the Transition Zone of the Chondro-Osseous Junction During Fracture Healing.* bioRxiv, 2020.
29. Hu, D. P., Ferro, F., Yang, F., Taylor, A. J., Chang, W., Miclau, T., Marcucio, R. S., and Bahney, C. S., *Cartilage to bone transformation during fracture healing is coordinated by the invading vasculature and induction of the core pluripotency genes.* Development, 2017. **144**(2): p. 221-234.
30. Morioka, K., Marmor, Y., Sacramento, J. A., Lin, A., Shao, T., Miclau, K. R., Clark, D. R., Beattie, M. S., Marcucio, R. S., Miclau, T., 3rd, Ferguson, A. R., Bresnahan, J. C., and Bahney, C. S., *Differential fracture response to traumatic brain injury suggests dominance of neuroinflammatory response in polytrauma.* Sci Rep, 2019. **9**(1): p. 12199.

31. Bahney, C. S., Hu, D. P., Taylor, A. J., Ferro, F., Britz, H. M., Hallgrimsson, B., Johnstone, B., Miclau, T., and Marcucio, R. S., *Stem cell-derived endochondral cartilage stimulates bone healing by tissue transformation.* J Bone Miner Res, 2014. **29**(5): p. 1269-82.
32. Hall, B.K. , *The role of movement and tissue interactions in the development and growth of bone and secondary cartilage in the clavicle of the embryonic chick.* J. Embryol. exp. Morph., 1986. **93**: p. 133-152.
33. Rivera, Kevin O., Cuylear, Darnell L., Duke, Victoria, O'Hara, Kelsey Marie, Kharbikar, Bhushan N., Kryger, Alex N., Miclau, Theodore, Bahney, Chelsea S., and Desai, Tejal A., *Localized delivery of β-NGF via injectable microrods accelerates endochondral fracture repair.* bioRxiv, 2021: p. 2021.11.16.468864.
34. Malhan, Deeksha, Muelke, Matthias, Rosch, Sebastian, Schaefer, Annemarie B., Merboth, Felix, Weisweiler, David, Heiss, Christian, Arganda-Carreras, Ignacio, and El Khassawna, Thaqif, *An Optimized Approach to Perform Bone Histomorphometry.* Frontiers in Endocrinology, 2018. **9**.
35. Pan, Leilei, Shi, Xiaoguang, Liu, Shuang, Guo, Xiaoying, Zhao, Ming, Cai, Ruoxin, and Sun, Guifan, *Fluoride promotes osteoblastic differentiation through canonical Wnt/β-catenin signaling pathway.* Toxicology letters, 2014. **225**(1): p. 34-42.
36. Agholme, F., Li, X., Isaksson, H., Ke, H. Z., and Aspenberg, P., *Sclerostin antibody treatment enhances metaphyseal bone healing in rats.* J Bone Miner Res, 2010. **25**(11): p. 2412-8.
37. DR, Schoenberg, *Mechanisms of endonuclease-mediated mRNA decay.* Wiley Interdiscip Rev RNA, 2011. **2**(4): p. 582-600.
38. Sultana, N., Magadum, A., Hadas, Y., Kondrat, J., Singh, N., Youssef, E., Calderon, D., Chepurko, E., Dubois, N., Hajjar, R. J., and Zangi, L., *Optimizing Cardiac Delivery of Modified mRNA.* Mol Ther, 2017. **25**(6): p. 1306-1315.
39. Zohra, F. T., Chowdhury, E. H., Tada, S., Hoshiba, T., and Akaike, T., *Effective delivery with enhanced translational activity synergistically accelerates mRNA-based transfection.* Biochem Biophys Res Commun, 2007. **358**(1): p. 373-8.
40. Mockey, M., Goncalves, C., Dupuy, F. P., Lemoine, F. M., Pichon, C., and Midoux, P., *mRNA transfection of dendritic cells: synergistic effect of ARCA mRNA capping with Poly(A) chains in cis and in trans for a high protein expression level.* Biochem Biophys Res Commun, 2006. **340**(4): p. 1062-8.
41. Ramunas, J., Yakubov, E., Brady, J. J., Corbel, S. Y., Holbrook, C., Brandt, M., Stein, J., Santiago, J. G., Cooke, J. P., and Blau, H. M., *Transient delivery of modified mRNA encoding TERT rapidly extends telomeres in human cells.* FASEB J, 2015. **29**(5): p. 1930-9.
42. Guo, Xiaomin, Wang, Huan, Li, Yang, Leng, Xiaopeng, Huang, Weiwei, Ma, Yanbing, Xu, Tao, and Qi, Xiaopeng, *Transfection reagent Lipofectamine triggers type I interferon signaling activation in macrophages.* Immunology & Cell Biology, 2019. **97**(1): p. 92-96.
43. Inglut, C. T., Sorrin, A. J., Kuruppu, T., Vig, S., Cicalo, J., Ahmad, H., and Huang, H. C., *Immunological and Toxicological Considerations for the Design of Liposomes.* Nanomaterials (Basel), 2020. **10**(2).
44. Choi, S., Yu, X., Jongpaiboonkit, L., Hollister, S. J., and Murphy, W. L., *Inorganic coatings for optimized non-viral transfection of stem cells.* Sci Rep, 2013. **3**: p. 1567.
45. Nelson, A. L., Fontana, G., Miclau, E., Rongstad, M., Murphy, W., Huard, J., Ehrhart, N., and Bahney, C., *Therapeutic approaches to activate the canonical Wnt pathway for bone regeneration.* J Tissue Eng Regen Med, 2022. **16**(11): p. 961-976.
46. Guo, Xiaoying, Wu, Sisi, He, Yang, Zhang, Zhiyu, and Sun, Guifan, *Effect of subchronic fluoride exposure on pathologic change and beta-catenin expression in rat bone tissue.* Wei Sheng yan jiu= Journal of Hygiene Research, 2011. **40**(3): p. 304-307.
47. Cai, Ting, Sun, Danqin, Duan, Ying, Wen, Ping, Dai, Chunsun, Yang, Junwei, and He, Weichun, *WNT/β-catenin signaling promotes VSMCs to osteogenic transdifferentiation and calcification*

through directly modulating Runx2 gene expression. Experimental cell research, 2016. **345**(2): p. 206-217.
48. Zhang, Chi, Cho, Kyucheol, Huang, Yehong, Lyons, Jon P, Zhou, Xin, Sinha, Krishna, McCrea, Pierre D, and De Crombrugghe, Benoit, *Inhibition of Wnt signaling by the osteoblast-specific transcription factor Osterix.* Proceedings of the National Academy of Sciences, 2008. **105**(19): p. 6936-6941.
49. de Gubareff, Nicholas and Platt, William R., *Influence of Sodium Fluoride on Healing of Experimental Fractures.* Archives of Environmental Health: An International Journal, 1969. **19**(1): p. 22-31.
50. SAVCHUCK, WILLIAM B., *Effects of Strontium and Fluoride on the Repair of Unreduced Humeral Fractures in the Adult Rat.* The Journal of Bone & Joint Surgery, 1957. **39**(1): p. 140-152.
51. Shteyer, A., Liberman, R., Simkin, A., and Gedalia, I., *Effect of local application of fluoride on healing of experimental bone fractures in rabbits.* Calcified Tissue Research, 1977. **22**(1): p. 297-302.
52. Du C, Xiao P, Gao S, Chen S, Chen B, Huang W and Zhao C, *High Fluoride Ingestion Impairs Bone Fracture Healing by Attenuating M2 Macrophage Differentiation.* Frontiers in Bioengineering and Biotechnology, 2022. **10**.
53. Grynpas, M. D., Chachra, D. & Limeback, H, *The action of fluoride on bone.* The Osteoporosis Primer, 2000: p. 318–330
54. Gao, X., Hwang, M. P., Wright, N., Lu, A., Ruzbarsky, J. J., Huard, M., Cheng, H., Mullen, M., Ravuri, S., Wang, B., Wang, Y., and Huard, J., *The use of heparin/polycation coacervate sustain release system to compare the bone regenerative potentials of 5 BMPs using a critical sized calvarial bone defect model.* Biomaterials, 2022. **288**: p. 121708.
55. Gao, X., Usas, A., Tang, Y., Lu, A., Tan, J., Schneppendahl, J., Kozemchak, A. M., Wang, B., Cummins, J. H., Tuan, R. S., and Huard, J., *A comparison of bone regeneration with human mesenchymal stem cells and muscle-derived stem cells and the critical role of BMP.* Biomaterials, 2014. **35**(25): p. 6859-70.

Chapter III: OPTIMIZING LIPID NANOPARTICLES FOR MRNA DELIVERY IN FRACTURES

III.1 Introduction

Liposomes continue to be one of the most explored drug delivery systems, and typically referred to as spherical phospholipid vesicles consisting of one or more lipid bilayers.[2] Since their initial fabrication in 1965, liposomes have been utilized to deliver proteins and nucleic acids, gaining considerable advancements in biomimetic properties and phospholipids over the last 30 years.[3-5] Liposomes have several distinctive advantages as delivery systems as they offer a wide array of tunable compositions, surface properties, stability profiles and can be fabricated at a relatively low cost.[3] Cationic lipids have been the most widely utilized liposomal formulation, specifically for gene delivery, as the positively charged lipids facilitates an electrostatic interaction with anionic nucleic acids. Often these liposomal-nucleic acid complexes, or lipoplexes, have been formulated in a solution containing helper lipids, which facilitate endosomal escape within the cytoplasm. Endosomal escape refers to the mechanism of pharmaceuticals released by the endosome and further as the endosome matures, it acidifies causing membrane destabilizing effects.[3, 6] Additionally, the component phospholipids of liposomes can vary in their structural components such as their hydrophilic head size, surface charge and length of their hydrophobic tail.[3] Due to the lack of knowledge on the impact that various lipid structures have in therapeutic applications, a trial and error method for selecting a liposomal formulation has been employed by several groups to determine the best lipoplex needed for each specific application.[7]

Two widely used commercially-available liposomes include Lipofectamine™ (manufacturer info) and TransIT® (manufacturer info) Lipofectamine employs cationic lipid DOSPA ({2,3-dioleyloxy-N-[2(sperminecarboxamido)ethyl]-N,N-dimethyl-l-propanaminium trifluoroacetate}) and helper lipid dioleoylphosphatidylethanolamine (DOPE), at a 3:1 ratio respectively.[3, 8] It is this multivalent cationic lipid that enhances nucleic acid packing within the liposome and the neutral helper lipid facilitates transfection efficacy.[3, 9, 10] Helper lipids alter the liposomal configuration to that of a hexagonal

conformation, allowing for membrane destabilization and thus, endosomal escape of the packaged nucleic acid.[3, 9, 11-13] While TransIT® Reagent is a proprietary blend of lipids and polymers to form lipoplexes, it is regarded as a liposome with high transfection efficacy amongst a wide array of cells.[14] Despite the high transfection efficiency, the commercially available liposomes have had limited clinical translation due to some undesirable effects. Specifically, the headgroups of cationic lipids have been found to activate pro-apoptotic and pro-inflammatory pathways.[15-17] Additionally, liposomal delivery have led to an enhance proinflammatory cytokine production in serum and the activation of the immune system.[18, 19]

Recently, there have been significant advancements in liposome nanotechnology for nucleic acid and drug delivery and these advances have resulted in the successful clinical translation of several novel and highly effective therapies. Specifically, optimization of particle size, surface charge, and increases in stability have promoted successful clinical translation.[20] Lipid nanoparticles (LNPs) have emerged as a new leader in drug delivery systems and are comprised of more complex phospholipid structures with enhanced stability.[21] The phospholipid structure of liposomes involves a phospholipid bilayer whereas the LNPs tend to have a more complex micelle-like structure comprised of other phospholipids, sterols and hydrophilic polymer, polyethylene glycol (PEG), covalently attached to a phospholipid head group.[2, 22] These PEGylated phospholipids mitigate clearance by the reticuloendothelial system, increasing blood circulation time and, importantly, enhance drug delivery.[23] While LNPs continue to cause an innate immune response with reports of toll-like receptor activation following intravenous administration, reviews have highlighted the reduced immunogenic profile seen with LNPs compared to cationic liposomes[24-27] Examples of LNPs currently used in the clinic include the FDA-approved nucleic acid drug, Onpattro, a liposomal drug encapsulating small interfering RNA that targets hepatocytes to treat amyloidosis, to the development of the highly successful COVID-19 mRNA vaccines.[28, 29]

LNPs comprised from ionizable phospholipids are positively charged at a low pH and net neutral at physiological pH.[20] Two ionizable phospholipid based LNPs that have been used in successful clinical trials are MC3 and SM102.[20] SM103 LNPs are composed of phospholipids structured with an ester

linkage located on the hydrophobic tail that was included in the design to facilitate elimination, with thus increased tolerability of the LNPs.[30] In contrast, the MC3 phospholipid-based LNP structure does not include an ester bond, which may suggest less biodegradation.[30, 31]

We hypothesized that LNPs have improved tolerability and enhanced mRNA delivery compared to that of cationic liposomes for delivery to a fracture callus by localized injection. To test this hypothesis, we compared two ionizable LNP formulations against two commercially available cationic liposomes. Differences in cationic and ionizable lipid nanoparticle formulations are shown in **FIGURE 10**. These LNPs were tested for transfection potential, immunogenicity, interference with bone healing, and biodistribution *in vitro* and in a murine fracture healing model. Together, this series of experiments explore efficacy of various lipid nanoparticles with the goal of finding a formulation best suited to effectively deliver mRNA to a fracture callus.

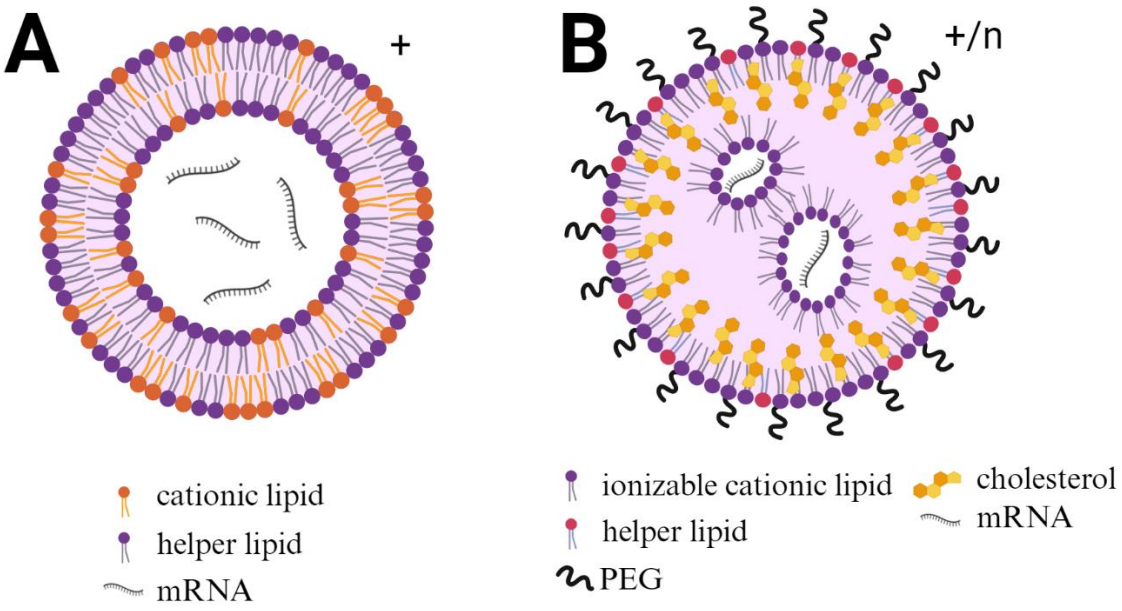

Figure 10. *Schematic depicting the differences between cationic* ***A).*** *LNPs and* ***B).*** *ionizable LNPs. Created with Biorender.com.[1]*

III.2 Methods & Materials

III.2.1 LNP Formulations

The two commercially available cationic LNP's, Lipofectamine and TransIT (see manufacturer details) were compared to one another to select the ideal cationic lipid nanoparticle to compare with the ionizable LNP's. Both Lipofectamine and TransIT were used according to manufacturer's instructions. Two different ionizable lipid nanoparticles (LNPs) were formulated for use in the following experiments to determine the most favorable formulation to deliver mRNA to the fracture callus. Firefly Luciferase mRNA was used as a reporter gene. Lipid nanoparticles containing mRNA were synthesized with the microfluidic system Benchtop Nanoassemblr. Briefly, 300 µg of mRNA were dissolved in 750 µl of sodium citrate buffer (150 mM, pH=4.5) to make up the aqueous phase, while the lipids DLin-MC3-DMA:DSPC:Cholesterol:DMG-PEG2000 (MC3), and the lipids SM-102:DOPC:Cholesterol:DMG-PEG2000 (molar ratios 50:10.5:38:1.5) (SM102) were dissolved in 250 µl of ethanol to make up the organic phase. Later, both phases were briefly warmed at 45°C, then loaded onto syringes for synthesis with the following parameters: the flow rate ratio was set at 1:3 (organic:aqueous), the total flow rate at 9ml/min, and the waste at 100 µl. The final N/P ratio (that is, the ratio between the positively charged amine groups of the ionizable lipids over the negatively charged phosphate groups of the mRNA) was set to 6 independently of the mRNA type. After synthesis, LNPs were dialyzed against 1x PBS (overnight, 4°C), then filtered with 0.22 µm syringe filters.

Physio-chemical properties of each LNP formulation were measured via dynamic light scattering (DLS, Malvern Zetasizer): 10 µl of LNPs were diluted in 990 µl of PBS for size (nm) and polydispersity index (PDI, a.u.) measurements, while the same amount of LNPs was diluted in 90µl of PBS and 900µl of double distilled water for zeta potential (mV) measurements. In all cases, the equipment was set to average three sets of measurements with 15 sub-runs each. mRNA encapsulation efficiency (EE%) was measured using the Ribogreen RNA assay. LNPs were initially diluted 1:100 in TE buffer, then subsequently diluted 1:2 in either TE buffer (to measure un-encapsulated RNA), or 2% (v/v) Triton-X in TE buffer (to burst

LNPs and measure encapsulated RNA), for a total volume of 100 µl. After a 15-minute incubation at 37°C, Ribogreen reagent was diluted 1:10 in TE buffer, then 100 µl were added to the previously diluted LNPs samples. Following a 10-minute incubation at room temperature, the plate was read at Ex/Em of 480nm/520nm. Results obtained from LNPs diluted in TE buffer were subtracted from those obtained for LNPs diluted in Triton-X to calculate the final mRNA concentration.

III.2.2 Testing transfection efficacy and cytotoxicity *in vitro*

The chondrogenic cell line, ATDC5 cells, were differentiated into hypertrophic chondrocytes and used for all *in vitro* experiments. Hypertrophic chondrocyte differentiation involved use of basal ATDC5 medium supplemented with 1 % L-Glutamine (ThermoFisher, Cat # 25030149), 10 µg/mL transferrin (Millipore Sigma, Cat # T8158-100mg), 3 x 10^{-8} M Selenite (Sigma Aldrich, Cat # S5261-10G), 0.2 mM Ascorbic Acid (Sigma Aldrich, Cat # A8960-5G), and 10 µg/mL Insulin (Millipore Sigma, Cat # I2643-25 MG) treated on cells for 7 days with replacing media every 2-3 days.[32] To measure transfection efficacy of the MC3 LNPs as compared to Lipofectamine™ complexes, reporter mRNA, firefly luciferase (FLuc) mRNA, was used to track transfection over a 48 hour time period. Lipofectamine™ was used according to manufacturer's protocol. 0.25 µg FLuc mRNA was used per well and Lipofectamine was used at 2 µL of reagent/well for the Lipofectamine treated groups. MC3 was delivered based on the encapsulation efficiency of FLuc mRNA and was also delivered at 0.25 µg/well. Cells were used at passage 5 and under for all experiments. ATDC5 cells were maintained using basal medium DMEM/F12 (Thermo Fisher, Cat# 11320033), 5 % fetal bovine serum (FBS, Thermo Fisher, Cat# 16000044) and 1 % penicillin/streptomycin (P/S, Thermo Fisher, Cat# 15140122). For all *in vitro* experiments, ATDC5 cells were plated at 20,000 cells/well in 12 well plates. Prior to transfection experiments, chondrocytes underwent serum starvation using basal media OPTI-MEM (Thermo Fisher, Cat# 31985070) 0.5 % FBS and 1 % P/S for 24 hours. All transfection protocols were executed using serum-free media, OPTI-MEM supplemented with 1 % P/S. The cytotoxic effects were assessed using PrestoBlue™ Cell Viability Reagent (Thermo Fisher, Cat#

A13261) according to the manufacturer's protocol. To quantify the number of metabolically active cells, a standard curve of ATDC5 cells was created and the absorbance values were related back to the number of cells for quantitation. The plate was read at 570 nm with a reference wavelength at 600 nm using a plate reader (TECAN infinite M200 Pro). RNA was isolated and made into cDNA as described previously using techniques described in Section II.2.4, and qRT-PCR was performed for *firefly luciferase* and *il-1β.*

hMSCs were grown in alphaMEM (VWR, Cat # 50-012-PC) supplemented with 10% FBS (Gibco, Cat # 16000-044) and 1% Penicillin/Streptomycin (Hyclone, VWR, Cat # SV30010). mRNA and LNPs were diluted in OptiMEM (Gibco, Cat # 11058021), delivered at 100 ng mRNA/well to human BM-MSCs and incubated overnight. Cells were treated for 24 hours and then were washed with PBS 2X and lysed (5:1 PBS to CCLR) (Promega, Cat # E1531). Firefly Luciferase activity was assayed by by mixing Firefly luciferase assay buffer (50mM Tris, 10mM MgSO4. 6 mM D/L cysteine, 20 µM Sodium Pyrophosphate, 1mM EDTA and 2g/L Bovine serum album) with ATP (1mM Final), and D-Luciferin (150 µg/mL). 100 uL of this assay buffer was added to 20 uL of lysate and read on a plate reader.

Celltiter Blue Reagent (Promega, Cat # G8080) was mixed 1:5 with cell culture media and incubated for 1 hour. Media was then collected and read on a plate reader per manufacturers recommendation. Metabolic activity was compared within treatment and untreated control groups. The CellTiter-Blue® Reagent is a buffered solution containing highly purified resazurin. The ingredients have been optimized for use as a cell viability assay. The spectral properties of CellTiter-Blue® Reagent change upon reduction of resazurin to resorufin. Resazurin is dark blue in color and has little intrinsic fluorescence until it is reduced to resorufin, which is pink and highly fluorescent (579Ex/584Em).

III.2.3 Murine tibia fracture and stabilization model

In vivo experiments were approved by and conducted in compliance with the Institutional Animal Care and Use Committee at Colorado State University (CSU). Mice were socially housed throughout the in-life period and permitted free ambulation. Mid-shaft tibial fractures were created in adult (12-14 weeks),

male C57BL/6J mice (Charles River # 027). (Describe treatment groups and numbers here) All animals received a pre-surgical analgesic, Buprenorphine SR (ZooPharm), at a dose of 0.6-1.0 mg/kg. Mice were placed under general anesthesia using inhaled 1-5 % isoflurane to effect. Left hind limbs were shaved and sterilely prepared using 70 % alcohol wipes and Chlorhexidine surgical scrub solution, repeated for a total of 3 times. Lubrication was provided for the eyes of each mouse using artificial tears ointment (Bausch & Lomb) and mice were then transferred to a heated operating table. Using aseptic technique, an incision was made along the tibia, and a hole was made at the top of the tibial plateau using a 23-gauge needle. An intermedullary pin (sterilized insect pin) was inserted through the hole made from the tibial plateau through the tibial cavity and into the distal tibia. One small hole was created in the mid-shaft of the tibia using a Dremel and pressure was applied to both proximal and distal ends to fracture the tibia to create a fracture which was not stabilized.{Wong, 2020 #13;Hu, 2017 #32} The surgical incision was then sutured using 5-0 Biosyn Sutures (Covidien, Cat #5687) and one surgical skin staple was applied over the skin incision to protect against chewing. A local anesthetic, 0.25% Bupivacaine Hydrochloride (NovaPlus, cat # RL-7562), was applied topically after the initial staple was placed. Mice were closely monitored for pain and signs of infections for 72 hours following the surgery. All treatments were suspended in 25 μL sterile PBS and vortexed before injecting. All experimental and control treatment groups were injected on day 6 post-fracture into the fracture callus using an insulin syringe (BD, Cat # 324702). Animals were sacrificed according to approved euthanasia protocols 2 days following injection into the fracture callus.

III.2.4 Localized injections of cationic lipoplexes

First, we performed a pilot study using a murine tibia fracture and stabilization model as described above to determine which commercially available cationic lipid nanoparticle was most effective for delivery of mRNA to the fracture callus and therefore appropriate to use to compare with ionizable LNP. First, 10 μg/mouse firefly luciferase (FLuc) mRNA as a reporter gene was encapsulated with either Lipofectamine™ MessengerMax or TransIT® per manufacturer's instructions. Following lipoplex formulation of

Lipofectamine™-FLuc or TransIT®-FLuc, 100 μg/mouse of MCMs were added and the lipoplex-MCM formulations were then incubated for 30 minutes at RT with moderate shaking. The negative control was sterile-filtered phosphate buffered saline (PBS). Following the incubation period, 50 μL of each MCM-lipoplex was injected locally at the site of the fracture callus (n=2/treatment).

III.2.5 Localized injections of MCM-LNPs

Initially, we tested the capacity for FMCM and MCM (as described in the previous chapter) in combination with cationic lipid nanoparticles to enhance or prolong mRNA transfection efficacy. Next, we compared cationic and ionizable lipid nanoparticles in combination with MCM or FMCM. Briefly MC3 LNPs were synthesized as described in Section III.2.1, using firefly luciferase 10 μg/mouse of firefly luciferase mRNA was used for *in vivo* studies. MC3 LNPs encapsulating firefly luciferase mRNA were incubated with MCM or FMCM (100 μg/mouse or 100 μg/well) for 30 minutes at RT with moderate shaking. The negative control was a sterile-filtered phosphate buffered saline (PBS) group. Following the incubation period, test articles were vortexed for 10 seconds and 25 μL of each MCM-MC3 or FMCM-MC3 combination was injected locally at the site of the fracture callus (n=5/group; n=3 for all PBS groups)

III.2.6 Localized injections of ionizable LNPs

To determine the ability of ionizable MC3 and SM-102 LNPs to deliver mRNA (without MCM or FMCM), MC3 and SM102 LNPs were concentrated to allow for a 25 μL injection volume using 100K protein concentrators (Sigma Aldrich, Cat # UFC510024), spun at 5000 x g for 5-10 minutes. Following fracture and stabilization, all treatments were injected on day 6. Similarly, to previous experiments, firefly luciferase (FLuc) mRNA was used as a reporter gene at 10 μg/mouse. Lipoplex delivery systems delivered 10 μg of encapsulated mRNA but were not normalized to deliver the same amount of phospholipid. Negative control groups included a sterile-filtered phosphate buffered saline (PBS) group. All treatments

were vortexed for 10 seconds prior to aspirating into the Hamilton 1800 series syringe and were then injected locally into the fracture callus region (n=5/treatment groups; n=3 for each PBS group).

III.2.7 Transfection efficacy and kinetics *in vivo*

Transfection efficacy and kinetics were measured using firefly luciferase mRNA and protein expression was quantified using IVIS bioluminescence imaging. IVIS imaging was performed 24 and 48 hours following injection. IVIS imaging was performed daily to quantitatively assess the magnitude and duration of luciferase expression from the time of delivery of reporter mRNA. All mice were anesthetized using isoflurane and injected with 100 µL of firefly luciferase substrate, D-luciferin, subcutaneously at 10 mg/mL in PBS. Continued isoflurane was maintained at 1-5% and mice were imaged 5 minutes following subcutaneous injection of D-luciferin. Bioluminescence was acquired using the 'Auto' setting and regions of interest were measured for bioluminescence using LivingImage software.

III.2.8 *In vivo* immunogenicity and fracture healing interference measurements

To further examine the immunogenic and osteogenic effects after delivering MC3 and SM-102 LNPs, qRT-PCR was performed on various markers. To isolate RNA from the fracture callus, the tissue was dissected, minced into small pieces and placed in 1 mL of TRIzol. The tissues were then homogenized using IKA Tissue Homogenizer (IKA, Cat# 0003737001) using a speed of 5 for 3 minutes, or at least until all large chunks were broken down. RNA was isolated using TRIzol™ Reagent (ThermoFisher, Cat# 15596026) according to the manufacturer's guidelines. RNA was then quantified by reading the absorbance values at 260 and 280 nm. 1 µg of RNA was then synthesized into cDNA using qScript cDNA SuperMix (QuantaBio, Cat# 95048-025). Next, primers were designed and are listed in **TABLE 4**. Quality measurements were used to confirm primer specificity and appropriate reaction temperatures by running PCR using DreamTaq Green PCR Master Mix (2X) (ThermoFisher, Cat# K1081) using a 3-step method with denaturation at 95°C for 30 sec, annealing at 60°C for 30 secs and extension at 72°C for 1 minute. The

bands were analyzed on a 1.5 % agarose gel with 2 µL GelStar Nucleic Acid Stain (Lonza, Cat # 50535) run at 150V for 25 minutes. Quantitative real-time PCR was run using SYBR Green Master Mix (Bio-Rad, Cat#1725270) to detect the amplified DNA. qRT-PCR was performed on a StepOnePlus™ instrument (Applied Biosystems). To analyze the output Ct values, the reference housekeeping gene (β-2-modulin) was used to determine ΔCt values. The value of 2-(ΔΔCt) was calculated for all graphs and to determine statistical significance. All 2(-ΔΔCt) values less than 1.0, were calculated as -1/(2(-ΔΔCt)) as followed and described in Schmittgen *et al.*[28] Local inflammatory response was measured using qRT-PCR while systemic inflammation was tested using a C-Reactive Protein (CRP) ELISA kit (R&D Systems, Cat# MCRP00) according to manufacturer's instructions on the serum collected at day 1 and 10 post-treatment.[33]

Table 4. *Primer sequences validated for use in qRT-PCR for use in all LNP treated fracture calluses.*

Gene	**Forward**	**Reverse**
β-2-modulin	ATACGCCTGCAGAGTTAAGCA	TCACATGTCTCGATCCCAGT
Collagen 10a1 (col10a1)	TTCTGCTGCTAATGTTCTTGACC	GGGATGAAGTATTGTGTCTTGGG
Alkaline Phosphatase (alp)	GTTGCCAAGCTGGGAAGAACAC	CCCACCCCGCTATTCCAAAC
interleukin-1β (il-1β)	TGGACCTTCCAGGATGAGGACA	GTTCATCTCGGAGCCTGTAGTG
Tumor necrosis factor- α (tnf α)	GGTGCCTATGTCTCAGCCTCTT	GCCATAGAACTGATGAGAGGGAG
firefly luciferase (fluc)	GTGGTGTGCAGCGAGAATAG	CGCTCGTTGTAGATGTCGTTAG

III.2.9 Biodistribution Study

IVIS imaging was performed at 6 and 18 hours following treatments to determine biodistribution. To acquire *ex-vivo* IVIS images, mice were sacrificed according to approved euthanasia protocols after 18 hours following localized treatments. Immediately following live IVIS imaging, fractured limb, liver, lung, spleen and kidney were harvested and imaged *ex-vivo*. Bioluminescence was acquired using the 'Auto' setting and regions of interest were measured for bioluminescence using LivingImage software. All tissues were then flash frozen immediately using liquid nitrogen and stored at -80°C.

III.2.10 Statistics

Animal sample size was determined *a priori* using the mean and standard deviation from our preliminary data, where a power analysis was conducted using R Studio to determine that 5 mice/group/time are required for IVIS outputs (total flux) to achieve a power level >80% with an effect size η^2=0.99 and a significance level of 5% (**SUPPLEMENTAL FIGURE 2**). Statistical analysis was performed using Graph Pad Prism 8. Log10 transformation was performed on all IVIS outputs and all statistics was executed on log transformed values. Data were plotted so that each sample represented a single dot on each graph. The bar indicates the mean with error bars representing standard deviation. Statistical difference was determined by ANOVAs and all post-hoc comparison performed using Tukey's HSD test.

III.3 Lipofectamine™ prolongs expression of FLuc at the fracture site as compared to TransIT

Both TransIT and Lipofectamine were tested for transfection efficacy. Following quantification of the IVIS images, the FLuc-Lipofectamine™-MCM group had the highest and most prolonged expression 24 hours following injection and expression was localized to the fracture site (**FIGURE 11**). Because of this efficacy, only cationic lipofectamine was used in subsequent experiments.

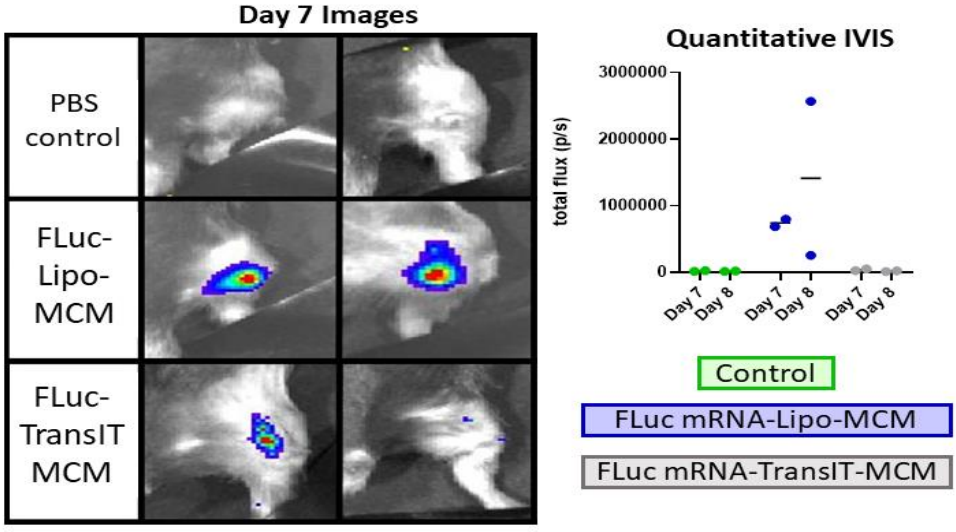

Figure 11. *IVIS images of two manufactured lipoplexes, Lipofectamine™ and TransIT®, revealed that Lipofectamine™ had consistently higher expression in all mice and at all time points tested.*

III.4 MC3-MCM/FMCM complex did not prolong transfection *in vivo*

Lipofectamine and MC3 LNPs were tested for their transfection potency using hypertrophic chondrocytes *in vitro*. In characterizing cytotoxicity following delivery of the lipoplexed FLuc mRNA, Lipofectamine™ was found to have significantly less cells at 6 and 24 hours following delivery as compared to the no treatment group, signifying some level of cytotoxicity with Lipofectamine delivery system (**FIGURE 12A**). No significant differences were found between MC3 LNPs and the no treatment group at any time point tested.

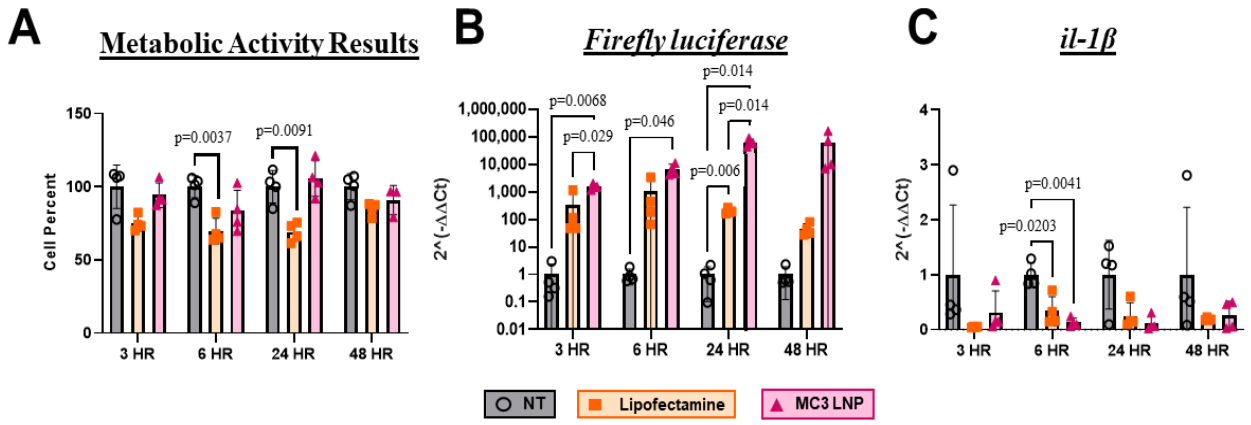

Figure 12. *MC3 LNP and Lipofectamine™ were tested in* ***A).*** *metabolic activity,* ***B).*** *firefly luciferase expression, and* ***C).*** *il-1β expression in hypertrophic chondrocytes in vitro.*

To evaluate transfection efficiency, temporal RNA expression for the reporter construct *firefly luciferase* was evaluated from 3 to 48 hours after delivery. MC3 LNPs delivering firefly luciferase mRNA had significantly higher luciferase expression at 3, 6 and 24 hours following treatment as compared to the no treatment group (**FIGURE 12B**). Additionally, MC3 LNPs had more luciferase expression than Lipofectamine™ groups at 3 and 24 hours (*p=0.0291, p=0.0143* respectively). Pro-inflammatory factor *il-1β* was quantified through qRT-PCR revealing that MC3 LNPs had the least amount of *il-1β* expression at 6 hours following treatment compared to the no treatment group (*p=0.0041*) (**FIGURE 12C**).

MC3 LNPs were then tested as an mRNA delivery vehicle in combination with MCM and FMCM technology and to further localize mRNA expression. Since our data support that MC3 LNPs have better transfection when tested *in vitro*, we then used these LNPs to generate an mRNA lipoplex to replace the

mRNA-Lipofectamine™ lipoplex that was used in studies within Chapter II. MCM-MC3 and FMCM-MC3 formulations were first tested *in vitro* in hypertrophic chondrocytes, resulting in FMCM-MC3 to significantly enhance transfection efficacy of MC3 LNPs at 6 hours after treatment (**FIGURE 13A**). Taken these promising results, we tested the MCM-MC3 and FMCM-MC3 in our murine tibia fracture model. Despite the promising *in vitro* results, the FMCM-MC3 group did not lead to significantly more transfection efficacy nor prolonged transfection *in vivo* (**FIGURE 13B-C**). The first two days following treatments, all groups (MC3, MCM-MC3 and FMCM-MC3) were found to have significantly more luciferase expression over the PBS control (*p=0.0062*, *p=0.0006*, *p=0.0005* respectively for day 1). All other p-values can be found on **FIGURE 13**.

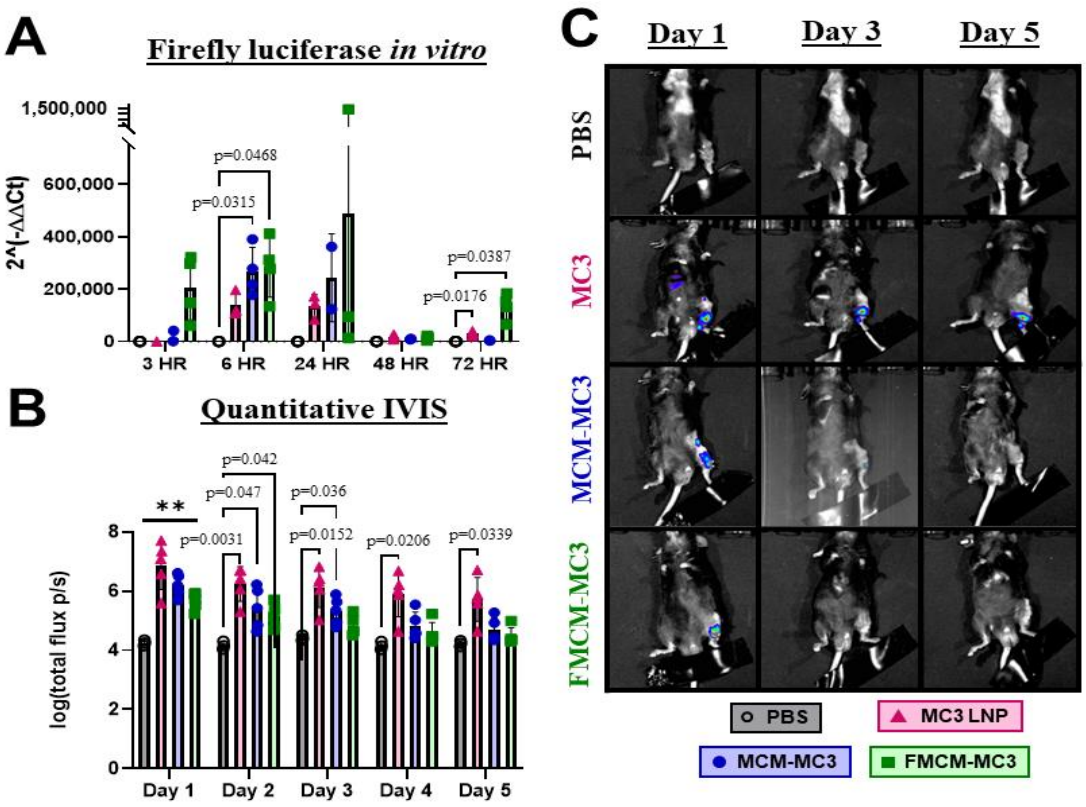

Figure 13.*MCM and FMCM were tested in their capacity to enhance MC3 LNPs in vitro and in vivo.* ***A).*** *First, MCM-MC3 and FMCM-MC3 formulations were tested for firefly expression in vitro using hypertrophic chondrocytes. Next, the formulations were tested in a murine fracture model and* ***B).*** *daily IVIS images were taken and* ***C).*** *quantified.*

No significant differences were detected between the treatment groups tested at day 1, yet MC3 was found to have significantly more luciferase signal over FMCM-MC3 at day 2, day 3 and day 4 (*p=0.042; p=0.0337; p=0.049* respectively). In fact, MC3 LNPs maintained significance over PBS control for all the 5 days tested, where MCM-MC3 lost significance over PBS at day 4.

III.5 SM-102 LNPs improved mRNA delivery characteristics as compared with MC3 LNPs *in vitro* and *in vivo*

SM-102 and MC3 LNPs were generated and then characterized to determine differences between the two formulations. First, we characterized the LNPs through size, polydispersity index (PDI) and surface charge (**FIGURE 14A**). MC3 and SM-102 LNPs were of similar size, with MC3 LNPs being 10 nm larger in diameter than SM-102 LNPs (97 nm and 87 nm respectively), but both under 100 nm according to current best practices. PDI reveals a monodisperse LNP sample set, as both are under a PDI of 0.15. In this application, a PDI of 0.0 suggests a perfectly uniform population and a PDI of 1.0 suggests a heterogenous population of particle size.[34] Lastly, the zeta potential, or the surface charge of nanoparticles in solution, analysis resulted in near net neutral surface charges for both of the LNPs. It has previously been published that net neutral nanoparticles fall within the range of -10 and +10 mV, while cationic and anionic nanoparticles are characterized as having a surface charge of ±30 mV and over/under.[35]

Transfection efficacy was assessed in human bone-marrow MSCs using firefly luciferase as a reporter gene to track and measure level of transfection. SM-102 was found to have significantly more transfection compared to MC3 LNPs and the no treatment group (**FIGURE 14B**). While MC3 did have significantly higher transfection when compared the PBS treatment group (*p=0.0411*), SM-102 LNPs was found to have the highest transfection in *in vitro* testing. No significant differences were determined between treatment groups in metabolically active cells revealing no cytotoxic effects with any treatment (**FIGURE 14C**).

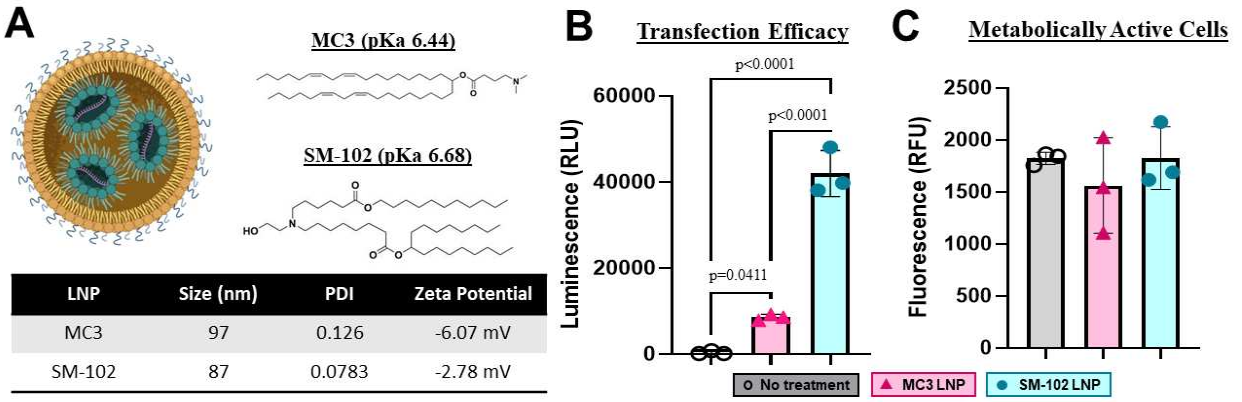

LNP	Size (nm)	PDI	Zeta Potential
MC3	97	0.126	-6.07 mV
SM-102	87	0.0783	-2.78 mV

Figure 14. *Characterization of MC3 and SM-102 ionizable LNPs.* ***A).*** *structure and characteristics,* ***B).*** *transfection efficacy of firefly luciferase loaded LNPs, and* ***C).*** *metabolic activity of LNPs in vitro. Schematic created with Biorender.com.*

Due to the promising transfection kinetics seen *in vitro*, both LNP formulations were tested in our murine tibia fracture model to assess transfection efficacy and kinetics. Daily IVIS images were taken of all treatment groups (**FIGURE 15A**) and the bioluminescence was quantified (**FIGURE 15B**) within the standardized region of interest (ROI). There was significantly greater luminescence within the ROI in the SM-102 LNPs group as compared with PBS controls at days 1-7 after delivery (**FIGURES 15A, B**). The MC3 LNPs group had significantly higher bioluminescence as compared with PBS controls on days 1-5 and day 8 following injection. There were no significant differences determined between MC3 and SM-102 treatment groups at any timepoint during analysis. SM-102 LNPs sustained transfection for 7 days following treatment as compared to MC3 LNPs which sustained transfection for 5 days. Further measures of transfection were taken as firefly luciferase RNA expression was quantified within the fracture callus (**FIGURE 15C**). Although SM-102 LNPs had the highest expression 1 day after injection, this difference did not reach significance.

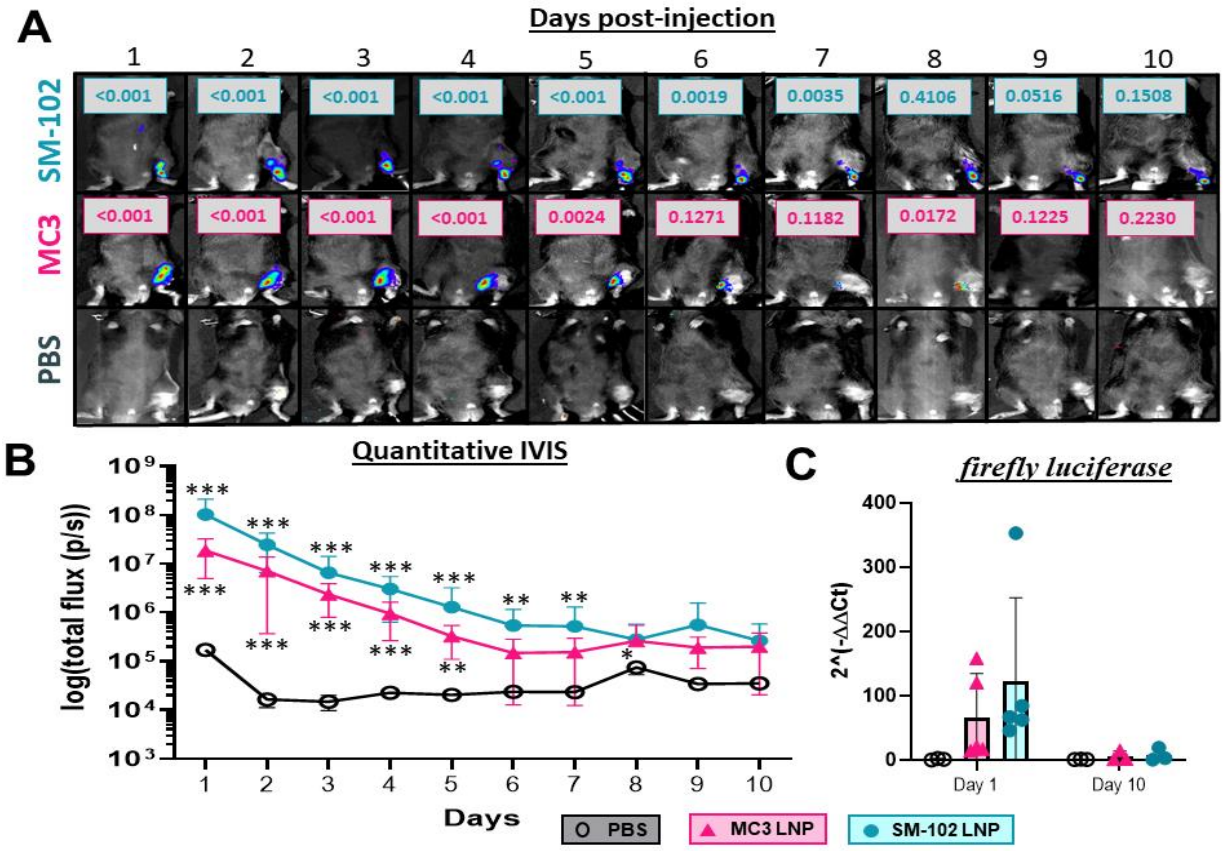

Figure 15. A). *Daily IVIS images after delivery of MC3 and SM-102 LNPs, and* ***B).*** *log-transformed quantitative IVIS.* ***C).*** *Firefly luciferase RNA expression was assessed within the fracture callus.*

Local inflammatory response to the LNPs was evaluated within the fracture callus using gene expression analysis. No significant differences were determined in *il-1β* levels within the fracture callus between any groups (**FIGURE 16A**). MC3 LNPs had significantly higher *tnfα* expression at day 10 following treatments as compared to both PBS and SM-102 treatment groups (**FIGURE 16B**). To assess systemic inflammatory response from delivery of LNPs, C-reactive protein (CRP) was measured in the serum 1 and 10 days following treatments (**FIGURE 16C**). Here, both LNP treatment groups showed elevations on day 1 injection relative to PBS, with MC3 LNPs having significantly elevated CRP levels, as compared with the PBS and SM-102 groups. No significant differences were found between any treatment group at 10 days after injection. To measure effect on fracture healing, the expression of osteogenic genes *alp* and *col10a1* were compared between groups. No significant differences were determined in the

expression of the early osteogenic marker *alp.* However, MC3 LNPs were found to have significantly less *col10a1* expression than the SM-102 group at days 1 and 10 post injection. No significant differences in *col10a1* were found between the MC3 and PBS groups, nor SM-102 and PBS at any time point.

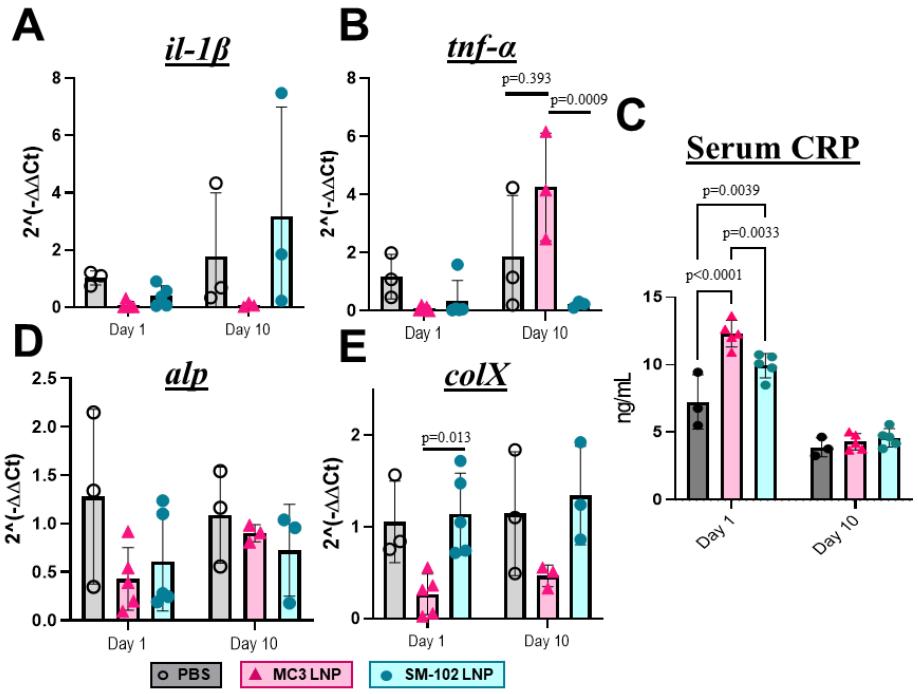

Figure 16. *Gene expression analysis of the fracture callus through qRT-PCR for markers of* ***A-B).*** *inflammation with il-1β and tnf-α, and* ***D-E).*** *osteogenesis with alkaline phosphatase and collagen 10a1 (colX).* ***C).*** *Additionally, C-reactive protein in serum was analyzed at days 1 and 10 after treatment.*

III.6 Biodistribution remained largely localized to the fracture site following LNP injection

A biodistribution study was performed to characterize the distribution of the LNPs following a localized injection to the site of the fracture callus. It is important to determine if the LNPs remained localized or if they were subjected to distribute through the reticuloendothelial system. Significantly more luciferase signal was determined at the fracture site after injections at 6 and 18 hours between MC3 LNPs and PBS control and additionally between SM-102 LNPs and PBS control (**FIGURE 17A,C**). *Ex-vivo* IVIS images depicted some luciferase signal in the liver, yet was not significantly different when compared to the PBS group (**FIGURE17B,D**). Further, no significance was noted in luciferase expression between any

of the groups tested in lung, spleen, or kidney tissues. MC3 and SM-102 had significantly higher luciferase signal in the fractured limbs when compared to the PBS control, but no significance was determined between the MC3 and SM-102 LNP groups.

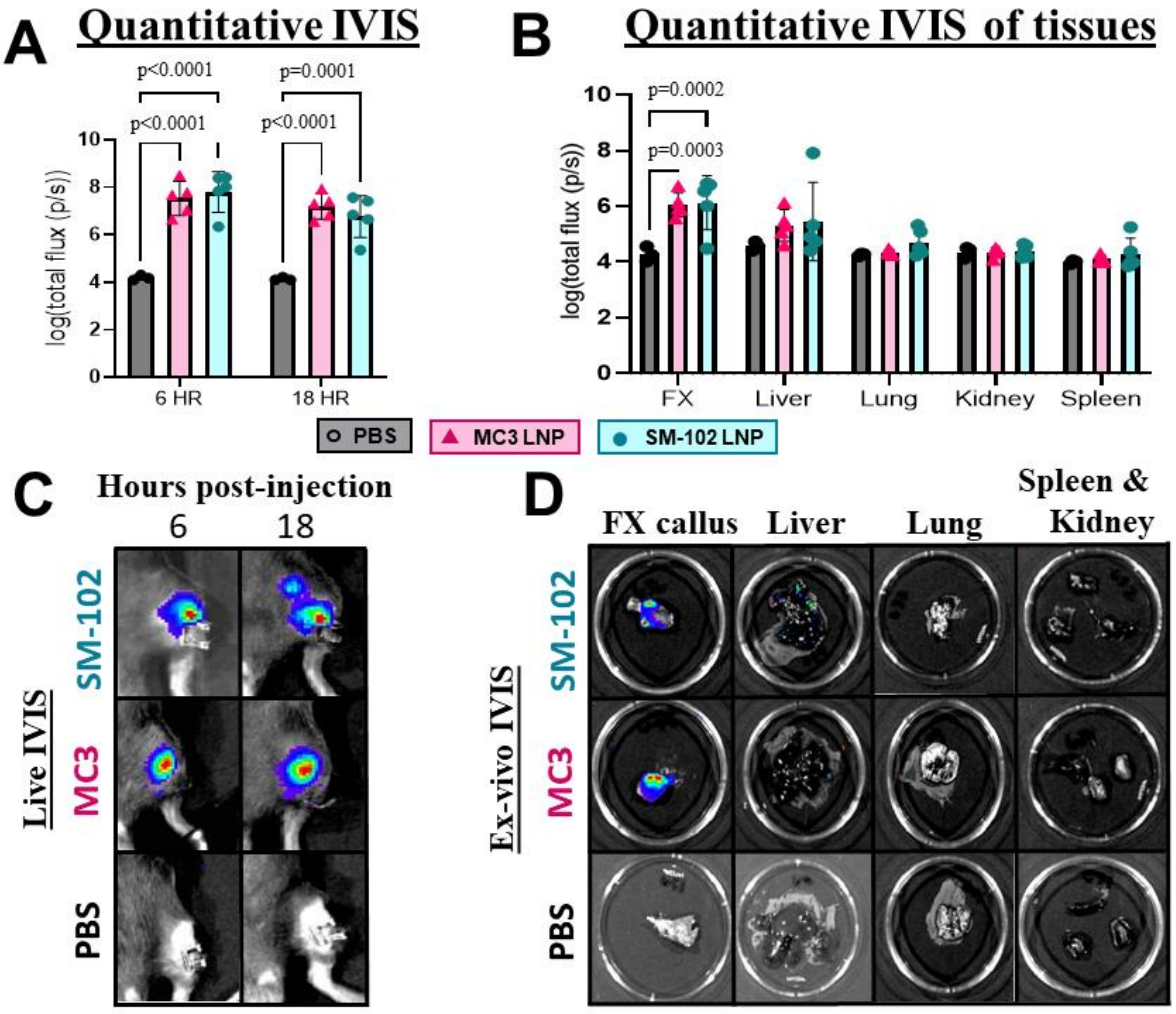

Figure 17. *Biodistribution study was performed to determine if the injections were localized to the fracture.* ***A,C).*** *Live IVIS imaging was performed at 6 and 18 hours following injections and* ***B,D).*** *ex-vivo IVIS was performed on various organs and tissues.*

III.7 Conclusions

In orthopaedic applications, viral gene therapy has made tremendous strides as evidenced by the success of early in-human trials showing efficacy of functional gene(s) to treat rheumatoid arthritis and osteoarthritis (OA).[36-39]. One such trial in patients suffering from rheumatoid arthritis was aimed to

reduce inflammation within the microenvironment through *ex-vivo*, intra-articular delivery of autologous transduced fibroblasts derived from the synovium using a retrovirus containing inhibitor of interleukin-1, interleukin-1 receptor antagonist (IL-1Ra) cDNA.[38, 40] Despite these successful clinical trials, the logistics of the *ex-vivo* treated synovium and the expense of viral gene therapy treatments have limited their clinical successes.[39] Several clinical trials for orthopaedic pathologies remain ongoing, however, to date, poor safety profiles and strong immunogenic responses using viral delivery systems have continued to hinder progression to FDA approval in the US.[44]

Non-viral gene delivery systems have the potential to overcome the challenges associated with viral gene therapy, with some of the main advantages being reduced immunogenicity and stronger safety profiles.[45, 46] Delivering mRNA to elicit a functional outcome is a promising approach for bone regeneration. However, for mRNA-based gene therapies to be successful in promoting the desired biological response, mRNA molecules must reach the targeted tissue and cell types. Targeted delivery and stability remain a critical need in mRNA therapeutics.[36, 47] The COVID vaccines successfully overcame this limitation by utilizing LNPs to deliver mRNA safely and efficaciously [28, 48] The 'bioinspired' design of the LNPs are advantageous due to their biocompatibility as they contain naturally occurring components, like cholesterol.[49] However, the use of mRNA delivery to address musculoskeletal diseases, specifically for bone healing remains a nascent field.[47] The recent work utilizing LNPs for use in bone tissue engineering have involved the use of surgically implanted collagen scaffolds to slow the release kinetics of the mRNA being delivered is one example of a successful approach, however an injectable system that does not require surgical implantation would be ideal, as this would mitigate risks and healthcare costs associated with surgery. [49-52] Another strategy using bone-targeting liposomes to deliver bisphosphonates locally in impaired fracture healing models increased liposomal localization to the site of the fracture without the use of a scaffold, yet immunogenicity was not tested.[53] The central advantageous feature of ionizable LNPs giving rise to their high transfection capacity is their pKa between 6 and 7, which enhances endosomal

escape of the mRNA through electrostatic interaction of the endosomal phospholipids and cationic ionizable lipids.[54, 55]

In this series of experiments, the cationic manufactured liposome Lipofectamine, superior transfection efficacy as compared to TransIT following localized injection to a fracture callus. Lipofectamine was then compared with 2 LNPs, MC3 and SM-102, to better understand reporter mRNA transfection efficiency within the fracture callus, immunogenicity and biodistribution following localized injection. Both MC3 LNPs and SM-102 LNPs were formulated with the same concentration of cholesterol, helper lipids, and pegylated lipids to ensure direct comparison of the two LNP formulations. We saw superior efficacy using ionizable LNPs as compared to manufactured liposomes (Lipofectamine and TransIT) and we proceeded with optimizing ionizable LNPs for fracture healing applications.

Charged LNPs, such as Lipofectamine and TransIT, often distribute to the lung and spleen when administered intravascularly *in vivo* putting these systems at risk of off-target effects.[56] Other studies have shown that intramuscular injections of neutral LNPs distribute to the liver, suggesting similar off-target risks.[31] In our work, a localized injection within the fracture callus was selected to enhance site-specificity.[31, 56, 57] Despite using a localized route of administration, mRNA-based pharmaceuticals have been found to diffuse within circulation and thus provoke an immunogenic response.[57] Due to the promiscuity of LNPs seen following localized administration, it is imperative to examine the biodistributive properties of pharmaceuticals. In this study, localized treatments of neutral LNPs did not show significant luciferase expression in liver, lung, spleen or kidney when tested *ex-vivo*.

SM-102 LNPs were found to enhance reporter mRNA transfection in *in vitro* When examining both formulations in our murine fracture and stabilization model, SM-102 LNPs prolonged transfection for a longer duration as compared with the MC3 formulation. This further signifies that SM-102 LNP improved stability of mRNA to facilitate greater endogenous protein expression. Taken these results, mRNA delivery with SM-102 LNPs has the potential to promote a greater biological outcome in a fracture healing application.

We initially felt it would be advantageous to combine mRNA-LNP with MCM or FMCM (see Chapter II) to minimize immune response and further localize the lipoplexes to the site of the fracture callus. Despite promising *in vitro* results showing enhanced transfection potential with combined FMCM-MC3 LNPs, no beneficial effect was seen when combining these technologies *in vivo*. In fact, the combination of these technologies reduced the transfection kinetics of MC3 LNPs. This may have been due in part to centrifugation requirements of MCM technologies which reduces the volume to suit a mouse fracture site, Further, mRNA-LNP complexes which were not bound to MCM may have undergone destabilizing effects with centrifugation or were removed through aspiration and resuspension of the solution. Importantly, this may signify insufficient interaction between MCM and ionizable LNPs which requires further optimization to facilitate proper binding of these two technologies.

Interestingly, when testing the use of combining MC3 LNPs with optimized mineral coated microparticles as developed in Chapter II, no beneficial effects were found in enhanced transfection. Further, it was proposed to combine these two technologies as an alternative approach for evading an immune response and additionally to further localize the lipoplexes to the site of the fracture callus. Despite promising *in vitro* results showing enhanced transfection potential with combined FMCM-MC3 LNPs, no beneficial effect seen when combining these technologies *in vivo*. In fact, the combination of these technologies reduced the transfection kinetic potential of MC3 LNPs. This may have been due in part to centrifugation requirements of MCM technologies which reduces the volume to suit a mouse fracture site. As this may signify insufficient interaction between MCM and ionizable LNPs, further optimization needs to be performed to facilitate proper binding of these two technologies.

Immunogenic effects, and any potential interference in osteogenesis were also tested *in vitro* and *in vivo*. No significant cytotoxic effects were noted when testing either LNP formulation *in vitro,* yet MC3 LNPs showed significantly more pro-inflammatory expression within the fracture callus. Despite MC3 being the only formulation to provoke a localized immunogenic response, all injections including the PBS control were shown to increase systemic CRP activity with MC3 formulation being the highest. MC3 also

significantly reduced osteogenic gene, *col10a1*, as compared to SM-102 formulation but no significance was noted between MC3 and PBS control at either osteogenic gene tested. While MC3 LNP caused a localized pro-inflammatory response, no interference of osteogenesis was noted within the fracture callus with either LNP formulation.

III.8 Limitations and Future Directions

This study has several limitations including the generation of all ionizable LNPs were prepared at within the Department of Musculoskeletal Regeneration at Houston Methodist, and specifically in Francesca Taraballi's laboratory prior to all *in vitro* and *in vivo* studies. Thus, the ionizable LNPs were not prepared and then immediately tested after preparation. Time from preparation to injection ranged from 1-2 weeks following formulation. Here, a shelf-life experiment testing firefly luciferase mRNA-MC3 LNP stability was performed to determine potential effects given this limitation. Here, MC3 LNPs showed significantly less firefly luciferase protein expression *in vitro* on ATDC5 cells (**SUPPLEMENTAL FIGURE 3**). Future studies should address shelf-life of mRNA by testing functional outcomes with varied shelf-life times. We also noted that manufactured cationic lipid vesicles showed lower transfection potential with increased shelf-life. To circumvent this limitation, manufactured reagents were ordered at the same time prior to each *in vivo* study to ensure both reagents are at their highest transfection potential. One last limitation is that all immunogenicity, fracture interference and biodistribution studies were performed following a single concentration of mRNA.

Delivery with higher mRNA concentrations may only heighten an innate immune reaction. Thus, future studies should address the use of higher mRNA concentrations on localized and systemic immune responses. To assess localized inflammation, pro-inflammatory markers can be tested on RNA expression within the fracture callus and for systemic inflammation, acute pro-inflammatory markers within serum can be used. In addition to immunogenicity, biodistributive properties should be re-measured with increased concentrations. While no significant luciferase expression levels were found when in the liver after a

localized delivery of 10 μg/mouse, a nearly five-fold increased dose may show a varied distribution profile. SM-102 LNPs prove to be a promising mRNA delivery vehicle and next steps in this platform include delivery of a functional gene to promote bone formation in this fracture model.

III.9 References

1. Żak, M. M. and Zangi, L., *Lipid Nanoparticles for Organ-Specific mRNA Therapeutic Delivery.* Pharmaceutics, 2021. **13**(10).
2. Nsairat, H., Khater, D., Sayed, U., Odeh, F., Al Bawab, A., and Alshaer, W., *Liposomes: structure, composition, types, and clinical applications.* Heliyon, 2022. **8**(5): p. e09394.
3. Balazs, D. A. and Godbey, W., *Liposomes for use in gene delivery.* J Drug Deliv, 2011. **2011**: p. 326497.
4. Chong, Z. X., Yeap, S. K., and Ho, W. Y., *Transfection types, methods and strategies: a technical review.* PeerJ, 2021. **9**: p. e11165.
5. Bangham, A. D., Standish, M. M., and Watkins, J. C., *Diffusion of univalent ions across the lamellae of swollen phospholipids.* J Mol Biol, 1965. **13**(1): p. 238-52.
6. Han, Geonhee, Noh, Dahye, Lee, Hokyung, Lee, Sangmin, Kim, Sehoon, Yoon, Hong Yeol, and Lee, Soo Hyeon, *Advances in mRNA Therapeutics for Cancer Immunotherapy: From Modification to Delivery.* Advanced Drug Delivery Reviews, 2023: p. 114973.
7. Han, R., Ye, Z., Zhang, Y., Cheng, Y., Zheng, Y., and Ouyang, D., *Predicting liposome formulations by the integrated machine learning and molecular modeling approaches.* Asian J Pharm Sci, 2023. **18**(3): p. 100811.
8. Yang, J. P. and Huang, L., *Time-dependent maturation of cationic liposome-DNA complex for serum resistance.* Gene Ther, 1998. **5**(3): p. 380-7.
9. Zuhorn, I. S., Bakowsky, U., Polushkin, E., Visser, W. H., Stuart, M. C., Engberts, J. B., and Hoekstra, D., *Nonbilayer phase of lipoplex-membrane mixture determines endosomal escape of genetic cargo and transfection efficiency.* Mol Ther, 2005. **11**(5): p. 801-10.
10. Uchida, E., Mizuguchi, H., Ishii-Watabe, A., and Hayakawa, T., *Comparison of the efficiency and safety of non-viral vector-mediated gene transfer into a wide range of human cells.* Biol Pharm Bull, 2002. **25**(7): p. 891-7.
11. Remy, J. S., Sirlin, C., Vierling, P., and Behr, J. P., *Gene transfer with a series of lipophilic DNA-binding molecules.* Bioconjug Chem, 1994. **5**(6): p. 647-54.
12. Koltover, I., Salditt, T., Rädler, J. O., and Safinya, C. R., *An inverted hexagonal phase of cationic liposome-DNA complexes related to DNA release and delivery.* Science, 1998. **281**(5373): p. 78-81.
13. Farhood, H., Serbina, N., and Huang, L., *The role of dioleoyl phosphatidylethanolamine in cationic liposome mediated gene transfer.* Biochim Biophys Acta, 1995. **1235**(2): p. 289-95.
14. Chen, R., Wang, S. K., Belk, J. A., Amaya, L., Li, Z., Cardenas, A., Abe, B. T., Chen, C. K., Wender, P. A., and Chang, H. Y., *Engineering circular RNA for enhanced protein production.* Nat Biotechnol, 2023. **41**(2): p. 262-272.
15. Lonez, Caroline, Vandenbranden, Michel, and Ruysschaert, Jean-Marie, *Cationic lipids activate intracellular signaling pathways.* Advanced drug delivery reviews, 2012. **64**(15): p. 1749-1758.
16. Bennett, Michael J, Aberle, Alfred M, Balasubramaniam, Rajiv P, Malone, Jill G, Malone, Robert W, and Nantz, Michael H, *Cationic lipid-mediated gene delivery to murine lung: correlation of lipid hydration with in vivo transfection activity.* Journal of medicinal chemistry, 1997. **40**(25): p. 4069-4078.
17. Cui, S., Wang, Y., Gong, Y., Lin, X., Zhao, Y., Zhi, D., Zhou, Q., and Zhang, S., *Correlation of the cytotoxic effects of cationic lipids with their headgroups.* Toxicol Res (Camb), 2018. **7**(3): p. 473-479.
18. Inglut, C. T., Sorrin, A. J., Kuruppu, T., Vig, S., Cicalo, J., Ahmad, H., and Huang, H. C., *Immunological and Toxicological Considerations for the Design of Liposomes.* Nanomaterials (Basel), 2020. **10**(2).
19. Kedmi, Ranit, Ben-Arie, Noa, and Peer, Dan, *The systemic toxicity of positively charged lipid nanoparticles and the role of Toll-like receptor 4 in immune activation.* Biomaterials, 2010. **31**(26): p. 6867-6875.

20. Akinc, A., Maier, M. A., Manoharan, M., Fitzgerald, K., Jayaraman, M., Barros, S., Ansell, S., Du, X., Hope, M. J., Madden, T. D., Mui, B. L., Semple, S. C., Tam, Y. K., Ciufolini, M., Witzigmann, D., Kulkarni, J. A., van der Meel, R., and Cullis, P. R., *The Onpattro story and the clinical translation of nanomedicines containing nucleic acid-based drugs.* Nat Nanotechnol, 2019. **14**(12): p. 1084-1087.
21. Tenchov, R., Bird, R., Curtze, A. E., and Zhou, Q., *Lipid Nanoparticles─From Liposomes to mRNA Vaccine Delivery, a Landscape of Research Diversity and Advancement.* ACS Nano, 2021. **15**(11): p. 16982-17015.
22. Zhang, G. and Sun, J., *Lipid in Chips: A Brief Review of Liposomes Formation by Microfluidics.* I nt J Nanomedicine, 2021. **16**: p. 7391-7416.
23. Suk, J. S., Xu, Q., Kim, N., Hanes, J., and Ensign, L. M., *PEGylation as a strategy for improving nanoparticle-based drug and gene delivery.* Adv Drug Deliv Rev, 2016. **99**(Pt A): p. 28-51.
24. Moghimi, Seyed Moein and Simberg, Dmitri, *Pro-inflammatory concerns with lipid nanoparticles.* Molecular Therapy, 2022. **30**(6): p. 2109-2110.
25. Tahtinen, Siri, Tong, Ann-Jay, Himmels, Patricia, Oh, Jaehak, Paler-Martinez, Andres, Kim, Leesun, Wichner, Sara, Oei, Yoko, McCarron, Mark J, and Freund, Emily C, *IL-1 and IL-1ra are key regulators of the inflammatory response to RNA vaccines.* Nature immunology, 2022. **23**(4): p. 532-542.
26. Parhiz, H., Brenner, J. S., Patel, P. N., Papp, T. E., Shahnawaz, H., Li, Q., Shi, R., Zamora, M. E., Yadegari, A., Marcos-Contreras, O. A., Natesan, A., Pardi, N., Shuvaev, V. V., Kiseleva, R., Myerson, J. W., Uhler, T., Riley, R. S., Han, X., Mitchell, M. J., Lam, K., Heyes, J., Weissman, D., and Muzykantov, V. R., *Added to pre-existing inflammation, mRNA-lipid nanoparticles induce inflammation exacerbation (IE).* J Control Release, 2022. **344**: p. 50-61.
27. Kulkarni, Jayesh A, Cullis, Pieter R, and Van Der Meel, Roy, *Lipid nanoparticles enabling gene therapies: from concepts to clinical utility.* Nucleic acid therapeutics, 2018. **28**(3): p. 146-157.
28. Meo, S. A., Bukhari, I. A., Akram, J., Meo, A. S., and Klonoff, D. C., *COVID-19 vaccines: comparison of biological, pharmacological characteristics and adverse effects of Pfizer/BioNTech and Moderna Vaccines.* Eur Rev Med Pharmacol Sci, 2021. **25**(3): p. 1663-1669.
29. Adams, D., Gonzalez-Duarte, A., O'Riordan, W. D., Yang, C. C., Ueda, M., Kristen, A. V., Tournev, I., Schmidt, H. H., Coelho, T., Berk, J. L., Lin, K. P., Vita, G., Attarian, S., Planté-Bordeneuve, V., Mezei, M. M., Campistol, J. M., Buades, J., Brannagan, T. H., 3rd, Kim, B. J., Oh, J., Parman, Y., Sekijima, Y., Hawkins, P. N., Solomon, S. D., Polydefkis, M., Dyck, P. J., Gandhi, P. J., Goyal, S., Chen, J., Strahs, A. L., Nochur, S. V., Sweetser, M. T., Garg, P. P., Vaishnaw, A. K., Gollob, J. A., and Suhr, O. B., *Patisiran, an RNAi Therapeutic, for Hereditary Transthyretin Amyloidosis.* N Engl J Med, 2018. **379**(1): p. 11-21.
30. Suzuki, Y. and Ishihara, H., *Difference in the lipid nanoparticle technology employed in three approved siRNA (Patisiran) and mRNA (COVID-19 vaccine) drugs.* Drug Metab Pharmacokinet, 2021. **41**: p. 100424.
31. Hassett, K. J., Benenato, K. E., Jacquinet, E., Lee, A., Woods, A., Yuzhakov, O., Himansu, S., Deterling, J., Geilich, B. M., Ketova, T., Mihai, C., Lynn, A., McFadyen, I., Moore, M. J., Senn, J. J., Stanton, M. G., Almarsson, Ö, Ciaramella, G., and Brito, L. A., *Optimization of Lipid Nanoparticles for Intramuscular Administration of mRNA Vaccines.* Mol Ther Nucleic Acids, 2019. **15**: p. 1-11.
32. Haffner-Luntzer, M., Heilmann, A., Rapp, A. E., Beie, S., Schinke, T., Amling, M., Ignatius, A., and Liedert, A., *Midkine-deficiency delays chondrogenesis during the early phase of fracture healing in mice.* PLoS One, 2014. **9**(12): p. e116282.
33. Pogue, A. I., Jaber, V., Zhao, Y., and Lukiw, W. J., *Systemic Inflammation in C57BL/6J Mice Receiving Dietary Aluminum Sulfate; Up-Regulation of the Pro-Inflammatory Cytokines IL-6 and*

TNFα, C-Reactive Protein (CRP) and miRNA-146a in Blood Serum. J Alzheimers Dis Parkinsonism, 2017. **7**(6).
34. Danaei, M., Dehghankhold, M., Ataei, S., Hasanzadeh Davarani, F., Javanmard, R., Dokhani, A., Khorasani, S., and Mozafari, M. R., *Impact of Particle Size and Polydispersity Index on the Clinical Applications of Lipidic Nanocarrier Systems.* Pharmaceutics, 2018. **10**(2).
35. Clogston, Jeffrey D and Patri, Anil K, *Zeta potential measurement.* Characterization of nanoparticles intended for drug delivery, 2011: p. 63-70.
36. Watson-Levings, R. S., Palmer, G. D., Levings, P. P., Dacanay, E. A., Evans, C. H., and Ghivizzani, S. C., *Gene Therapy in Orthopaedics: Progress and Challenges in Pre-Clinical Development and Translation.* Front Bioeng Biotechnol, 2022. **10**: p. 901317.
37. Evans, Christopher H, Mankin, Henry J, Robbins, Paul D, Ghivizzani, Steve C, Herndon, James H, Kang, Richard, Bahnson, Alfred B, Barranger, John A, Elders, Elaine M, and Gay, Steffen, *Clinical Trial to Assess the Safety, Feasibility, and Efficacy of Transferring a Potentially Anti-Arthritic Cytokine Gene to Human Joints with Rheumatoid Arthritis. University of Pittsburgh School of Medicine, Pittsburgh, Pennsylvania.* Human gene therapy, 1996. **7**(10): p. 1261-1280.
38. Evans, Christopher H, Ghivizzani, SC, Herndon, JH, Wasko, MC, Reinecke, J, Wehling, P, and Robbins, PD, *Clinical trials in the gene therapy of arthritis.* Clinical Orthopaedics and Related Research (1976-2007), 2000. **379**: p. S300-S307.
39. Wehling, Peter, Reinecke, Julio, Baltzer, Axel WA, Granrath, Markus, Schulitz, Klaus P, Schultz, Carl, Krauspe, Rüdiger, Whiteside, Theresa W, Elder, Elaine, and Ghivizzani, Steven C, *Clinical responses to gene therapy in joints of two subjects with rheumatoid arthritis.* Human gene therapy, 2009. **20**(2): p. 97-101.
40. Evans, Christopher H, Robbins, Paul D, Ghivizzani, Steven C, Wasko, Mary Chester, Tomaino, Matthew M, Kang, Richard, Muzzonigro, Thomas A, Vogt, Molly, Elder, Elaine M, and Whiteside, Theresa L, *Gene transfer to human joints: progress toward a gene therapy of arthritis.* Proceedings of the National Academy of Sciences, 2005. **102**(24): p. 8698-8703.
41. Shirley, J. L., de Jong, Y. P., Terhorst, C., and Herzog, R. W., *Immune Responses to Viral Gene Therapy Vectors.* Mol Ther, 2020. **28**(3): p. 709-722.
42. Naldini, L., *Gene therapy returns to centre stage.* Nature, 2015. **526**(7573): p. 351-60.
43. Collins, Mary and Thrasher, Adrian, *Gene therapy: progress and predictions.* Proceedings of the Royal Society B: Biological Sciences, 2015. **282**(1821): p. 20143003.
44. Li, X., Shen, L., Deng, Z., and Huang, Z., *New treatment for osteoarthritis: Gene therapy.* Precis Clin Med, 2023. **6**(2): p. pbad014.
45. Puhl, D. L., D'Amato, A. R., and Gilbert, R. J., *Challenges of gene delivery to the central nervous system and the growing use of biomaterial vectors.* Brain Res Bull, 2019. **150**: p. 216-230.
46. Ramamoorth, M. and Narvekar, A., *Non viral vectors in gene therapy- an overview.* J Clin Diagn Res, 2015. **9**(1): p. Ge01-6.
47. De la Vega, RODOLFO E, Atasoy-Zeybek, Aysegul, Panos, Joseph A, Van Griensven, Martijn, Evans, Christopher H, and Balmayor, Elizabeth R, *Gene therapy for bone healing: lessons learned and new approaches.* Translational Research, 2021. **236**: p. 1-16.
48. Al Kaabi, Nawal, Zhang, Yuntao, Xia, Shengli, Yang, Yunkai, Al Qahtani, Manaf M, Abdulrazzaq, Najiba, Al Nusair, Majed, Hassany, Mohamed, Jawad, Jaleela S, and Abdalla, Jehad, *Effect of 2 inactivated SARS-CoV-2 vaccines on symptomatic COVID-19 infection in adults: a randomized clinical trial.* Jama, 2021. **326**(1): p. 35-45.
49. Burdușel, Alexandra-Cristina and Andronescu, Ecaterina, *Lipid Nanoparticles and Liposomes for Bone Diseases Treatment.* Biomedicines, 2022. **10**(12): p. 3158.
50. Zhou, Limin, Wu, Haojun, Gao, Xiang, Zheng, Xiaoyan, Chen, Hang, Li, Hailong, Peng, Jun, Liang, Weichong, Wang, Wenxing, and Qiu, Zuocheng, *Bone-targeting liposome-encapsulated salvianic acid a improves nonunion healing through the regulation of HDAC3-mediated endochondral ossification.* Drug Design, Development and Therapy, 2020: p. 3519-3533.

51. De La Vega, Rodolfo E., van Griensven, Martijn, Zhang, Wen, Coenen, Michael J., Nagelli, Christopher V., Panos, Joseph A., Peniche Silva, Carlos J., Geiger, Johannes, Plank, Christian, Evans, Christopher H., and Balmayor, Elizabeth R., *Efficient healing of large osseous segmental defects using optimized chemically modified messenger RNA encoding BMP-2.* Science Advances. **8**(7): p. eabl6242.
52. Wei, Bangguo, Wang, Wenrui, Liu, Xiangyu, Xu, Chenxi, Wang, Yanan, Wang, Ziqi, Xu, Jinnuo, Guan, Jianzhong, Zhou, Pinghui, and Mao, Yingji, *Gelatin methacrylate hydrogel scaffold carrying resveratrol-loaded solid lipid nanoparticles for enhancement of osteogenic differentiation of BMSCs and effective bone regeneration.* Regenerative Biomaterials, 2021. **8**(5): p. rbab044.
53. Liu, Yanzhi, Jia, Zhenshan, Akhter, Mohammed P, Gao, Xiang, Wang, Xiaobei, Wang, Xiaoyan, Zhao, Gang, Wei, Xin, Zhou, You, and Wang, Xiuli, *Bone-targeting liposome formulation of Salvianic acid A accelerates the healing of delayed fracture Union in Mice.* Nanomedicine: Nanotechnology, Biology and Medicine, 2018. **14**(7): p. 2271-2282.
54. Buschmann, Michael D, Carrasco, Manuel J, Alishetty, Suman, Paige, Mikell, Alameh, Mohamad Gabriel, and Weissman, Drew, *Nanomaterial delivery systems for mRNA vaccines.* Vaccines, 2021. **9**(1): p. 65.
55. Cullis, Pieter R and Hope, Michael J, *Lipid nanoparticle systems for enabling gene therapies.* Molecular Therapy, 2017. **25**(7): p. 1467-1475.
56. Carrasco, Manuel J, Alishetty, Suman, Alameh, Mohamad-Gabriel, Said, Hooda, Wright, Lacey, Paige, Mikell, Soliman, Ousamah, Weissman, Drew, Cleveland IV, Thomas E, and Grishaev, Alexander, *Ionization and structural properties of mRNA lipid nanoparticles influence expression in intramuscular and intravascular administration.* Communications biology, 2021. **4**(1): p. 956.
57. Xu, X. and Xia, T., *Recent Advances in Site-Specific Lipid Nanoparticles for mRNA Delivery.* ACS Nanosci Au, 2023. **3**(3): p. 192-203.

CHAPTER IV: NON-DESTRUCTIVE β-CATENIN MRNA PROMOTES BONE IN FRACTURE MODEL

IV.1 Introduction

Gene therapy to enhance bone regeneration using viral vectors for delivery of complementary DNA (cDNA) has been extensively studied in preclinical models.[1-4] As an example, bone formation was enhanced using BMP-2 gene therapy in preclinical models and circumvented some of the challenges associated with BMP-2 protein delivery, such as the need for supraphysiologic doses of protein *in vivo.*[2] In fact, the expression resulting from gene delivery using viral vector methods has been shown to persist up to 6 weeks in rabbit and mouse femoral defect models.[1, 2] While prolonged protein expression is desirable in some cases, it can also be associated with untoward effects, like immunogenicity of the viral vector. Gene therapy using mRNA-based technologies direct transient gene expression, or expression of the mRNA for only a short period of time, which has the potential to be efficacious in fracture healing applications. Bone repair is a transient process involving the temporal regulation of proteins throughout the various bone healing stages. However, delivery of mRNA provokes an immunostimulatory effect as seen when tested preclinically and clinically.[5, 6] Thus, mRNA-based therapies aim to maximize endogenous protein expression while minimizing immunogenicity.

It has been found that using mRNA as a therapeutic requires 50-1,000 fold higher concentration as compared to using mRNA as a vaccine in order to provoke a therapeutic response.[7] High concentrations of mRNA are associated with activation of the innate immune system. Thus, there is a need to optimize transfection efficiency and subsequent protein expression, while reducing immunogenicity of the mRNA transcript and the delivery mechanism.[8] Recent advancements in transcript engineering and in packaging materials, specifically lipid nanoparticles (as covered in Chapter 3), are promising strategies to address these limitations.

Various transcript engineering approaches have been studied to enhance protein expression and to minimize immunogenicity.[9] These techniques include nucleoside modifications, cap analogs and sequence optimization. Of these, nucleoside modifications are the most commonly utilized strategy in successful mRNA technologies.[7] The most frequent modified nucleoside in cellular RNA is pseudouridine, an isomer of uridine.[10-12] The substitution of pseudouridine for uridine is a post-translational modification which has been shown to reduce activation of the innate immune response.[7, 13, 14] The SARS-COV-2 vaccines developed by Pfizer and Moderna were generated using N1-methyl-pseudouridine to enhance protein translation and thus enhance efficacy of the vaccine.[7, 15]

Cap analogs located on both 5'and 3' ends have also been shown to enhance translation. Standard cap analogs, or Cap0 structure, have a N7-methyl guanosine (m7G) connected to the 5' nucleotide. This cap analog is protects the RNA from 5' exonuclease degradation and also aids in initiation of transcription through cap-dependent initiation.[16, 17] When using Cap0 structure for *in vitro* transcription (IVT), it elongates the transcript resulting in both forward and reverse oriented products.[16] Anti-reverse cap analog (ARCA), or Cap1 structure, transformed IVT as the cap analog is added exclusively in the forward direction, further enhancing translation of the desired product by two fold.[18, 19] Following this advance, a co-transcriptional capping method using CleanCap AG trimer which results in higher transcription efficiency over Cap1, 94% efficiency compared to 70% efficiency respectively.[20, 21]

To further exemplify the necessity of mRNA modifications, and specifically nucleoside modifications, one of the SARS-CoV-2 mRNA vaccine candidates, Curevac, can be reviewed. Curevac was developed to encode the same spike protein as both Pfizer-BioNTech and Moderna Therapeutics, yet the sequence used unmodified nucleosides.[15] When testing the clinical efficacy in a clinical trial, Curevac resulted in only 47% efficacy rates against SARS-CoV-2 symptoms and preventing disease.[22, 23] Additionally, when delivering Curevac at high doses, an aberrant immunogenic response and high rates of side effects were found in several participants, such as severe flu-like symptoms, headaches and fatigue.[22] While participants developed antibodies against the spike protein, the amount of antibodies was found to

be comparatively low especially to the antibody level seen from both Pfizer-BioNTech and Moderna Therapeutics vaccines.[22]

In addition to stability and immunogenicity, the challenge with orthopaedic adoption of mRNA therapies is finding an effective target. Prior work in Dr. Bahney's laboratory has detailed the imperative role of canonical Wnt pathway in endochondral ossification, a process in which cartilage forms between the fracture gap before transforming into bone.[24, 25] First, genetic loss- and gain-of-function experiments conditionally inhibiting or expressing canonical Wnt in hypertrophic chondrocytes were performed in a fracture callus to determine β-catenin's role in endochondral bone repair.[25] Importantly, these experiments were executed through conditional inhibition or expression of a stabilized form of β-catenin in Aggrecan-Cre^{ERT2} mice, with daily injections of Tamoxifen at 6-10 days post-fracture.[25] Loss-of-function experiments showed significantly less bone at 2 and 3 weeks after fracture and conversely, gain-of-function experiments displayed significantly more bone at these time points.[25] Further, day 6 was selected to conditionally express or inhibit canonical Wnt this represents the beginning of the soft callus phase in mouse fracture remodeling, following the initial hematoma.[26, 27] Additionally, this data reveals canonical Wnt's imperative role in endochondral ossification and specifically in chondrocyte-to-osteoblast transdifferentiation.

In this series of experiments, we aimed to develop and test an mRNA construct encoding a non-destructive β-catenin sequence, β-catenin^{GOF}, for stimulating bone regeneration by activating the canonical Wnt signaling pathway at a temporally optimized time within bone repair. The β-catenin^{GOF} mRNA was generated using GMP-compliant techniques at Houston Methodist within the RNA Core Facility and was subsequently encapsulated in SM-102 LNPs. Here, we validate β-catenin^{GOF} bioactivity and efficacy in promoting bone *in vitro* and *in vivo* after localized delivery to the fracture site in a murine tibia fracture model. We hypothesized that delivery of chemically modified β-catenin^{GOF} mRNA encapsulated in SM-102 LNPs would activate canonical Wnt pathway and promoted bone formation in a murine tibia fracture model.

IV.2 Methods & Materials

IV.2.1 LNP Formulations

SM-102 LNPs were synthesized as detailed in Section III.2 Methods & Materials. For these experiments cargo mRNA encoded β-catenin^{GOF} sequence (**SUPPLEMENTAL FIGURE 1**). β-catenin^{GOF} sequence was developed based on gain-of-function phenotypes that have been previously published.[28] The sequence was then optimized using online codon optimality tool, icodon.org. N1-methyl-pseudouridine was used as a modified nucleoside to replace all uridines and Clean Cap technology was used as a 5' cap. The mRNA construct was generated at the RNA Core facility at Houston Methodist, a GMP compliant facility. The RNA Core facility uses proprietary untranslated regions (UTRs) and additionally a long poly A tail of 150 bases.

IV.2.2 Testing bioactivity of β-catenin mRNA *in vitro*

To test bioactivity of β-catenin mRNA, β-catenin mRNA was encapsulated in SM-102 LNPs as described in Section IV.2.1 and 0.25 μg mRNA was delivered per well. Canonical Wnt activation was measured using experiments including Topflash assay and qRT-PCR for *axin2* and *runx2*, downstream genes from canonical Wnt. The chondrogenic cell line, ATDC5 cells were differentiated into hypertrophic chondrocytes. Hypertrophic chondrocyte differentiation involved use of basal ATDC5 medium supplemented with 1 % L-Glutamine (ThermoFisher, Cat # 25030149), 10 μg/mL transferrin (Millipore Sigma, Cat # T8158-100mg), 3 x 10-8 M Selenite (Sigma Aldrich, Cat # S5261-10G), 0.2 mM Ascorbic Acid (Sigma Aldrich, Cat # A8960-5G), and 10 μg/mL Insulin (Millipore Sigma, Cat # I2643-25 MG) treated on cells for 7 days with replacing media every 2-3 days.[19]). Passage 5 and under wasused for all *in vitro* experiments. ATDC5 cells were maintained using basal medium DMEM/F12 (Thermo Fisher, Cat# 11320033), 5 % fetal bovine serum (FBS, Thermo Fisher, Cat# 16000044) and 1 % penicillin/streptomycin (P/S, Thermo Fisher, Cat# 15140122) until hypertrophic differentiation. For all *in vitro* experiments, ATDC5 cells were plated at 20,000 cells/well in 12 well plates. Prior to transfection experiments,

chondrocytes underwent serum starvation using basal media OPTI-MEM (Thermo Fisher, Cat# 31985070) 0.5 % FBS and 1 % P/S for 24 hours. All transfection protocols were executed using serum-free media, OPTI-MEM supplemented with 1 % P/S. Following transfection, RNA was isolated 6 hours after treatments, made into cDNA and qRT-PCR was performed for *axin2* and *runx2* to evaluate Wnt activation. Topflash assay was used to measure bioactivity of β-catenin mRNA *in vitro*. First, plasmid vectors M50 (Addgene, Cat # 12456), M51 (Addgene, Cat # 12457) and Renilla (Addgene, Cat # 27163) were grown on amp-resistant agar plates (Thermo Fisher, Cat # J63197EQF) overnight at 37°C. A single colony was then amplified in liquid amp-resistant LB broth overnight at 37°C. Plasmids were then isolated using ZymoPure II Plasmid Maxiprep Kit (Zymo Research, Cat # D4202) according to manufacturer's instructions. ATDC5 cells were transfected with plasmid vectors using Lipofectamine 3000, according to manufacturer's instructions, using 1 μg of pDNA/well, Renilla was used at $1/10^{th}$ the concentration of M50 and M51. The plasmids were transfected for 2 days prior to treating with 100 ng/mL rhWnt3a (R&D Systems, Cat # 5036-WN-010), as the positive control, or with 2 μg/well β-catenin mRNA. Lipofectamine MessengerMax was used to deliver mRNA according to manufacturer's instructions. Treatments were incubated for 48 hours prior to analysis. Firefly/Renilla Dual Luciferase Assay (Sigma Aldrich, Cat # SCT152) was used as a reporter assay to quantify both firefly and renilla luciferase expression and was used per manufacturer's protocol. Topflash results were reported as a ratio of Firefly to Renilla signal.

IV.2.3 Murine tibia fracture and stabilization model

In vivo experiments were approved by and conducted in compliance with the Institutional Animal Care and Use Committee at Colorado State University (CSU). Mid-shaft tibial fractures were created in adult (12-14 weeks), male C57BL/6J mice (Charles River # 027). All animals received a pre-surgical analgesic, Buprenorphine SR (ZooPharm), at a dose of 0.6-1.0 mg/kg. Mice were placed under general anesthesia using inhaled 1-5 % isoflurane to effect. Left hind limbs were shaved and sterilely prepared using 70 % alcohol wipes and Chlorhexidine surgical scrub solution, repeated for a total of 3 times.

Lubrication was provided for the eyes of each mouse using artificial tears ointment (Bausch & Lomb) and mice were then transferred to a heated operating table. Using aseptic technique, an incision was made along the tibia, and a hole was made at the top of the tibial plateau using a 23-gauge needle. An intermedullary pin (sterilized insect pin) was inserted through the hole made from the tibial plateau through the tibial cavity and into the distal tibia. One small hole was created in the mid-shaft of the tibia using a Dremel and pressure was applied to both proximal and distal ends to fracture the tibia.[25, 29] The surgical incision was then sutured using 5-0 Biosyn Sutures (Covidien, Cat #5687) and one surgical skin staple was applied over the skin incision to protect against chewing. A local anesthetic, 0.25% Bupivicaine Hydrochloride (NovaPlus, cat # RL-7562), was applied topically after the initial staple was placed. Mice were then allowed to recover individually in a heated cage before being transferred back to their original cage. Mice were socially housed throughout the in-life period, and permitted free ambulation. Mice were closely monitored for pain and signs of infections for 72 hours following the surgery. All treatments were suspended in 25 μL sterile PBS and vortexed before injecting. All experimental and control treatment groups were injected on day 6 post-fracture into the fracture callus using an insulin syringe (BD, Cat # 324702). Animals were sacrificed according to approved euthanasia protocols at 2 weeks after fracture.

IV.2.4 Localized injections of β-catenin mRNA – SM-102 LNPs

All treatments were injected locally to the site of the fracture callus 6 days following fracture. To inject the mice, SM-102 β-catenin mRNA was concentrated allow for a 25-30 μL injection volume/mouse using 100K protein concentrators (Sigma Aldrich, Cat # UFC510024), spun at 5000 x g for 5-10 minutes. *In vivo* studies used sterile filtered 1X phosphate buffer solution (PBS, Thermo Fisher, Cat # 10010023) as the solvent to produce the various solutions. The negative control group was sterile-filtered phosphate buffered saline (PBS) group. Positive control was rhWnt3a (R&D Systems, Cat # 5036-WN-010), at a concentration of 1 μg/mL at similar volume (*n=7-10*).

IV.2.5 Histology and histomorphometry

Fractured tibias of treated mice were collected 2 and 8 days post injection, immersion fixed in 4 % paraformaldehyde, and decalcified using 19 % ethylenediaminetetraacetic acid (EDTA). The tissues were then processed in increased ethanol solutions (50%, 70%, 95% and 100%), processed in xylene (x2) and then placed in paraffin for 1.5 hours each. Samples were embedded in paraffin, sectioned at 8 μm thickness, and mounted onto glass slides. To perform quantitative histomorphometry, serial sections were obtained using the first section beginning in the fracture callus and every 10^{th} section afterwards. Standard histomorphometry principles were used and quantification of the fracture callus components including bone, cartilage and fibrous tissues were determined.[29, 30] Hall Brundt Quadruple stain was used to identify the dense collagenous fibrils of bone, stained red by direct red, and proteoglycans in the cartilage matrix, stained by alcian blue.[31] Quantification of callus composition was determined using the Trainable Weka Segmentation2 add-on in Fiji ImageJ (version 1.54f; NIH, Maryland, USA).[32] Volume of specific tissue types was determined by summing the individual compositions relative to the whole fracture callus compositions. Tissues were imaged using a Nikon Eclipse Ti microscope. Additionally, photoshop (version 24.7.0, Adobe) was used to isolate fractured tissue from the adjacent muscle and skin tissues.

IV.2.6 μCT analysis

Mice were sacrificed at 2 weeks following fracture and stabilization and the fractured tibia was dissected and fixed in 4% paraformaldehyde (PFA). MicroCT and microCT analysis was performed as previously published.[33, 34] Briefly, `fixed bones were scanned using MicroCT (Viva CT-40, Scanco Medical, Switzerland) at 15 μm resolution, 70 kVP and 112 μA X-ray energy. Bone volume was quantified using Scanco evaluation software according to the guidelines of the American Society of Bone and Mineral Research (ASBMR). The mid-point of fracture callus was selected and 150 slices above and below were analyzed for a total of 300 slices to be evaluated per mouse. Trabecular bone quantity was analyzed with a Gauss = 0.8, Sigma = 1, threshold of 184. Bone volume, total volume, trabecular number, trabecular

separation, trabecular thickness, connectivity density, structure model index, and volumetric bone density were all CT parameters.

IV.2.7 Statistics

Animal sample size was determined *a priori* using the mean and standard deviation from our preliminary data, where a power analysis was conducted using RStudio to determine that 7 mice/group/time are required for histomorphometry analysis to achieve a power level >80% with an effect size d =0.24 and a significance level of 5%. Moreover, a significance level of 5% was chosen for all studies. Statistical analysis was performed using Graph Pad Prism 8. Data were plotted so that each sample represented a single dot on each graph. The bar indicates the mean with error bars representing standard deviation. Statistical difference was determined by ANOVAs and all post-hoc comparison performed using Tukey's HSD test.

IV.3 β-catenin mRNA activates canonical Wnt *in vitro* and stimulates bone formation *in vivo*

Hypertrophic chondrocytes had significantly increased axin2 expression as compared to both the PBS control and positive control, rhWnt3a. Following a 6 hour exposure to β-catenin^{GOF} mRNA lipoplexes, (**FIGURE 18A**). Axin2 expression was significantly higher in the rhWnt3a treated group as compared with the PBS control (*p=0.0003*), but no difference was seen when compared with β-catenin^{GOF} mRNA. β-catenin^{GOF} mRNA significantly increased *runx2* expression as compared with PBS controls and was not significantly different as compared with the rhWnts3a group(**FIGURE 18B**). Topflash did not detect a significant increase in Wnt signaling in the β-catenin^{GOF} mRNA group, however the β-catenin^{GOF} mRNA group did show trends for higher bioactivity than the PBS control (**FIGURE 18C**). As expected, positive control rhWnt3a significantly enhanced Wnt activity in Topflash study. SM-102-

β-catenin^{GOF}mRNA was then tested histomorphometrically in its abilities to promote bone formation in a murine tibia fracture model. Histomorphometric analysis demonstrated that both 25 μg and

45 µg /mouse of SM-102 LNPs encapsulating β-catenin^{GOF} mRNA resulted in significantly more total bone area than PBS controls (**FIGURE 19A,C**). Additionally, β-catenin^{GOF}mRNA at 45 µg had significantly more total bone area than the 10 µg/mouse group. Not only did the higher concentrations of SM-102 β-catenin^{GOF}mRNA have more bone histologically, but there was significantly less cartilage composition within the fracture callus in both 25 and 45 µg groups. Not only did these two concentrations have less cartilage than the PBS control group, but the 25 µg group also had less cartilage composition than the 10 µg group (*p=0.0420*).

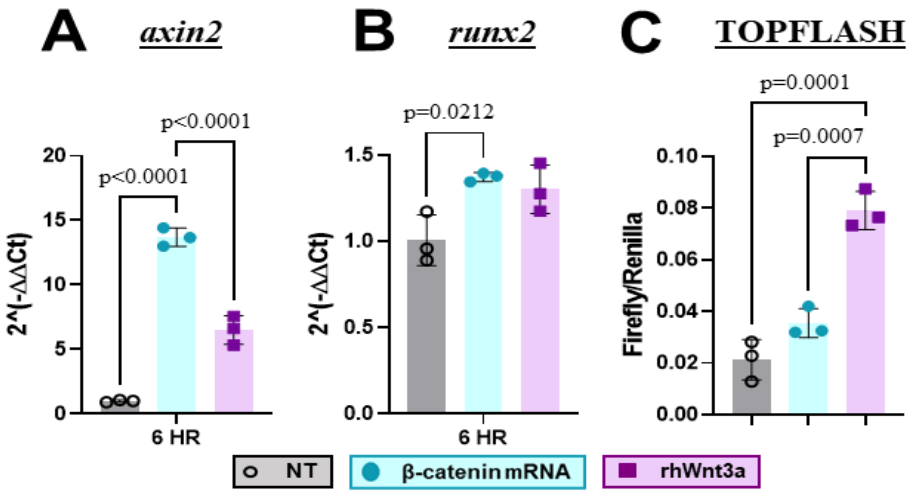

Figure 18. *Canonical Wnt bioactivity of β-catenin^{GOF}mRNA in vitro in a hypertrophic chondrocyte model. Specifically,* ***A).*** *genes downstream from canonical Wnt pathway were tested and* ***B).*** *a canonical Wnt reporter assay, Topflash.*

MicroCT quantification of bone were consistent with the histomorphometry results and showed significantly more bone volume following the delivery of 45 µg SM-102 LNPs encapsulating β-catenin^{GOF}mRNA compared to the control (**FIGURE 19 B, D**). No significant differences were found in any of the other groups tested, or in any of the other measurements acquired.

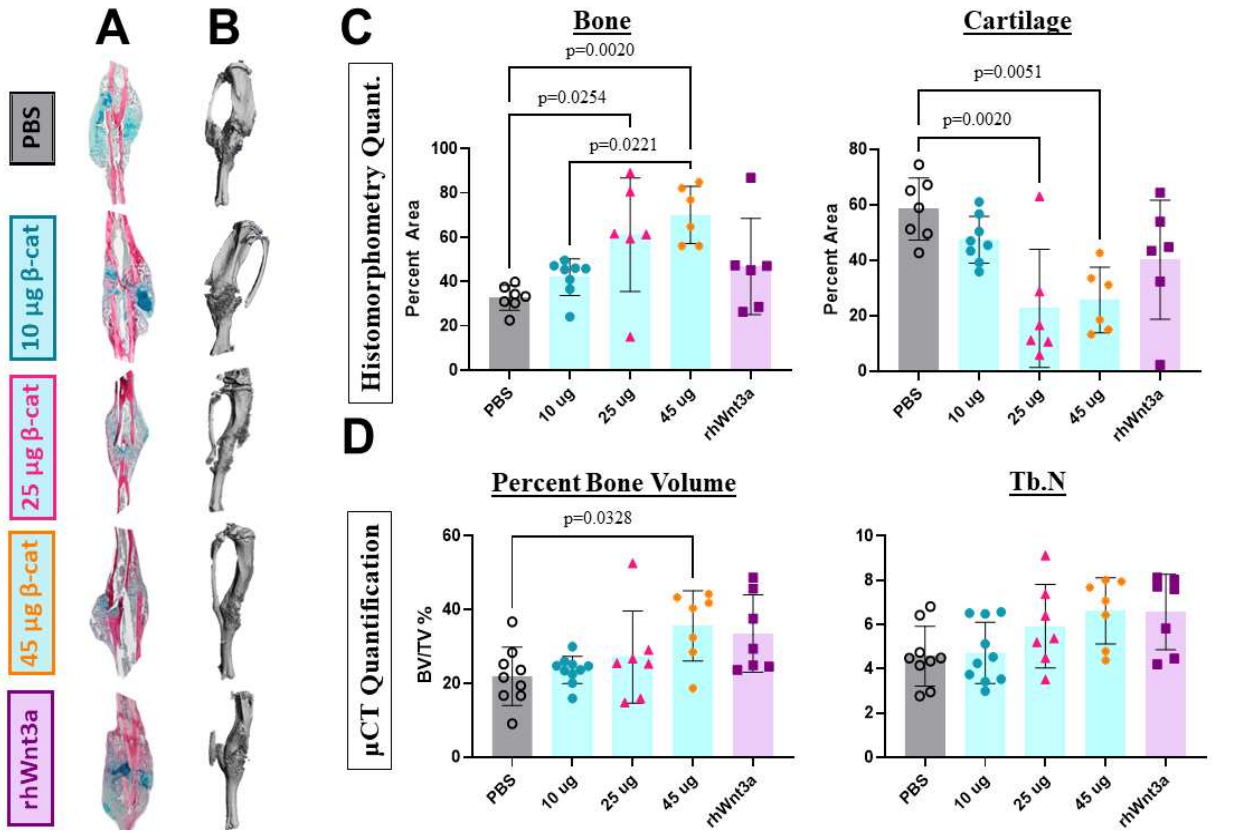

Figure 19. *SM-102 LNPs encapsulating β-catenin^{GOF}mRNA were tested in their capabilities to promote bone in a murine tibia fracture model.* ***A).*** *Histomorphometry was employed to* ***C).*** *quantify bone and cartilage tissues and* ***B).*** *uCT was used to evaluate* ***D).*** *bone volume/ total volume.*

IV.4 Conclusions

The success of the vaccines has heightened interest in mRNA-based therapeutics for many applications. Transcript engineering was found to be imperative to create a clinically effective of the mRNA vaccine and these lessons have been pivotal in developing mRNA therapies to date. Both of the Pfizer BioNTech and Moderna Therapeutics mRNA constructs use modified nucleosides, and specifically both use N1-methyl-pseudouridine, and optimized 5' cap structures, based on cap1 analogs.[16, 35] The success of these mRNA vaccines is based off of their good safety profiles and over 90% efficacy rates against SARS-CoV-2 symptoms.[36, 37]

This chapter focuses on developing and validating a functional mRNA sequence encoding a non-destructive β-catenin to promote bone regeneration during fracture repair by activating the canonical Wnt

signaling pathway. We hypothesized that Wnt signaling activation during fracture repair was an ideal therapeutic target as an alternative to BMP based on our discovery that this pathway plays a key role in the transformation of chondrocytes to osteoblast during the endochondral phase of fracture healing.[25] An in depth review on canonical Wnt for bone healing is described in Chapter I of this dissertation. Non-destructive β-catenin was selected as the target mRNA sequence to activate the Wnt pathway as they are associated with enhanced β-catenin expression and protection from proteolytic destruction as compared to wild-type β-catenin.[28, 38] This constitutive stabilization of β-catenin, β-catenin^{GOF}, was proposed in this study as this will facilitate maximal β-catenin expression of the mRNA therapeutic with potentially lower doses.

We further translated this non-destructive mRNA β-catenin sequence by chemically modifying the mRNA for improved therapeutic efficacy using state-of-the-art mRNA engineering techniques. First, N1-methyl-pseudouridine was selected to replace all uridines in the β-catenin^{GOF} transcript. Another main mRNA modification which influences stability is selecting optimal codons which have a faster translation elongation by the ribosome than non-optimal codons, while encoding for the same protein.[39, 40] To further maximize translation efficiency, an online codon optimality tool was selected for use to enhance mRNA stability, icodon.org.[40]

Several other groups have generated mRNA therapeutics to promote bone healing, primarily focused on the canonical bone target of BMP. Balmayor *et al.* reported that a chemically modified mRNA (cmRNA) encoding BMP-2 in a collagen sponge resulted in local delivery of significant amounts of BMP-2 cmRNA, induced more collagen 1 and osteocalcin genes, and generated higher mineral content *in vitro*.[41] Zhang *et al.* has specifically sought to enhance osteogenesis by chemically modifying a BMP-2 mRNA transcript using alternative nucleoside modifications such as substituting pyrimidines with 2-thiouridine and 5-methylcytidine and optimizing untranslated regions (UTRs).[42] Similarly, Elangovan *et al.* incorporated 100% substitution with N1-meethyl-pseudouridine and 5-methylcytidine resulting in diminished interferon-α expression.[43, 44] The use of these modified nucleosides has also been associated

with reduced immunogenicity and increased half-life of the chemically modified mRNA (cmRNA). Despite the use of modified nucleosides to enhance immunogenicity, most of the cmRNA strategies for bone repair have used cap0 structures.[42, 43, 45]

Here, we have validated canonical Wnt activation with delivery of β-catenin^{GOF} mRNA lipoplexed with SM-102 LNPs as developed in Chapter III. We verified that this sequence activated canonical Wnt through qRT-PCR quantification the downstream genes *axin2* and *runx2*. The delivery of SM-102-β-catenin^{GOF} mRNA had higher *axin2* expression as compared to the rhWnt3a positive control, yet this was not found when analyzing the Wnt reporter assay, Topflash. Interestingly, Wnt reporter assay, which expresses firefly luciferase every time TCF/LEF transcription is activated, revealed higher TCF/LEF activity with Wnt ligand, rhWnt3a. However, this may be a limitation of the study as β-catenin was delivered with Lipofectamine instead of SM-102 LNPs. Thus, the canonical Wnt activity measured may not fully recapitulate the therapeutic efficacy of generated SM-102- β-catenin mRNA.

Interventions which stimulate osteoblast differentiation and proliferation have the capacity to accelerate fracture healing.[46] Our results show that SM-102-β-catenin^{GOF} mRNA promotes bone formation *in vivo* in a dose-dependent manner. Significantly more bone composition was determined in the 25 and 45 μg β-catenin^{GOF} mRNA groups on μCT analysis. The only group which revealed significantly more bone in both histomorphometry and μCT was the 45 μg β-catenin^{GOF} mRNA group, suggesting this dose may accelerate bone healing in our murine tibia fracture model.

IV.5 Limitations and Future Directions

This study has several limitations including the difference in volume between the treatment groups. While the lower concentration SM-102- β-catenin^{GOF} mRNA lipoplexes were able to reduce in volume to 25 μL/mouse, the highest concentration tested was unable to reduce in volume to this degree. Thus, the highest dose tested (45 μg) was delivered using a volume of 30 μL/mouse. Several implications could occur

with this increased volume including increased immunogenicity and potentially altering transfection kinetics. Another limitation includes that only one time point was tested in murine tibia fracture model at 2 weeks following fracture. Aberrant bone growth has been reported to occur in mice at 4 months following treatment with BMP-2.[47] Thus, it is important to test long-term effects of the mRNA treatments. Further, to confirm that SM-102- β-catenin^{GOF} mRNA accelerates fracture healing, longer time points need to be assessed through uCT and histomorphometry. Time points displaying this group has fully healed prior to the PBS control needs to be performed, such as at 4 and 6 weeks post-fracture. For this model, additional time points for μCT and histomorphometry at 4 and 6 weeks after fracture would sufficiently determine earlier healing.

To fully examine if the β-catenin^{GOF} sequence has a higher transfection capability, additional groups should be tested. Further an experimental group which encodes the full β-catenin mRNA sequence should be tested for transfection capacity against the β-catenin^{GOF} sequence. Not only could the β-catenin^{GOF} sequence give rise to more robust transfection but may prompt differing immune responses. Future studies should include varying time points to fully examine the osteogenic profile of the treated mice with SM-102- β-catenin^{GOF} mRNA lipoplexes. Additionally, as immunogenicity was only examined with the SM-102 LNPs-Firefly luciferase mRNA at a concentration of 10 μg/mouse, future studies should also examine immunogenicity with the proposed SM-102 β-catenin^{GOF} mRNA lipoplexes. Systemic and localized immunogenic responses should be evaluated at each of the doses and time points tested for SM-102 β-catenin^{GOF} mRNA lipoplexes.

IV.6 References

1. Baltzer, A. W., Lattermann, C., Whalen, J. D., Braunstein, S., Robbins, P. D., and Evans, C. H., *A gene therapy approach to accelerating bone healing. Evaluation of gene expression in a New Zealand white rabbit model.* Knee Surg Sports Traumatol Arthrosc, 1999. **7**(3): p. 197-202.
2. Baltzer, A. W., Lattermann, C., Whalen, J. D., Wooley, P., Weiss, K., Grimm, M., Ghivizzani, S. C., Robbins, P. D., and Evans, C. H., *Genetic enhancement of fracture repair: healing of an experimental segmental defect by adenoviral transfer of the BMP-2 gene.* Gene Ther, 2000. **7**(9): p. 734-9.
3. Bougioukli, S., Jain, A., Sugiyama, O., Tinsley, B. A., Tang, A. H., Tan, M. H., Adams, D. J., Kostenuik, P. J., and Lieberman, J. R., *Combination therapy with BMP-2 and a systemic RANKL inhibitor enhances bone healing in a mouse critical-sized femoral defect.* Bone, 2016. **84**: p. 93-103.
4. Alluri, R., Song, X., Bougioukli, S., Pannell, W., Vakhshori, V., Sugiyama, O., Tang, A., Park, S. H., Chen, Y., and Lieberman, J. R., *Regional gene therapy with 3D printed scaffolds to heal critical sized bone defects in a rat model.* J Biomed Mater Res A, 2019. **107**(10): p. 2174-2182.
5. Salleh, M. Z., Norazmi, M. N., and Deris, Z. Z., *Immunogenicity mechanism of mRNA vaccines and their limitations in promoting adaptive protection against SARS-CoV-2.* PeerJ, 2022. **10**: p. e13083.
6. Lee, Yeji, Jeong, Michaela, Park, Jeongeun, Jung, Hyein, and Lee, Hyukjin, *Immunogenicity of lipid nanoparticles and its impact on the efficacy of mRNA vaccines and therapeutics.* Experimental & Molecular Medicine, 2023.
7. Rohner, Eduarde, Yang, Ran, Foo, Kylie S., Goedel, Alexander, and Chien, Kenneth R., *Unlocking the promise of mRNA therapeutics.* Nature Biotechnology, 2022. **40**(11): p. 1586-1600.
8. van Asbeck, A. H., Dieker, J., Oude Egberink, R., van den Berg, L., van der Vlag, J., and Brock, R., *Protein Expression Correlates Linearly with mRNA Dose over Up to Five Orders of Magnitude In Vitro and In Vivo.* Biomedicines, 2021. **9**(5).
9. Balmayor, E. R., *Synthetic mRNA - emerging new class of drug for tissue regeneration.* Curr Opin Biotechnol, 2022. **74**: p. 8-14.
10. Carlile, Thomas M., Martinez, Nicole M., Schaening, Cassandra, Su, Amanda, Bell, Tristan A., Zinshteyn, Boris, and Gilbert, Wendy V., *mRNA structure determines modification by pseudouridine synthase 1.* Nature Chemical Biology, 2019. **15**(10): p. 966-974.
11. Cerneckis, J., Cui, Q., He, C., Yi, C., and Shi, Y., *Decoding pseudouridine: an emerging target for therapeutic development.* Trends Pharmacol Sci, 2022. **43**(6): p. 522-535.
12. Cohn, Waldo E. and Volkin, Elliot, *Nucleoside-5'-Phosphates from Ribonucleic Acid.* Nature, 1951. **167**(4247): p. 483-484.
13. Karikó, Katalin, Muramatsu, Hiromi, Welsh, Frank A, Ludwig, János, Kato, Hiroki, Akira, Shizuo, and Weissman, Drew, *Incorporation of pseudouridine into mRNA yields superior nonimmunogenic vector with increased translational capacity and biological stability.* Molecular therapy, 2008. **16**(11): p. 1833-1840.
14. Andries, Oliwia, Mc Cafferty, Séan, De Smedt, Stefaan C, Weiss, Ron, Sanders, Niek N, and Kitada, Tasuku, *N1-methylpseudouridine-incorporated mRNA outperforms pseudouridine-incorporated mRNA by providing enhanced protein expression and reduced immunogenicity in mammalian cell lines and mice.* Journal of Controlled Release, 2015. **217**: p. 337-344.
15. Morais, P., Adachi, H., and Yu, Y. T., *The Critical Contribution of Pseudouridine to mRNA COVID-19 Vaccines.* Front Cell Dev Biol, 2021. **9**: p. 789427.
16. Shanmugasundaram, Muthian, Senthilvelan, Annamalai, and Kore, Anilkumar R., *Recent Advances in Modified Cap Analogs: Synthesis, Biochemical Properties, and mRNA Based Vaccines.* The Chemical Record, 2022. **22**(8): p. e202200005.

17. Ramanathan, A., Robb, G. B., and Chan, S. H., *mRNA capping: biological functions and applications.* Nucleic Acids Res, 2016. **44**(16): p. 7511-26.
18. STEPINSKI, JANUSZ, WADDELL, CLINT, STOLARSKI, RYSZARD, DARZYNKIEWICZ, EDWARD, and RHOADS, ROBERT E, *Synthesis and properties of mRNAs containing the novel "anti-reverse" cap analogs 7-methyl (3'-O-methyl) GpppG and 7-methyl (3'-deoxy) GpppG.* Rna, 2001. **7**(10): p. 1486-1495.
19. Peng, Zheng-Hong, Sharma, Vivek, Singleton, Scott F, and Gershon, Paul D, *Synthesis and application of a chain-terminating dinucleotide mRNA cap analog.* Organic letters, 2002. **4**(2): p. 161-164.
20. Henderson, Jordana M., Ujita, Andrew, Hill, Elizabeth, Yousif-Rosales, Sally, Smith, Cory, Ko, Nicholas, McReynolds, Taylor, Cabral, Charles R., Escamilla-Powers, Julienne R., and Houston, Michael E., *Cap 1 Messenger RNA Synthesis with Co-transcriptional CleanCap® Analog by In Vitro Transcription.* Current Protocols, 2021. **1**(2): p. e39.
21. Tusup, Marina, French, Lars E, De Matos, Mara, Gatfield, David, Kundig, Thomas, and Pascolo, Steve, *Design of in vitro Transcribed mRNA Vectors for Research and Therapy.* Chimia, 2019. **73**(5): p. 391-391.
22. Dolgin, Elie, *Covid vaccine Flop Spotlights Mrna Design Challenges.* Nature, 2021. **594**: p. 483-483.
23. Kremsner, Peter, Guerrero, Rodolfo Andrés Ahuad, Arana, Eunate, Martinez, Gustavo Jose Aroca, Bonten, Marc JM, Chandler, Reynaldo, Corral, Gonzalo, Block, Eddie Jan Louis De, Ecker, Lucie, and Gabor, Julian Justin, *Efficacy and safety of the CVnCoV SARS-CoV-2 mRNA vaccine candidate: results from herald, a phase 2b/3, randomised, observer-blinded, placebo-controlled clinical trial in ten countries in Europe and Latin America.* 2021.
24. Bahney, C. S., Zondervan, R. L., Allison, P., Theologis, A., Ashley, J. W., Ahn, J., Miclau, T., Marcucio, R. S., and Hankenson, K. D., *Cellular biology of fracture healing.* J Orthop Res, 2019. **37**(1): p. 35-50.
25. Wong, Sarah Anne, Hu, Diane, Shao, Tiffany, Niemi, Erene, Barruet, Emilie, Morales, Blanca M., Boozarpour, Omid, Miclau, Theodore, Hsiao, Edward C., Nakamura, Mary, Bahney, Chelsea S., and Marcucio, Ralph S., *Beta-catenin Signaling Regulates Cell Fate Decisions at the Transition Zone of the Chondro-Osseous Junction During Fracture Healing.* bioRxiv, 2020.
26. Williams, J. N., Li, Y., Valiya Kambrath, A., and Sankar, U., *The Generation of Closed Femoral Fractures in Mice: A Model to Study Bone Healing.* J Vis Exp, 2018(138).
27. Niedermair, T., Straub, R. H., Brochhausen, C., and Grässel, S., *Impact of the Sensory and Sympathetic Nervous System on Fracture Healing in Ovariectomized Mice.* Int J Mol Sci, 2020. **21**(2).
28. Harada, N., Tamai, Y., Ishikawa, T., Sauer, B., Takaku, K., Oshima, M., and Taketo, M. M., *Intestinal polyposis in mice with a dominant stable mutation of the beta-catenin gene.* Embo j, 1999. **18**(21): p. 5931-42.
29. Hu, D. P., Ferro, F., Yang, F., Taylor, A. J., Chang, W., Miclau, T., Marcucio, R. S., and Bahney, C. S., *Cartilage to bone transformation during fracture healing is coordinated by the invading vasculature and induction of the core pluripotency genes.* Development, 2017. **144**(2): p. 221-234.
30. Rivera, Kevin O., Cuylear, Darnell L., Duke, Victoria, O'Hara, Kelsey Marie, Kharbikar, Bhushan N., Kryger, Alex N., Miclau, Theodore, Bahney, Chelsea S., and Desai, Tejal A., *Localized delivery of β-NGF via injectable microrods accelerates endochondral fracture repair.* bioRxiv, 2021: p. 2021.11.16.468864.
31. Hall, B.K. , *The role of movement and tissue interactions in the development and growth of bone and secondary cartilage in the clavicle of the embryonic chick.* J. Embryol. exp. Morph., 1986. **93**: p. 133-152.

32. Malhan, Deeksha, Muelke, Matthias, Rosch, Sebastian, Schaefer, Annemarie B., Merboth, Felix, Weisweiler, David, Heiss, Christian, Arganda-Carreras, Ignacio, and El Khassawna, Thaqif, *An Optimized Approach to Perform Bone Histomorphometry.* Frontiers in Endocrinology, 2018. **9**.
33. Bouxsein, Mary L, Boyd, Stephen K, Christiansen, Blaine A, Guldberg, Robert E, Jepsen, Karl J, and Müller, Ralph, *Guidelines for assessment of bone microstructure in rodents using micro–computed tomography.* Journal of bone and mineral research, 2010. **25**(7): p. 1468-1486.
34. Sun, Xuying, Gao, Xueqin, Deng, Zhenhan, Zhang, Linlin, McGilvray, Kirk, Gadomski, Benjamin C., Amra, Sarah, Bao, Gang, and Huard, Johnny, *High bone microarchitecture, strength, and resistance to bone loss in MRL/MpJ mice correlates with activation of different signaling pathways and systemic factors.* The FASEB Journal, 2020. **34**(1): p. 789-806.
35. Nance, Kellie D and Meier, Jordan L, *Modifications in an emergency: the role of N1-methylpseudouridine in COVID-19 vaccines.* ACS Central Science, 2021. **7**(5): p. 748-756.
36. Baden, Lindsey R, El Sahly, Hana M, Essink, Brandon, Kotloff, Karen, Frey, Sharon, Novak, Rick, Diemert, David, Spector, Stephen A, Rouphael, Nadine, and Creech, C Buddy, *Efficacy and safety of the mRNA-1273 SARS-CoV-2 vaccine.* New England journal of medicine, 2021. **384**(5): p. 403-416.
37. Polack, Fernando P, Thomas, Stephen J, Kitchin, Nicholas, Absalon, Judith, Gurtman, Alejandra, Lockhart, Stephen, Perez, John L, Pérez Marc, Gonzalo, Moreira, Edson D, and Zerbini, Cristiano, *Safety and efficacy of the BNT162b2 mRNA Covid-19 vaccine.* New England journal of medicine, 2020. **383**(27): p. 2603-2615.
38. Vijaya Chandra, Shree Harsha, Wacker, Ingrid, Appelt, Uwe Kurt, Behrens, Jürgen, and Schneikert, Jean, *A common role for various human truncated adenomatous polyposis coli isoforms in the control of beta-catenin activity and cell proliferation.* PloS one, 2012. **7**(4): p. e34479.
39. Presnyak, V., Alhusaini, N., Chen, Y. H., Martin, S., Morris, N., Kline, N., Olson, S., Weinberg, D., Baker, K. E., Graveley, B. R., and Coller, J., *Codon optimality is a major determinant of mRNA stability.* Cell, 2015. **160**(6): p. 1111-24.
40. Diez, Michay, Medina-Muñoz, Santiago Gerardo, Castellano, Luciana Andrea, da Silva Pescador, Gabriel, Wu, Qiushuang, and Bazzini, Ariel Alejandro, *iCodon customizes gene expression based on the codon composition.* Scientific Reports, 2022. **12**(1): p. 12126.
41. *Modified mRNA for BMP-2 in Combination with Biomaterials Serves as a Transcript-Activated Matrix for Effectively Inducing Osteogenic Pathways in Stem Cells.* Stem Cells and Development, 2017. **26**(1): p. 25-34.
42. Zhang, Wen, De La Vega, Rodolfo E, Coenen, Michael J, Müller, Sebastian A, Peniche Silva, Carlos J, Aneja, Manish K, Plank, Christian, Van Griensven, Martijn, Evans, Christopher H, and Balmayor, Elizabeth R, *An improved, chemically modified RNA encoding BMP-2 enhances osteogenesis in vitro and in vivo.* Tissue Engineering Part A, 2019. **25**(1-2): p. 131-144.
43. Khorsand, B., Elangovan, S., Hong, L., Dewerth, A., Kormann, M. S., and Salem, A. K., *A Comparative Study of the Bone Regenerative Effect of Chemically Modified RNA Encoding BMP-2 or BMP-9.* Aaps j, 2017. **19**(2): p. 438-446.
44. Elangovan, S., Khorsand, B., Do, A. V., Hong, L., Dewerth, A., Kormann, M., Ross, R. D., Sumner, D. R., Allamargot, C., and Salem, A. K., *Chemically modified RNA activated matrices enhance bone regeneration.* J Control Release, 2015. **218**: p. 22-8.
45. De La Vega, R. E., van Griensven, M., Zhang, W., Coenen, M. J., Nagelli, C. V., Panos, J. A., Peniche Silva, C. J., Geiger, J., Plank, C., Evans, C. H., and Balmayor, E. R., *Efficient healing of large osseous segmental defects using optimized chemically modified messenger RNA encoding BMP-2.* Sci Adv, 2022. **8**(7): p. eabl6242.
46. Aspenberg, P., *Special Review: Accelerating fracture repair in humans: a reading of old experiments and recent clinical trials.* Bonekey Rep, 2013. **2**: p. 244.

47. Prados, B., Del Toro, R., MacGrogan, D., Gómez-Apiñániz, P., Papoutsi, T., Muñoz-Cánoves, P., Méndez-Ferrer, S., and de la Pompa, J. L., *Heterotopic ossification in mice overexpressing Bmp2 in Tie2+ lineages.* Cell Death Dis, 2021. **12**(8): p. 729.

CHAPTER V: SUMMARY, IMPLICATIONS, CONCLUSIONS AND FUTURE DIRECTIONS

There remains an unmet clinical need to develop and test novel strategies to promote bone regeneration and fracture repair. Conventional methods use protein-based therapeutics, including the single FDA-approved osteoanabolic, recombinant human bone morphogenetic protein-2 (BMP-2).[1-5] However, BMP-2 has frequently been associated with adverse side effects and high complication rates ranging from 20-70%.[6, 7] Mechanistic data has elucidated the key role that canonical Wnt plays in chondrocyte to osteoblast transdifferentiation in endochondral ossification, making this pathway a desirable target for bone repair therapeutics.[8] Because Wnt ligands are post-translationally modified through palmitoylation and thus, hydrophobic in nature, hindered their translation into the clinic and make them difficult to manufacture and deliver therapeutically.[9, 10] Gene therapy is a promising strategy to promote fracture repair through the activation of the canonical Wnt pathway and has the potential to circumvent limitations seen with current techniques to activate canonical Wnt. Additionally, recent advancements in nanotechnology have highlighted the potential of using mRNA as a therapeutic for bone tissue engineering.

While mRNA therapeutics have recently gained traction, to date there have been very few studies using mRNA as a therapeutic modality for bone tissue regeneration.[11, 12] Most approaches have employed mRNA encoding bone morphogenetic proteins (BMPs). Elangovan *et al*. used a cationic polymer to complex with the negatively charged nucleic acid, termed polyplex, loaded onto a collagen scaffold and tested in a rat calvarial bone defect model.[11] It was reported that this chemically modified mRNA (cmRNA) encoding BMP-2 significantly increased bone volume as compared to the plasmid DNA polyplex encoding BMP-2.[11] Other approaches using lipoplexes encapsulating cmBMP-2 have used various scaffolding materials including collagen sponge, poly-lactic-co-glycolic acid (PLGA) microparticles and also calcium phosphate cement.[13-16] Interestingly, Fayed *et al.* used a cmRNA BMP-2 transcript in combination with a polymeric film to enhance integration of titanium surfaces, finding increased alkaline phosphatase (ALP) activity leading to higher mineralized content with the transcript activated matrix.[17]

Another study co-delivered cmRNA BMP-2 and vascular endothelial growth factor (VEGF) in bone marrow-mesenchymal stem cells (BMSCs) showing improved osteogenesis compared to protein delivery *in vitro,* and accelerated fracture healing when delivered on a collagen scaffold in a rat cranial defect model at both 4 and 12 weeks as compared to untransfected and protein controls.[18] Importantly, all studies have reported therapeutic efficacy with incorporation of cmRNA encoding BMP-s *in vitro*, bone defect or integration models.[11, 13-16] Despite these therapeutic benefits seen, all strategies have required surgical intervention to implement treatment.

Ex-vivo gene therapy strategies have shown to be more efficacious in bone regeneration with advantages including reduced cytotoxicity from mitigating direct administration of viral delivery vectors and lipid vehicles. In fact, when comparing direct *in vivo* delivery with *ex-vivo* delivery of the same adenoviral-based BMP-2 construct, the *ex-vivo* administration was proven to be more effective following implementation in a rat cavarial bone defect model.[19] Additionally, *ex-vivo* gene therapy has shown to be more efficacious than direct protein delivery in promoting bone.[19, 20] These results support the concept that *ex-vivo* transfection can mitigate some of the challenges seen with direct viral gene delivery, including reduced immunogenicity, yet this approach has been associated with high manufacturing costs associated from logistics with *ex-vivo* procedures.[21]

Our work employed a modified mRNA encoding a stabilized, non-destructive β-catenin transcript that was delivered using an optimized lipid-nanoparticle in a murine fracture model. While other strategies have used transcripts for bone regeneration, there has been limited research exploring transcripts activating the canonical Wnt pathway to promote bone regeneration.[12, 22] Our approach for activating canonical Wnt more directly activates canonical Wnt as β-catenin is a direct modulator of the pathway and also regulates *Runx2* expression.[23] β-catenin was found to play an imperative role in endochondral ossification and mechanistically drives chondrocytes to differentiate into osteoblasts.[8] Additionally, Balmayor *et al.* determined endochondral healing with the BMP-2 cmRNA group in a rat defect model and intramembranous healing with the BMP-2 protein group.[24] As fractures heal through endochondral

ossification, this signifies a more native like healing route as compared to delivery with the protein.[24]Taken together, delivering β-catenin in the form cmRNA provides a direct and native approach to effectively produce bone through driving endochondral ossification.

After reviewing current clinical strategies and emerging technologies in canonical Wnt therapeutics for bone repair, we have developed a novel mRNA-based therapeutic activating the canonical Wnt pathway and have tested this mRNA therapeutic in its capacity to promote bone in a murine tibia fracture model. The approach chosen for this research was novel in that we explored the feasibility of novel, injectable local and non-viral delivery of a cmRNA designed to activate canonical Wnt to promote bone in a fracture setting. Despite promising *in vitro* results showing higher transfection when delivering lipoplexes (LPX) complexed with MCM and FMCM, these combined MCM-LPX and FMCM-LPX delivery mechanisms did not significantly increase transfection, yet FMCM-LPX did prolong transfection when tested in a murine tibia fracture model. Localized delivery of SM-102 LNPs were determined to significantly improve transfection efficacy and kinetics, minimize immunogenicity and did not interfere with bone healing in a murine fracture model. Combined with the optimized SM-102 LNPs, a novel mRNA sequence was synthesized encoding a non-destructive β-catenin mRNA, β-catenin^{GOF}, containing modified nucleosides and CleanCap technology to maximize mRNA stability and reduce immunogenicity. When tested, the SM-102-β-catenin^{GOF} mRNA activated canonical Wnt genes *in vitro* and increased bone formation when delivered at 45 μg/mouse in a murine tibia fracture model. Stabilized β-catenin mRNA transcript in combination with optimized lipid nanoparticles, provides an injectable application system which circumvents the need to surgically deliver the construct.

Despite the novelty of these findings there are several challenges that need further exploration and remain as potential limitations with our approach. One of the main limitations include that only one dose of the optimized SM-102 LNP was tested for immunogenicity. Previously studied mRNA therapies encoding BMP-2 for a critical sized defect have found success in using 50 μg mRNA delivered on a collagen sponge.[24] In this study, a similar, yet slightly lower dose of 45 μg was found to be clinically effective

when tested at 2 weeks after fracture. However, immunogenicity was only tested using a dose of 10 μg/mouse. Our work did not explore the immunological impact with higher doses. This poses a limitation as the dose that showed efficacy for improved bone formation *in vivo* was not tested for its capabilities to cause an immunogenic response. It would be expected that the near 4.5-fold increase in dose would provoke an even higher acute inflammatory response as compared with the 10 μg dose tested. Nonetheless, the improved bone formation in a fracture healing setting suggests that any potential immunogenic influence did not negatively impact bone healing outcomes. Robust testing of systemic and localized immunological responses with the 45 μg mRNA dose remains to be explored in future studies. Additional systemic inflammatory measurements should be taken in addition to CRP, as this protein is a minor acute phase reactant (APR) in mice. The major APR for mice, serum amyloid P-component (SAP), should also be evaluated amongst other signaling mechanisms known to recruit macrophages such as chemokine CCL2.[25] To investigate the localized inflammatory profile from delivery with higher doses of mRNA, pro-inflammatory cytokines IL-1, IL-6, TNF-α and IFN-γ and anti-inflammatory cytokines IL-10 and TGF-β should be assessed through analysis of RNA expression within the fracture callus.[26] Fractures activate a temporally regulated inflammatory response which necessitates several time points to determine the full inflammatory profile of a therapeutic. Thus, these systemic and localized inflammatory responses should be measured at time points following treatments including days 1, 3, 5 and 10 to determine elevated pro-inflammatory response and its temporal resolution.

Another main limitation of these set of experiments includes that only one time point was tested following delivery of SM-102-β-catenin^{GOF} mRNA at 2 weeks following fracture. By testing later time points for measures of bone formation, validating fully healed fractures can be determined with each treatment group. Further, this measure can assess acceleration of bone volume and adverse events, like heterotopic ossification which has been found to occur in mice as early as 4 weeks after fracture.[27] Future studies should incorporate later time points to analyze bone formation through uCT and histomorphometry,

such as at 4 and at 6 weeks following fracture. Expectations of 4 week images would depict a fully healed fracture in the 45 μg SM-102-β-catenin^{GOF} mRNA treatment group with potentially increased bone volume found in the 25 μg and rhWnt3a groups compared to the PBS control. This would further suggest a dose dependency of the β-catenin^{GOF} mRNA as seen through histomorphometry. Lastly, at this time point, adverse effects frequently associated with osteoanabolics, like heterotopic ossification can be determined. Later time points, like 6 weeks after fracture, have shown near complete fracture healing in a murine tibia fracture and stabilization model using similar methods.[28] Bone healing measurements at this time point would begin to show any delays in fracture healing.

Additional tests need to be performed in diverse fracture types to determine if the developed therapeutic is efficacious in impaired fracture healing models. For the purposes of this study, a mid-shaft tibia fracture was performed in young mice and an intermedullary rod was employed to facilitate relative stability of the fracture site. However, this fracture model does not recapitulate delayed or non-union models. Several models have been established for delayed and non-union, yet these models have not been standardized. Models of atrophic nonunion typically involve critical sized defects with or without periosteal injury and stabilized with either pins or with a plate and screws.[29-33] Similarly, models of hypertrophic non-union typically involve defects with or without periosteal injury yet are employed by using an unstabilized fixation technique, creating a large callus.[29, 34] Delayed union models also use defect and stabilization techniques combined with additional injuries to the periosteum or vasculature.[29, 35, 36] Additional fracture types due to traumatic injuries include comminuted fractures, or fractures resulting in bone broken into multiple fragments. Typically this fracture type is treated surgically and depending on the severity of comminution, reports of non-union can occur more frequently.[37] Surrounding soft tissues, like muscle, influence fractures by increasing angiogenesis and providing a source of stem cells.[38] Extensive insult to muscle impedes fracture healing.[38] Traumatic injuries resulting in loss of soft tissue and other fracture models such as craniofacial models, were not in the scope of this dissertation and thus should be further investigated in their respective fracture models. Many studies have concluded that femoral fractures

treated surgically with intermedullary rods serve as a leading model to evaluate therapies to accelerate bone repair.[29, 39] To test our therapeutic for treatment of non-union or delayed union, these models or similar models must be employed. It would be expected that these impaired fracture models would benefit from anabolic agents which augment the biologic microenvironment. Previous studies have shown benefits following treatment with osteoanabolic agent rhBMP-2 and rhBMP-7 in non-union cases, but many of these trials reported complications, such as heterotopic ossification.[40-43] The need to develop therapeutics to accelerate fracture healing in impaired fracture healing cases remains to be met.

Different delivery platforms and routes of administration are necessary depending on each specific application. For instance, modes of delivery can be optimized for critical sized defect models. These cases may present a lack of soft callus completely bridging both the ends of the fracture which require implementation of a structural support in addition to an osteoanabolic treatment. For these cases, the developed therapeutic SM-102-β-catenin^{GOF} mRNA would be complexed within an osteoconductive support, such as allograft material demineralized bone matrix. For these types of applications, further dose responses need to be explored.

One such limitation seen when using MCM as an mRNA delivery platform was that the binding efficacy of MC3 LNPs were not tested when complexed with MCM or FMCM. While the combination of these two technologies provided promising *in vitro* results showing enhanced transfection efficacy with the FMCM-MC3 group. However, binding efficiencies of the MC3 LNPs with FMCM/MCM vehicles were not assessed prior to *in vivo* studies. The immense variation of luciferase signal between mice within MCM-MC3 and FMCM-MC3 groups can potentially be reduced by optimizing the binding protocol between the two technologies. The net neutral surface charge seen with ionizable LNPs hinders any electrostatic interaction with calcium and phosphate ions located in mineral coating of MCMs. Future studies should assess various binding buffers to facilitate an electrostatic interaction between these two technologies, such as MES buffers adjusted to pH of 4.5. Reports with this buffer have supplemented with CaCl2 to counteract the loss of calcium within acidic pH ranges.[44]

Post-hoc power analyses are typically performed to determine the proper effect size for the model. In this case, a priori power analysis for histomorphometry analysis revealed that a major effect would present significant results with an n-value of 6 per sample. The low sample size performed for histomorphometry analysis could give rise to a type II error, or false negative, which would suggest that there were differences between groups despite not finding differences.[45] A post-hoc power analysis exposed that the effect size for testing MCM and FMCM for osteogenesis *in vivo* was $\eta^2 = 0.15$ giving rise to an n-value of 123 per group to reach significance. Conversely, a p-value can be used to examine type I error, or false positive, in a power analysis where the lower the p-value the lower possibility of type I error to occur.[45] Given the results of this study, a low power of 8% was determined for histomorphometric analysis. This may inhibit future work from being performed and ultimately leading to not determining potential differences between MCM, FMCM and controls. Future studies should aim to increase power by potentially increasing effect size through increasing delivered doses or increasing n-values.

Here we presented the development and testing of a novel mRNA-based therapeutic activating the canonical Wnt pathway. Additionally, we hypothesized that the β-catenin^{GOF} transcript would reduce the efficacious dose as it is a non-destructible form of β-catenin, yet this was not explicitly tested. Thus, future studies should determine whether wild-type (WT) β-catenin is just as efficacious as the β-catenin^{GOF} transcript. To determine activation, and thus nuclear localization of β-catenin, following delivery of the stabilized and WT β-catenin mRNA treatments then nuclear β-catenin staining can be performed. Following nuclear β-catenin staining, positively stained cells can be quantified and averaged in at least 3-5 sections per sample. Through quantification of the nuclear β-catenin staining, efficacy of the β-catenin^{GOF} transcript over the WT β-catenin transcript can be determined. Expected outcomes involve higher nuclear β-catenin staining with β-catenin^{GOF} treated mice.

In summary, we have developed an injectable and biocompatible method to deliver functional mRNA modalities specifically for bone tissue regeneration. Despite the promise of using a MCM-LPX complex in a bone healing application, the lipid nanoparticles (LNPs) were found to more consistently

express mRNA within the fracture without interfering with fracture healing. SM-102-β-catenin^{GOF} mRNA was found to increase bone formation in a murine tibia fracture model, indicating its potential to be used to accelerate fracture healing. Given the high number of delayed or non-union fractures, the approach has the potential for significant clinical impact and deserves further development.[46] Our injectable SM-102-β-catenin^{GOF} mRNA therapeutic may prove to accelerate fracture healing, without requiring additional surgeries, thereby reducing healthcare costs and morbidity associated with impaired fracture healing.

V.1 References

1. Dumic-Cule, I., Peric, M., Kucko, L., Grgurevic, L., Pecina, M., and Vukicevic, S., *Bone morphogenetic proteins in fracture repair.* Int Orthop, 2018. **42**(11): p. 2619-2626.
2. Tsuji, K., Bandyopadhyay, A., Harfe, B. D., Cox, K., Kakar, S., Gerstenfeld, L., Einhorn, T., Tabin, C. J., and Rosen, V., *BMP2 activity, although dispensable for bone formation, is required for the initiation of fracture healing.* Nat Genet, 2006. **38**(12): p. 1424-9.
3. Garrison KR, Shemilt I, Donell S, Ryder JJ, Mugford M, Harvey I, Song F, *Bone morphogenetic protein (BMP) for fracture healing in adults.* Cochrane Database ofSystematic Reviews, 2008(1).
4. Lissenberg-Thunnissen, S. N., de Gorter, D. J., Sier, C. F., and Schipper, I. B., *Use and efficacy of bone morphogenetic proteins in fracture healing.* Int Orthop, 2011. **35**(9): p. 1271-80.
5. Gillman, C. E. and Jayasuriya, A. C., *FDA-approved bone grafts and bone graft substitute devices in bone regeneration.* Mater Sci Eng C Mater Biol Appl, 2021. **130**: p. 112466.
6. Shields, Lisa B. E., Raque, George H., Glassman, Steven D., Campbell, Mitchell, Vitaz, Todd, Harpring, John, and Shields, Christopher B., *Adverse Effects Associated With High-Dose Recombinant Human Bone Morphogenetic Protein-2 Use in Anterior Cervical Spine Fusion.* Spine, 2006. **31**(5): p. 542-547.
7. James, A. W., LaChaud, G., Shen, J., Asatrian, G., Nguyen, V., Zhang, X., Ting, K., and Soo, C., *A Review of the Clinical Side Effects of Bone Morphogenetic Protein-2.* Tissue Eng Part B Rev, 2016. **22**(4): p. 284-97.
8. Wong, Sarah Anne, Hu, Diane, Shao, Tiffany, Niemi, Erene, Barruet, Emilie, Morales, Blanca M, Boozarpour, Omid, Miclau, Theodore, Hsiao, Edward C, Nakamura, Mary, Bahney, Chelsea S, and Marcucio, Ralph S, *β-catenin Signaling Regulates Cell Fate Decisions at the Transition Zone of the Chondro-Osseous Junction During Fracture Healing.* bioRxiv, 2020: p. 2020.03.11.986141.
9. Janda, C. Y. and Garcia, K. C., *Wnt acylation and its functional implication in Wnt signalling regulation.* Biochem Soc Trans, 2015. **43**(2): p. 211-6.
10. Hanna, C. C., Kriegesmann, J., Dowman, L. J., Becker, C. F. W., and Payne, R. J., *Chemical Synthesis and Semisynthesis of Lipidated Proteins.* Angew Chem Int Ed Engl, 2022. **61**(15): p. e202111266.
11. Elangovan, S., Khorsand, B., Do, A. V., Hong, L., Dewerth, A., Kormann, M., Ross, R. D., Sumner, D. R., Allamargot, C., and Salem, A. K., *Chemically modified RNA activated matrices enhance bone regeneration.* J Control Release, 2015. **218**: p. 22-8.
12. Rajendran, A. K., Amirthalingam, S., and Hwang, N. S., *A brief review of mRNA therapeutics and delivery for bone tissue engineering.* RSC Adv, 2022. **12**(15): p. 8889-8900.
13. Balmayor, Elizabeth R, Geiger, Johannes P, Aneja, Manish K, Berezhanskyy, Taras, Utzinger, Maximilian, Mykhaylyk, Olga, Rudolph, Carsten, and Plank, Christian, *Chemically modified RNA induces osteogenesis of stem cells and human tissue explants as well as accelerates bone healing in rats.* Biomaterials, 2016. **87**: p. 131-146.
14. Utzinger, Maximilian, Jarzebinska, Anita, Haag, Nicolas, Schweizer, Martin, Winter, Gerhard, Dohmen, Christian, Rudolph, Carsten, and Plank, Christian, *cmRNA/lipoplex encapsulation in PLGA microspheres enables transfection via calcium phosphate cement (CPC)/PLGA composites.* Journal of Controlled Release, 2017. **249**: p. 143-149.
15. Zhang, Wen, De La Vega, Rodolfo E, Coenen, Michael J, Müller, Sebastian A, Peniche Silva, Carlos J, Aneja, Manish K, Plank, Christian, Van Griensven, Martijn, Evans, Christopher H, and Balmayor, Elizabeth R, *An improved, chemically modified RNA encoding BMP-2 enhances osteogenesis in vitro and in vivo.* Tissue Engineering Part A, 2019. **25**(1-2): p. 131-144.
16. Khorsand, B., Elangovan, S., Hong, L., Dewerth, A., Kormann, M. S., and Salem, A. K., *A Comparative Study of the Bone Regenerative Effect of Chemically Modified RNA Encoding BMP-2 or BMP-9.* Aaps j, 2017. **19**(2): p. 438-446.

17. Fayed, Omnia, van Griensven, Martijn, Tahmasebi Birgani, Zeinab, Plank, Christian, and Balmayor, Elizabeth R., *Transcript-Activated Coatings on Titanium Mediate Cellular Osteogenesis for Enhanced Osteointegration.* Molecular Pharmaceutics, 2021. **18**(3): p. 1121-1137.
18. Geng, Yingnan, Duan, Huichuan, Xu, Liang, Witman, Nevin, Yan, Bingqian, Yu, Zheyuan, Wang, Huijing, Tan, Yao, Lin, Liqin, and Li, Dong, *BMP-2 and VEGF-A modRNAs in collagen scaffold synergistically drive bone repair through osteogenic and angiogenic pathways.* Communications Biology, 2021. **4**(1): p. 82.
19. Bukharova, Tatiana Borisovna, Nedorubova, Irina Alekseevna, Mokrousova, Viktoria Olegovna, Meglei, Anastasiia Yurevna, Basina, Viktoriia Pavlovna, Nedorubov, Andrey Anatolevich, Vasilyev, Andrey Vyacheslavovich, Grigoriev, Timofei Evgenevich, Zagoskin, Yuriy Dmitrievich, Chvalun, Sergei Nicolaevich, Kutsev, Sergey Ivanovich, and Goldshtein, Dmitry Vadimovich, *Adenovirus-Based Gene Therapy for Bone Regeneration: A Comparative Analysis of In Vivo and Ex Vivo BMP2 Gene Delivery.* Cells, 2023. **12**(13): p. 1762.
20. Lin, Hang, Tang, Ying, Lozito, Thomas P., Oyster, Nicholas, Wang, Bing, and Tuan, Rocky S., *Efficient in vivo bone formation by BMP-2 engineered human mesenchymal stem cells encapsulated in a projection stereolithographically fabricated hydrogel scaffold.* Stem Cell Research & Therapy, 2019. **10**(1): p. 254.
21. Bashor, Caleb J., Hilton, Isaac B., Bandukwala, Hozefa, Smith, Devyn M., and Veiseh, Omid, *Engineering the next generation of cell-based therapeutics.* Nature Reviews Drug Discovery, 2022. **21**(9): p. 655-675.
22. Uchida, Satoshi, Yanagihara, Kayoko, Matsui, Akitsugu, Kataoka, Kazunori, and Itaka, Keiji, *mRNA as a Tool for Gene Transfection in 3D Cell Culture for Future Regenerative Therapy.* Micromachines, 2020. **11**(4): p. 426.
23. Haxaire, C., Haÿ, E., and Geoffroy, V., *Runx2 Controls Bone Resorption through the Down-Regulation of the Wnt Pathway in Osteoblasts.* Am J Pathol, 2016. **186**(6): p. 1598-609.
24. De La Vega, Rodolfo E., van Griensven, Martijn, Zhang, Wen, Coenen, Michael J., Nagelli, Christopher V., Panos, Joseph A., Peniche Silva, Carlos J., Geiger, Johannes, Plank, Christian, Evans, Christopher H., and Balmayor, Elizabeth R., *Efficient healing of large osseous segmental defects using optimized chemically modified messenger RNA encoding BMP-2.* Science Advances. **8**(7): p. eabl6242.
25. Mortensen, RICHARD F, Beisel, K, Zeleznik, NJ, and Le, PT, *Acute-phase reactants of mice. II. Strain dependence of serum amyloid P-component (SAP) levels and response to inflammation.* Journal of immunology (Baltimore, Md.: 1950), 1983. **130**(2): p. 885-889.
26. McCauley, James, Bitsaktsis, Constantine, and Cottrell, Jessica, *Macrophage subtype and cytokine expression characterization during the acute inflammatory phase of mouse bone fracture repair.* Journal of Orthopaedic Research, 2020. **38**(8): p. 1693-1702.
27. Chakkalakal, S. A. and Shore, E. M., *Heterotopic Ossification in Mouse Models of Fibrodysplasia Ossificans Progressiva.* Methods Mol Biol, 2019. **1891**: p. 247-255.
28. Deng, Z., Gao, X., Sun, X., Cui, Y., Amra, S., and Huard, J., *Gender differences in tibial fractures healing in normal and muscular dystrophic mice.* Am J Transl Res, 2020. **12**(6): p. 2640-2651.
29. Garcia, P., Histing, T., Holstein, J. H., Klein, M., Laschke, M. W., Matthys, R., Ignatius, A., Wildemann, B., Lienau, J., Peters, A., Willie, B., Duda, G., Claes, L., Pohlemann, T., and Menger, M. D., *Rodent animal models of delayed bone healing and non-union formation: a comprehensive review.* Eur Cell Mater, 2013. **26**: p. 1-12; discussion 12-4.
30. Choi, P., Ogilvie, C., Thompson, Z., Miclau, T., and Helms, J. A., *Cellular and molecular characterization of a murine non-union model.* J Orthop Res, 2004. **22**(5): p. 1100-7.

31. Garcia, P., Holstein, J. H., Maier, S., Schaumlöffel, H., Al-Marrawi, F., Hannig, M., Pohlemann, T., and Menger, M. D., *Development of a reliable non-union model in mice.* J Surg Res, 2008. **147**(1): p. 84-91.
32. Garcia, P., Herwerth, S., Matthys, R., Holstein, J. H., Histing, T., Menger, M. D., and Pohlemann, T., *The LockingMouseNail--a new implant for standardized stable osteosynthesis in mice.* J Surg Res, 2011. **169**(2): p. 220-6.
33. Wagner, Johannes M, Schmidt, Sonja V, Dadras, Mehran, Huber, Julika, Wallner, Christoph, Dittfeld, Stephanie, Becerikli, Mustafa, Jaurich, Henriette, Reinkemeier, Felix, and Drysch, Marius, *Inflammatory processes and elevated osteoclast activity chaperon atrophic non-union establishment in a murine model.* Journal of Translational Medicine, 2019. **17**(1): p. 1-8.
34. Oetgen, Matthew E, Merrell, Greg A, Troiano, Nancy W, Horowitz, Mark C, and Kacena, Melissa A, *Development of a femoral non-union model in the mouse.* Injury, 2008. **39**(10): p. 1119-1126.
35. Gröngröft, I., Wissing, S., Meesters, D. M., Poeze, M., Matthys-Mark, R., Ito, K., and Zeiter, S., *Development of a novel murine delayed secondary fracture healing in vivo model using periosteal cauterization.* Arch Orthop Trauma Surg, 2019. **139**(12): p. 1743-1753.
36. Lu, Chuanyong, Miclau, Theodore, Hu, Diane, and Marcucio, Ralph S, *Ischemia leads to delayed union during fracture healing: a mouse model.* Journal of orthopaedic research, 2007. **25**(1): p. 51-61.
37. Park, S. H., Kong, G. M., Ha, B. H., Park, J. H., and Kim, K. H., *Nonunion of subtrochanteric fractures: Comminution or Malreduction.* Pak J Med Sci, 2016. **32**(3): p. 591-4.
38. Shah, K., Majeed, Z., Jonason, J., and O'Keefe, R. J., *The role of muscle in bone repair: the cells, signals, and tissue responses to injury.* Curr Osteoporos Rep, 2013. **11**(2): p. 130-5.
39. Williams, J. N., Li, Y., Valiya Kambrath, A., and Sankar, U., *The Generation of Closed Femoral Fractures in Mice: A Model to Study Bone Healing.* J Vis Exp, 2018(138).
40. Emara, K. M., Diab, R. A., and Emara, A. K., *Recent biological trends in management of fracture non-union.* World J Orthop, 2015. **6**(8): p. 623-8.
41. Friedlaender, Gary E, Perry, Clayton R, Cole, J Dean, Cook, Stephen D, Cierny, George, Muschler, George F, Zych, Gregory A, Calhoun, Jason H, LaForte, Amy J, and Yin, Samuel, *Osteogenic protein-1 (bone morphogenetic protein-7) in the treatment of tibial nonunions: a prospective, randomized clinical trial comparing rhOP-1 with fresh bone autograft.* The Journal of bone and joint surgery. American volume, 2001. **83**(Pt 2): p. S151.
42. Ekrol, Ingri, Hajducka, Carol, Court-Brown, Charles, and McQueen, Margaret M, *A comparison of RhBMP-7 (OP-1) and autogenous graft for metaphyseal defects after osteotomy of the distal radius.* Injury, 2008. **39**: p. S73-S82.
43. Jones, Alan L., Bucholz, Robert W., Bosse, Michael J., Mirza, Sohail K., Lyon, Thomas R., Webb, Lawrence X., Pollak, Andrew N., Golden, Jane Davis, Valentin-Opran, Alexandre, and Group, the BMP-2 Evaluation in Surgery for Tibial Trauma–Allograft Study, *Recombinant Human BMP-2 and Allograft Compared with Autogenous Bone Graft for Reconstruction of Diaphyseal Tibial Fractures with Cortical Defects: A Randomized, Controlled Trial.* JBJS, 2006. **88**(7): p. 1431-1441.
44. Schröder, E., Jönsson, T., and Poole, L., *Hydroxyapatite chromatography: altering the phosphate-dependent elution profile of protein as a function of pH.* Anal Biochem, 2003. **313**(1): p. 176-8.
45. Shreffler, J. and Huecker, M. R., *Type I and Type II Errors and Statistical Power*, in *StatPearls*. 2023, StatPearls Publishing Copyright © 2023, StatPearls Publishing LLC.: Treasure Island (FL).
46. Bastian, O. W., Kuijer, A., Koenderman, L., Stellato, R. K., van Solinge, W. W., Leenen, L. P., and Blokhuis, T. J., *Impaired bone healing in multitrauma patients is associated with altered leukocyte kinetics after major trauma.* J Inflamm Res, 2016. **9**: p. 69-78.

ATGGCTACTCAAGATATCGACGGGCAGTATGCAATGACCAGGGCTCAGCGAGTCCGAGCTGCCATGTTC
CCAGAGACCCTAGATGAGGGAATGCAGATCCCATCCACGCAGTTTGACGCTGCTCATCCCACTAATGTCC
AGCGTCTTGCTGAACCATCCCAGATGTTGAAACATGCTGTTGTCAATCTTATTAACTATCAGGATGACGC
AGAACTTGCCACAAGAGCAATTCCTGAACTGACAAAACTGCTAAACGATGAGGACCAGGTGGTCGTTAA
TAAGGCTGCTGTTATGGTCCATCAGCTTTCCAAAAAGGAAGCTTCCAGACATGCTATCATGAGATCCCCT
CAGATGGTGTCTGCCATTGTACGTACCATGCAGAATACAAATGATGTTGAGACCGCTCGTTGTACTGCTG
GTACTCTGCACAACCTTTCTCACCACCGCGAAGGACTGCTGGCCATCTTTAAATCTGGTGGAATCCCTGC
TCTGGTCAAAATGCTGGGATCACCTGTCGATTCTGTACTGTTCTACGCCATTACAACACTGCATAATCTCC
TGCTCCACCAGGAAGGAGCAAAGATGGCTGTGCGCCTAGCTGGTGGACTGCAGAAAATGGTGGCTTTG
CTCAACAAAACAAATGTGAAGTTTTTGGCTATTACGACGGACTGCCTGCAGATCTTAGCTTACGGAAATC
AAGAGTCTAAGCTCATCATTCTGGCCTCTGGAGGACCCCAAGCCTTAGTCAACATCATGAGGACCTACAC
TTATGAGAAGCTTCTGTGGACAACCAGCAGAGTGCTGAAGGTGCTGTCTGTCTGCTCTAGCAATAAGCC
GGCCATTGTAGAAGCTGGAGGGATGCAGGCACTGGGACTGCATCTGACAGATCCATCCCAGCGACTTG
TGCAGAACTGTCTTTGGACTCTCAGAAATCTTTCCGATGCAGCGACTAAGCAAGAAGGGATGGAAGGCC
TCCTGGGGACTCTGGTTCAGCTTCTGGGTTCCGATGATATAAATGTGGTCACCTGCGCAGCTGGAATTCT
CTCTAACCTCACCTGCAATAATTACAAAAATAAGATGATGGTGTGCCAAGTGGGTGGCATAGAGGCTCT
GGTACGCACCGTCCTTCGTGCTGGTGATCGTGAAGACATCACTGAGCCTGCGATCTGTGCTCTGCGTCAC
CTGACCAGCCGGCATCAGGAAGCAGAGATGGCCCAGAATGCTGTTCGCCTTCATTACGGTCTGCCTGTT
GTGGTTAAACTTCTGCACCCACCTTCTCACTGGCCCCTGATAAAGGCAACTGTTGGATTGATTCGAAACC
TTGCTCTTTGCCCAGCTAATCATGCTCCTCTGCGAGAACAGGGAGCTATCCCACGACTGGTTCAGCTTCTT
GTCCGTGCTCATCAGGACACCCAACGTCGCACCTCCATGGGTGGAACGCAGCAGCAATTTGTTGAGGGC
GTGAGAATGGAGGAGATCGTGGAAGGGTGTACCGGAGCTCTCCACATCCTCGCTCGAGACGTCCACAA
CCGGATCGTAATCAGAGGACTTAATACCATTCCATTGTTTGTGCAACTGCTTTACTCGCCTATTGAAAACA
TCCAAAGAGTCGCTGCTGGGGTCCTCTGTGAACTTGCTCAGGATAAGGAGGCTGCCGAGGCCATTGAA
GCTGAGGGAGCTACCGCTCCTCTGACAGAGTTACTGCACTCCCGTAATGAGGGAGTCGCAACCTACGCA
GCTGCAGTCCTGTTCCGAATGTCTGAGGACAAGCCACAGGATTACAAGAAGCGGCTGTCCGTTGAGCTC
ACCAGTTCCCTCTTCCGTACCGAGCCAATGGCTTGGAACGAGACTGCAGATCTTGGACTGGATATTGGT
GCCCAGGGAGAAGCCCTTGGATATCGTCAGGACGACCCCAGCTACCGTTCTTTTCATTCTGGTGGATAC
GGTCAGGATGCCTTGGGGATGGACCCTATGATGGAGCATGAAATGGGTGGCCATCACCCTGGAGCTGA
CTATCCAGTTGATGGACTGCCTGATCTGGGACATGCCCAGGACCTCATGGATGGGCTGCCCCCAGGTGA
TTCAAATCAGCTCGCCTGGTTCGATACTGACCTGTAA

Supplemental Figure 1. Optimized open reading frame (ORF) of β-catenin sequence without exon 3.

IVIS Output from 1st Pilot Study (10/2020):

Trtmnt	Flux
MCM	1.32E+04
MCM	2.31E+04
Lipo	7.97E+05
Lipo	6.87E+05
TransIT	5.12E+04
TransIT	2.32E+04

R Studio Output -- effect size for preliminary IVIS data set:

```
Parameter | Sum_Squares | df | Mean_Square |      F |      p
-----------------------------------------------------------
Trtmnt    |    6.81e+11 |  2 |    3.40e+11 | 157.30 | < .001
Residuals |    6.49e+09 |  3 |    2.16e+09 |        |

Anova Table (Type 1 tests)

# Effect Size for ANOVA (Type I)

Parameter |   η² |       95% CI
------------------------------
Trtmnt    | 0.99 | [0.92, 1.00]

- One-sided CIs: upper bound fixed at [1.00].
```

Power analysis for effect size f=0.99::

```
     Balanced one-way analysis of variance power calculation

              k = 3
              n = 4.444027
              f = 0.99
      sig.level = 0.05
          power = 0.8

NOTE: n is number in each group
```

R Studio Code:

```
#install.packages("pwr")
library(knitr)
library(tidyverse)
library(emmeans)
library(pwr)
knitr::opts_chunk$set(echo = FALSE, warning=FALSE)
knitr::opts_chunk$set(message = FALSE, comment=NA)
library(effectsize)

seven <- read.csv("U:/PhD/Dissertation/Stats calculations/IVIS preliminary da
ta.csv", quote = " ' ", header=TRUE)
str(seven)

m <- lm(Flux ~ Trtmnt, data = seven)
parameters::model_parameters(anova(m))
options(es.use_symbols = TRUE) # get nice symbols when printing! (On Windows,
requires R >= 4.2.0)


eta_squared(m, partial = FALSE)
pwr.anova.test(k=3,f=0.99, sig.level=.05,power=.8)
```

Supplemental Figure 2. Preliminary data from IVIS output was used to calculate effect size (η^2), which was then used to determine the smallest sample size to reach a power of 80%. Smallest sample size was determined to be n=4.4. R Studio code provided on the right.

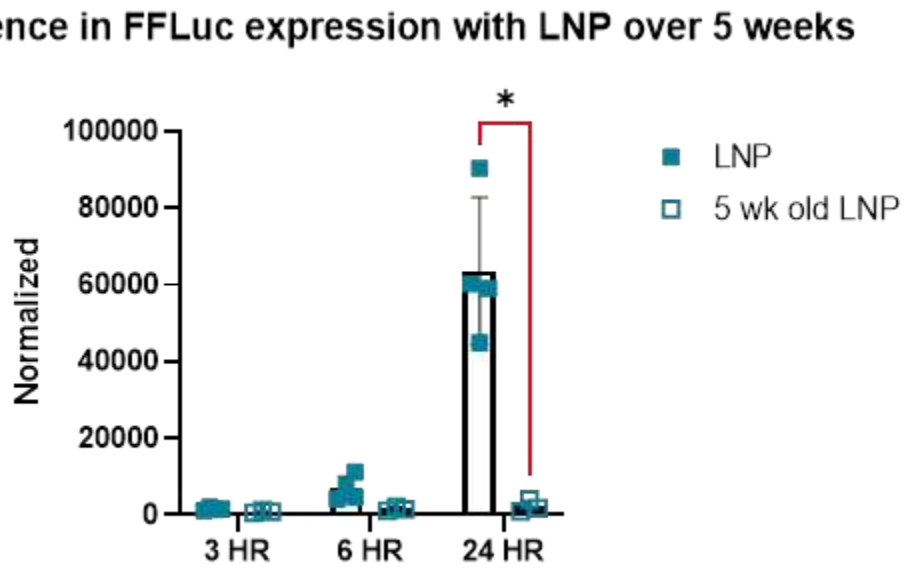

Supplemental Figure 3. MC3 LNPs were tested for transfection efficacy using reporter gene, firefly luciferase mRNA. Firefly luciferase was tested through qRT-PCR as described in Chapter III. Shelf-life of firefly luciferase mRNA-MC3 LNPs were tested within receiving LNPs 1-2 weeks after formulation and again at 5 weeks after formulation.

Supplemental Table 1. Histopathology results used a Semi-quantitative scoring method using a modification of ISO10993-6 Annex E: Biological evaluation of medical devices – Part 6: Tests for local effects after implantation.

	Score				
Cell type/response	**0**	**1**	**2**	**3**	**4**
Polymorphonuclear cells (PMNs)	None	Rare, 1-5/HPF*	5-10/HPF	Heavy infiltrate	Packed
Lymphocytes	None	Rare, 1-5/HPF	5-10/HPF	Heavy infiltrate	Packed
Plasma cells	None	Rare, 1-5/HPF	5-10/HPF	Heavy infiltrate	Packed
Macrophages (Mϕ)	None	Rare, 1-5/HPF	5-10/HPF	Heavy infiltrate	Packed
Giant cells	None	Rare, 1-2/HPF	3-5/HPF	Heavy infiltrate	Sheets
Necrosis	None	Minimal	Mild	Moderate	Severe
Edema	None	Minimal	Mild	Moderate	Severe[+]
Hemorrhage	None	Minimal	Mild	Moderate	Severe[#]
Neovascularization[&]	None	Minimal	Mild	Moderate	Severe
Fibrosis	None	Minimal	Mild	Moderate	Severe
Signs of implant degradation	None	Minimal	Mild	Moderate	Severe
Particulate debris	None	Minimal	Mild	Moderate	Severe
*HPF – high powered field [&] Neovascularization – severe suggests numerous neovascular vessels					

APPENDIX B: COPYRIGHT PERMISSION LETTER

Order Details

1. Journal of tissue engineering and regenerative medicine

Billing Status: Open

Article: Therapeutic approaches to activate the canonical Wnt pathway for bone regeneration

Order License ID	1407044-1	**Type of Use**	Republish in a thesis/dissertation
Order detail status	Completed	**Publisher**	JOHN WILEY & SONS, LTD.
ISSN	1932-7005	**Portion**	Chapter/article

0.00 USD
Republication Permission

LICENSED CONTENT

Publication Title	Journal of tissue engineering and regenerative medicine	**Publication Type**	e-Journal
Article Title	Therapeutic approaches to activate the canonical Wnt pathway for bone regeneration	**Start Page**	961
		End Page	976
		Issue	11
		Volume	16
Date	01/01/2007	**URL**	http://www3.interscience.wiley.com/cgi-bin/jhome/113389949
Language	English		
Country	United Kingdom of Great Britain and Northern Ireland		
Rightsholder	John Wiley & Sons - Books		

REQUEST DETAILS

Portion Type	Chapter/article	**Rights Requested**	Main product
Page Range(s)	5-45	**Distribution**	Worldwide
Total Number of Pages	150	**Translation**	Original language of publication
Format (select all that apply)	Electronic	**Copies for the Disabled?**	No
Who Will Republish the Content?	Not-for-profit entity	**Minor Editing Privileges?**	No
		Incidental Promotional Use?	No
Duration of Use	Life of current edition	**Currency**	USD
Lifetime Unit Quantity	Up to 499		

NEW WORK DETAILS

Title	PhD Student	**Institution Name**	Colorado State University
Instructor Name	Anna Laura Nelson	**Expected Presentation Date**	2023-10-23

ADDITIONAL DETAILS

The Requesting Person/Organization to Appear on the License	Anna Laura Nelson

REQUESTED CONTENT DETAILS

Title, Description or Numeric Reference of the Portion(s)	Chapter 1	**Title of the Article/Chapter the Portion Is From**	Therapeutic approaches to activate the canonical Wnt pathway for bone regeneration
Editor of Portion(s)	Nelson, Anna Laura; Fontana, GianLuca; Miclau, Elizabeth; Rongstad, Mallory; Murphy, William; Huard, Johnny; Ehrhart, Nicole; Bahney, Chelsea	**Author of Portion(s)**	Nelson, Anna Laura; Fontana, GianLuca; Miclau, Elizabeth; Rongstad, Mallory; Murphy, William; Huard, Johnny; Ehrhart, Nicole; Bahney, Chelsea
Volume / Edition	16		
Page or Page Range of Portion	961-976	**Publication Date of Portion**	2022-10-31

John Wiley & Sons - Books Terms and Conditions

No right, license or interest to any trademark, trade name, service mark or other branding ("Marks") of WILEY or its licensors is granted hereunder, and you agree that you shall not assert any such right, license or interest with respect thereto. You may not alter, remove or suppress in any manner any copyright, trademark or other notices displayed by the Wiley material. This Agreement will be void if the Type of Use, Format, Circulation, or Requestor Type was misrepresented during the licensing process. In no instance may the total amount of Wiley Materials used in any Main Product, Compilation or Collective work comprise more than 5% (if figures/tables) or 15% (if full articles/chapters) of the (entirety of the) Main Product, Compilation or Collective Work. Some titles may be available under an Open Access license. It is the Licensors' responsibility to identify the type of Open Access license on which the requested material was published, and comply fully with the terms of that license for the type of use specified Further details can be found on Wiley Online Library http://olabout.wiley.com/WileyCDA/Section/id-410895.html.

Total Items: 1

Subtotal: 0.00 USD

Order Total: 0.00 USD